INTEGRATING AIRBORNE LIDAR AND TERRESTRIAL LASER SCANNER FOREST PARAMETERS FOR ACCURATE ESTIMATION OF ABOVE-GROUND BIOMASS/CARBON IN AYER HITAM TROPICAL FOREST RESERVE, MALAYSIA

MULUKEN NEGA BAZEZEW

February, 2017

SUPERVISORS:
Dr. Yousif A. Hussin
Drs. E. H. Kloosterman

INTEGRATING AIRBORNE LIDAR AND TERRESTRIAL LASER SCANNER FOREST PARAMETERS FOR ACCURATE ESTIMATION OF ABOVE-GROUND BIOMASS/CARBON IN AYER HITAM TROPICAL FOREST RESERVE, MALAYSIA

MULUKEN NEGA BAZEZEW

Enschede, The Netherlands, February, 2017

Thesis submitted to the Faculty of Geo-Information Science and Earth Observation of the University of Twente in partial fulfilment of the requirements for the degree of Master of Science in Geo-information Science and Earth Observation.
Specialization: Natural Resource Management

SUPERVISORS:
Dr. Yousif A. Hussin
Drs. E. H. Kloosterman

THESIS ASSESSMENT BOARD:
Dr. A.G. Toxopeus (Chair)
Dr. Tuomo Kauranne (External Examiner, Lappeenranta University of Technology, Finland)
Dr. Yousif A. Hussin (1st Supervisor)
Drs. E. H. Kloosterman (2nd Supervisor)

DISCLAIMER

This document describes work undertaken as part of a programme of study at the Faculty of Geo-Information Science and Earth Observation of the University of Twente. All views and opinions expressed therein remain the sole responsibility of the author, and do not necessarily represent those of the Faculty.

ABSTRACT

Efficient and accurate estimation of tropical forests above-ground biomass (AGB) is a major concern of Reduced Emission from Deforestation and Forest Degradation (REDD+) in its climate change mitigation program. However, retrieving tree parameters of tropical forests has been continued as challenging process since these forests are with complex vertical structure. Application of single remote sensing has, therefore, challenging to retrieve all trees parameter of tropical forests. This thesis presents an approach for accurate AGB assessment by integrating Airborne LiDAR scanning (ALS) and Terrestrial laser scanning (TLS). Integrative use of ALS and TLS of modern remote sensing technologies has enabled to detect a comparable number of manually recorded trees. ALS and TLS were used to detect and extract upper and lower canopies tree parameters, respectively. About 62% of trees were detected by ALS while the remaining 38% were detected by TLS. The height of upper and lower canopy trees was then measured from corresponding ALS and TLS point cloud data. Diameter at breast height (DBH) of all trees was measured by TLS, and ALS detected trees were matched and linked with the corresponding tree stems detected by TLS for DBH use. DBH derived from TLS was validated using manually measured field DBH. On the other hand, two way of tree height validation were implemented; upper canopy and lower canopies tree height. Upper canopy trees height measured from ALS was used as a ground-truth reference to validate corresponding field-based tree heights.

For lower canopy trees height measurement validation, controlled field experiment was performed to assess the accuracy and height measurement variation of the TLS and handheld laser instruments (Leica DISTO 510, TruPulse and Forestry Laser Rangefinder). Height measurements were done in the known height of the windowsills, and selected solitary and complex cluster of trees. The result showed TLS provides highly accurate height approaching to the actual heights of the windowsills with Root Mean Square (RMSE) of 5 cm while Leica DISTO 510, TruPulse and Forestry Laser Rangefinder provided RMSE of 60, 73 and 85 cm, respectively. Height measurement with handheld laser instruments showed deviations from regression line with increasing distance and height of the object. On the other hand, handheld laser instruments height measurement of selected trees showed significant differences among observers and distances to the tree.

Coefficient of determination (R^2) and RMSE between field and TLS based DBH were 0.989 and 1.30 cm (6.52%), respectively. The R^2 and RMSE between upper canopy trees field-based height and the corrosponding heights identified by ALS were 0.61 and 3.24 m (20.18%), respectively. On the other hand, R^2 of 0.69 and RMSE of 1.45 m (14.77%) were found for lower canopy tree heights when field-based height validated with TLS measured tree heights.

The AGB calculated from combination of ALS and TLS derived parameters was compared with traditional field-based AGB at the plot level, and R^2 of 0.966 and RMSE of 0.62 Mg (7.64%) were achieved

Keywords: ALS, Handheld laser instruments, Lower canopy trees, Point cloud data, REDD+, TLS, Upper canopy trees

ACKNOWLEDGEMENTS

I express my sincere gratitude to Faculty of Geo-information and Earth Observation Science (ITC), University of Twente and Netherland Fellowship Program (NFP) who granted me scholarship to pursue MSc. degree in Geo-information and Earth Observation Science for Natural Resource Management. I'm also very thankful to Dilla University, Ethiopia for allowing me to study in the Netherlands.

I would like to express my deepest appreciation to Dr. Yousif A. Hussin, my first supervisor, who has given me constructive and indispensable comments in all phases of the research. He has been interested in all process of my study and encouraged me through his scientific discussion. I'm very thankful to Drs. E. H. Kloosterman, my second supervisor, who provided me invaluable support in intensive fieldwork and guidance from the beginning to final submission of the study.

I'm very grateful to Dr.Ir. T.A. Groen and Dr. A.G. Toxopeus for their valuable feedback during the proposal and mid-term presentation. I'm also thankful to Dr. T. Wang and Mr. X. Zhu for their cooperation and technical support on the use Terrestrial laser scanner. I'm also gratified to Mr. Ojoatre Sadadi who have done a lot in the processing of Airborne LiDAR data and made available for this study. Drs. R.G. Nijmeijer, NRM Course Director; I'm really thankful in my heart for his warm welcome, support and advice especially in mentor sessions. He really made me feel like home during my stay in ITC.

I'm indebted to University of Putra Malaysia (UPM) for collaboration in providing Airborne LiDAR data and support for fieldwork. I'm very thankful to Dr. Mohd Hasmadi, Faculty of Forestry, UPM for facilitating of the entrance to Malaysia and guidance in fieldwork. I would like to thank Mrs. Siti Zurina, Mr. Fasil Bin, Mr. Jelani Bin, Mr. Fazrul Azree, Mr. Mohd Fakhrullah and Mr. Razael for their immeasurable assistance in intensive fieldwork.

I'm also grateful to my fieldwork crews Miss Mariam Salim of Kenya, Mr. John Reuben and Mr. Yuvenal Pantaleo of Tanzania, and Mr. Solomon Mulat of Ethiopia for their productive discussion and experience throughout my study. I would like to thank NRM classmates for the academic experience and joyful time we shared.

Last but not least, my eternal thanks goes to my parents; my father Nega Bazezew and my Mother Simegn Muluneh who always helping and encouraging me. You have been patient all the time in my study. My brothers Asmare, Eyayu, Chekille and Bekele, and my sisters Yeshalem and Mamey; I'm always grateful for your encouragement to move forward.

Muluken Nega
Enschede, The Netherlands
February, 2017

TABLE OF CONTENTS

LIST OF FIGURES

LIST OF TABLES

LIST OF EQUATIONS

LIST OF APPENDICES

LIST OF ACRONYMS

AGB	Above-ground Biomass
AGBC	Above-ground Biomass Carbon
ALS	Airborne LiDAR Scanner
CF	Conversion Factor
CHM	Canopy Height Model
CPA	Crown Projection Area
DBH	Diameter at Breast Height
DSM	Digital Surface Model
DTM	Digital Terrain Model
FAO	Food and Agricultural Organization of the United Nations
GFDRR	Global Facility for Disaster Reduction and Recovery
GHGs	Greenhouse Gases
GPS	Global Positioning System
IGI	Integrated Geospatial Innovation
IPCC	Intergovernmental Panel on Climate Change
LiDAR	Light Detection and Ranging
MRV	Measurement, Reporting and Verification
MSA	Multi-station Adjustment
NOAA	National Oceanic and Atmospheric Administration
OBIA	Object Based Image Analysis
PPM	Parts Per Million
REDD+	Reducing Emission from Deforestation and Forest Degradation
RMSE	Root Mean Square Error
RS	Remote Sensing
SOCS	Scanner Own Coordinate System
TLS	Terrestrial Laser Scanner
UNFCCC	United Nations Conventions on Climate Change
UPM	University Putra Malaysia

1. INTRODUCTION

1.1. Background

Forests play an important role in regulating global climate by their capacity which serve as sink and source of carbon (Pan et al., 2011). Through absorbing of atmospheric carbon by photosynthesis, forest ecosystems are crucial in atmospheric CO_2 emission balance. Forest ecosystems can sequester approximately 3 billion of tons of anthropogenic carbon per year in their net growth; this means absorbing 30% of all carbon emission from fossil burning and deforestation (Canadell & Raupach, 2008). Tropical forests are known by storing large amounts of carbon than any other terrestrial ecosystem (Soares-Filho et al., 2010).

Eventhough the importance of forests in off-setting atmospheric CO_2 is well-known, increment of atmospheric carbon is one of today's major concern since it is the principal causal factor for climate change (Crowley, 2000). The concentration of this atmospheric CO_2 is still increasing due to human activity. Recent 2016 National Oceanic and Atmospheric Administrative (NOAA) records show that the continuous rise of atmospheric CO_2 currently reached 408.97 PPM which has been 385.21 PPM 10 years back (NOAA, 2016). Anthropogenic greenhouse gases (GHGs) emission and lack of data on the role of forests in emission balance contributes to severity of the problem (Boudreau et al., 2008).

Accurate measurement and spatial coverage of forest carbon stock to monitor emission balance have both a political and a scientific dimension (Patenaude et al., 2004). Though the need of atmospheric carbon balance has been discussed for the past years, in which most countries still do not have accurate yearly forest carbon inventory data. Therefore, efficient and accurate forest carbon inventory in most countries is still challenging which affects achieving terrestrial carbon sink plan. Thus, the reliability of the difference between the amounts of carbon emitted from anthropogenic activities and sequestrated carbon from forests is ambiguous for most of the countries (Garcia et al., 2010).

Efficient and accurate ways of quantifying and monitoring of carbon stock at regional, continental and global scale is highlighted to be very important (Boudreau et al., 2008). Therefore, countries agreed under the Kyoto protocol of United Nations Framework Convention on Climate Change (UNFCCC) it is required to reporting annually on their emissions and offsets of CO_2 from the atmosphere (UNFCCC, 2015). The agreement comprises regular information on emissions and sequestrations from land use land cover changes such as deforestation, afforestation, and reforestation of each country. Hence, Reduced Emission from Deforestation and Forest Degradation (REDD+) has been initiated to implement forest projects and ensure accurate Measurement, Reporting and Verification (MRV) of forest carbon stocks of countries (Gupta et al., 2013).

Accurate estimation and regular reporting of forest biomass carbon require global integrity as countries have to comply with UNFCCC convention. The Ministry of Natural Resources and Environment (NRE) of Malaysian Federal Government has therefore abided to the convention to be devoted to forest monitoring primarily for their carbon sink (NRE, 2014). REDD+ was developed for implementation of national and sub-national levels of forestry plans taking MRV mechanism as a principal goal. Therefore, exploring accurate techniques for spatial coverage and forest biomass assessment has been given central emphasis.

Accurate biomass measurement would require a destructive method of cutting and weighing tree parts which is not environmentally practical. The use of allometric equations is widely recognized methods for forest carbon inventory by using mathematical estimation models, which are mainly derived based on field measured height and diameter at breast height (DBH) parameters (Parresol, 1999, cited in Segura & Kanninen, 2005). Although field-

based estimation of forest carbon stock is commonly used, this method is time-consuming and labor intensive. Besides, lack of field inventory data in remote areas and inconsistent inventory methods over large regions or overseas are constraints of acquiring reliable biomass estimations. Ground inventory method requires tedious effort over large areas and so are not well suited for monitoring and estimating carbon stock changes. As a result, single biomass carbon measurement have been used for several years without an update. Furthermore, relying on ground-based allometric equations generates uncertainties due to the inadequate site based model diagnosis (Sileshi, 2014).

Uncertainties in above-ground biomass (AGB) estimation occurs mainly in tree parameter measurement errors. Tree height from traditional field based instruments like hypsometers and handheld lasers height measure devices are associated with uncertainties due to structural nature of forests. Especially, traditional field-based height measurement accuracy in tropical forests is ambiguous, as these forests have a dense and multi-layered structure which makes it difficult to see tree tops. Larjavaara & Muller-Landau (2013) highlighted that using handheld laser instruments for tree height measurements in closed complex forest where tree tops are not visible, provides inaccurate tree height readings.

The growing need for spatially-explicit mapping and monitoring change in forest biomass and the use of earth observation satellites has grown continuously in order to acquire forest inventory data over a large areas at regular intervals (Dong et al., 2003). This remote sensing approach could improve spatial forest inventory and reduce efforts in field assessment. On the other hand, Hyde et al. (2006) stated that some remote sensing techniques; like the use of low and medium resolution images have drawbacks, especially in dense forests, due to the difficulty of canopy penetration.

The use of modern earth observation technologies of Light Detection and Ranging (LiDAR) which includes Airborne LiDAR or Laser Scanner (ALS) and Terrestrial Laser Scanner (TLS) are growing fast as these methods can provide vertical and horizontal structure of the forest through target scanning with laser pulses (Jung et al., 2011). Now a day's these methods are found to be the most favorable remote sensing as it is possible to delineate individual tree crowns (Lindberg et al., 2012). Several researches showed that ALS and TLS provide height, DBH, crown area and the position of trees with high accuracy (Hyyppa et al., 2012; Ramirez et al., 2013; Ferraz et al., 2016).

The ALS provides accurate geospatial data of Digital Terrain Model (DTM) and Digital Surface Model (DSM) (Popescu et al., 2002) which are useful for extracting absolute height of the trees. Studies indicated that ALS technology provides tree height with high accuracy (Kumar, 2012; Sadadi, 2016). Andersen et al. (2006) confirmed that ALS provide tree height with accuracy ranges from 0.02 ± 0.73 m. Thus, ALS method has recognized as it is more precise and efficient way than field and optical remote sensing methods (Lim et al., 2003). On the other hand, recently TLS which is a ground based LiDAR has also been used in forest trees inventory parameters for biomass estimation. The instrument provides efficient and accurate extraction of basic tree inventory parameters of DBH and height (Bienert et al., 2006). Henning et al. (2006) also proved that TLS provides excellent accuracy of DBH with error not exceeding 1 cm, and height accuracy of <2 cm from height of trees up to 13 m.

Although these remote sensing technologies are confirmed to provide accurate forest inventory parameters, independent application of these instruments seems challenging to consider all trees in complex multiple canopy structure of tropical forests. Airborne LiDAR is providing highly accurate tree heights of the top emergent trees of dense forest while TLS is accurately provide all trees DBH, and lower canopy trees height. In the circumstance of tropical rainforest having more than one canopy layer, integrative use of ALS and TLS data potentially provide more accurate AGB output than independent application of these technologies. Recently, complimentary use of

ALS and TLS derived parameters at plot level has been tested, and promising accuracy has been achieved in the estimation of AGB in tropical rainforest (Lawas, 2016). Therefore, integrative application of ALS and TLS provides highly accurate tree height and DBH measurements which can contribute to REDD+ MRV program of accurate AGB assessment.

The main objective of this study is to present an approach for estimating AGB through integrative application of ALS and TLS derived tree parameters of height and DBH in complex structure of Ayer Hitam tropical rainforest.

1.2. Research Problems

REDD+ has been initiated as a follow-up mechanism aiming to avoid deforestation and forest degradation and provides financial compensation to countries conserving their forest for enhancing carbon stock (UN-REDD, 2016). Thus, Measurement, Reporting and Verification (MRV) of accurate and transparent forest carbon stock is required for each country to monitor emission balance. Therefore, accurate measurement of forest parameters mainly tree height and DBH, which have a direct link for above-ground biomass (AGB) assessment are of major concern to REDD+ MRV. However, accurate measurement of these tree parameters is challenging in most measurement approaches especially in dense complex forests.

In order to efficiently and timely quantifying AGB, use of remotely sensed data is considered to be a good method for MRV of forest carbon stock assessment of the REDD+ program. Optical sensor data can be used for mapping and monitoring in relatively simple forest structures. Previous studies have shown that estimating accurate AGB of tropical forests using Landsat Thematic Mapper (TM) and synthetic aperture radar (SAR) is difficult due to spectral response saturation and overlap of many species from optical sensors and backscatter from SAR (Steininger, 2000; Foody, 2003). Dengsheng (2006) indicated that rely on only low and medium resolution imagery approaches in dense forest areas lead to high uncertainties due to saturation problem.

Now a day's the use of active remote sensing techniques of ALS and TLS provides more accurate AGB than other optical remote sensors as these technologies can provide direct tree height, DBH and other tree parameters which have direct relationship with biomass (Lindberg et al., 2012; Apostol et al., 2016). Studies showed that ALS can provide accurate crown area and height under a wide range of canopy conditions (Clark et al., 2004). On the other hand, TLS approach can also provide tree parameters with high accuracy and can replace tedious traditional forest inventory methods (Watt & Donoghue, 2005; Maas et al., 2008; Kaasalainen et al., 2014).

In temperate and boreal forests, the performance of ALS and TLS in terms of number of tree extraction and parameter measurements for biomass estimation is found to be fairly accurate (Naesset & Gobakken, 2008; Garcia et al., 2010). Extracting all trees in tropical forests on the other hand is challenging, as its' complex vertical structure makes it unable to detect all trees by a single independent technique. In multiple canopies of tropical forests, ALS can only be used to detect upper canopy trees for height and canopy projection area (CPA) (Jung et al., 2011). Terrestrial laser scanner has been also used to extract tree height and DBH with high accuracy through ground observation (Hunter et al., 2013). But, application of TLS independently in a tropical forest results high uncertainty in tree height measurement of the higher trees since the complex structure of forest canopy and very tall trees makes it difficult for the instrument to view all tree tops (Strahler et al., 2008). Hence, application of TLS mainly apply for understory tree height detection and parameter measurements.

Thus, using only ALS in the tropical rainforest can only provide the upper canopy trees parameter while understories vegetation would remain undetected. In the same way using TLS independently mainly provide accurate measurements of clearly viewed understory trees. Integrating ALS and TLS derived tree parameters is

likely to increase the accuracy of AGB estimation. Figure 1.1 demonstrates research problems and approaches followed to overcome the problem of estimating accurate AGB in tropical forests.

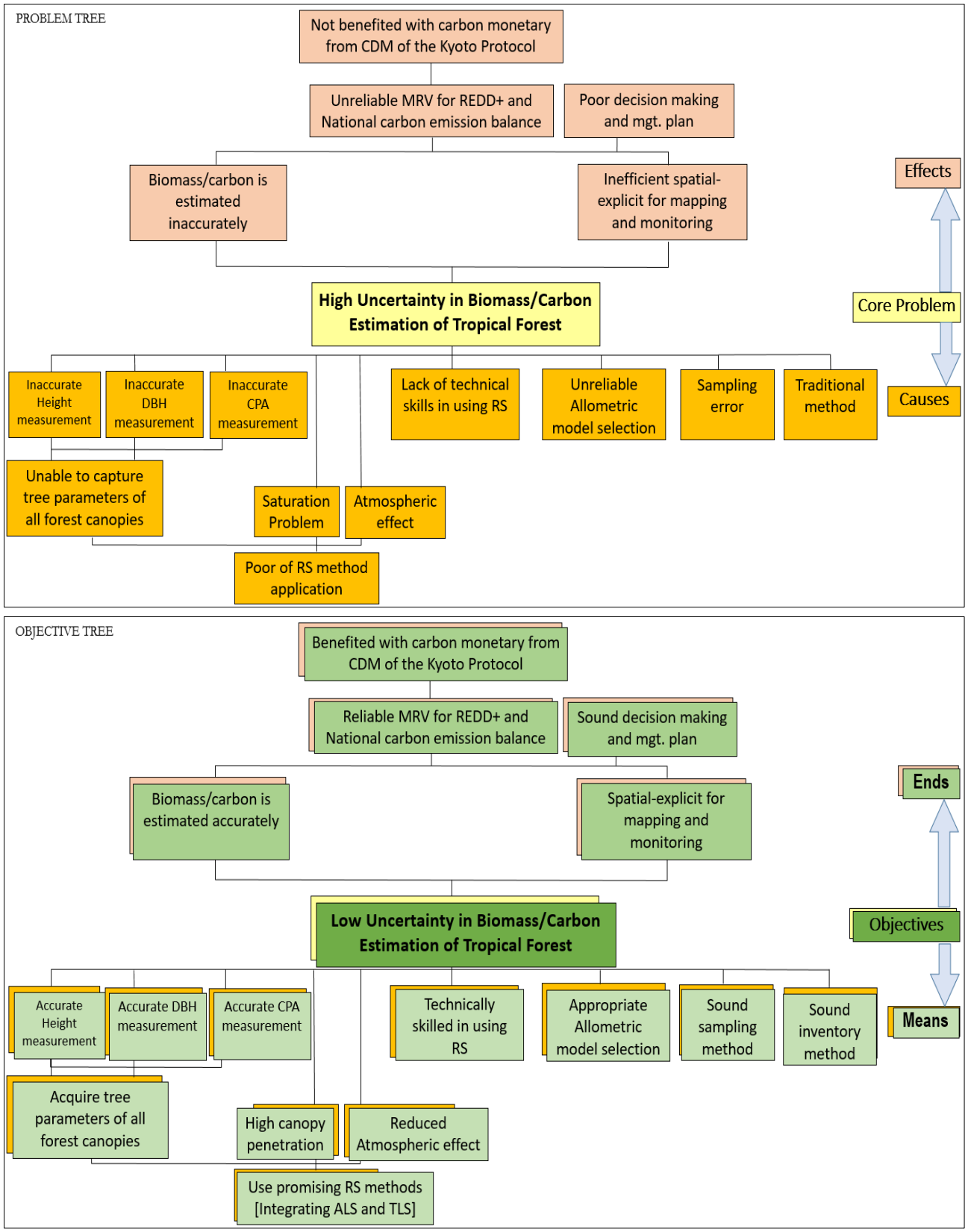

Figure 1.1. Research Problems (Problem Tree) and approaches to overcome AGB estimation uncertainty (Objective Tree)

1.3. Research Objectives

1.3.1. General Objective

The main objective of this study is to develop an approach for accurate estimation of AGB and carbon of tropical rainforest through remote sensing methods of integrating ALS and TLS derived forest parameters in comparison to traditional field methods.

1.3.2. Specific Objectives

1. To assess the accuracy of TLS and field handheld laser instruments for tree height in controlled field experiment,
2. To assess the accuracy of DBH of upper and lower canopies measured from TLS as compared to field DBH measurements of the tropical forest,
3. To assess the accuracy of segmentation of individual tree Canopy Projection Area (CPA) of tropical forest from Airborne LiDAR image,
4. To assess the accuracy of field trees height of the upper canopies as compared to the ALS measurement of tropical forest,
5. To assess the accuracy of field trees height of lower canopies as compared to the TLS measurement of tropical forest, and
6. To assess AGB/carbon by integrating ALS and TLS derived forest parameters and compare remote sensing and field-based AGB estimation per plot.

1.4. Research Questions

1. How accurate is tree height measurement of TLS and field handheld laser instruments in controlled field experiment?
2. How accurate are trees DBH of upper and lower canopies tropical forest derived from TLS as compared with field measured DBH?
3. How accurate are individual trees Canopy Projection Area (CPA) segmented from Airborne LiDAR image?
4. How accurate is trees height of upper canopies tropical forest derived from the field as compared with ALS measured height?
5. How accurate is trees height of lower canopies tropical forest derived from the field as compared with TLS measured height?
6. What are the amount and the difference between estimated AGB derived from integrating ALS and TLS forest parameters compared to field based AGB per plot?

1.5. Hypotheses

1. **Ho:** There is no significant difference between the accuracy of tree height measured from TLS and handheld laser instruments.
   H_1: There is a significant difference between the accuracy of the tree height measured from TLS and field handheld laser instruments.

2. **Ho:** There is no significant difference between the accuracy of tropical forest upper and lower canopies tree DBH derived from TLS and field.
   H_1: There is a significant difference between the accuracy of tropical forest upper and lower canopies tree DBH derived from TLS and field.

3. **Ho:** CPA of individual tree derived from ALS of the tropical rainforest cannot be segmented with > 70% accuracy.
   H_1: Segmented CPA of individual tree derived from ALS of the tropical rainforest can be segmented with > 70% accuracy.
4. **Ho:** There is no significant difference between the accuracy of upper canopies tree height derived from ALS and field.
   H_1: There is a significant difference between the accuracy of lower canopies tree height derived from ALS and field.

5. **Ho:** There is no significant difference between the accuracy of lower canopies tree height derived from TLS and field.
   H_1: There is a significant difference between the accuracy of lower canopies tree height derived from TLS and field.

6. **Ho:** There is no significant difference between remote sensing method of integrating ALS and TLS and field based AGB per plot.
   H_1: There is a significant difference between remote sensing method of integrating ALS and TLS and field based AGB per plot.

2. LITERATURE REVIEW

2.1. Airborne Laser Scanning

Airborne LiDAR scanner (ALS) is an active remote sensing technology stands for light detection and ranging. This technology uses in near infrared light ranging 900 to 1064 nm, where there is high reflectance of vegetation. ALS enables accurate and details 3D geometry of ground surface and objects; aided by small beam width, multiple pulses, and waveform digitization (Wehr & Lohr, 1999). It operates from airborne platform with set of instruments; laser scanner device, inertial navigation measurement unit (IMU) which records aircraft's altitude vector continuously, high-precision global positioning system (GPS) which records three-dimensional position of the aircraft, and computer interface used to manage communication between the device and data (Gallay, 2013) (Figure 2.1).

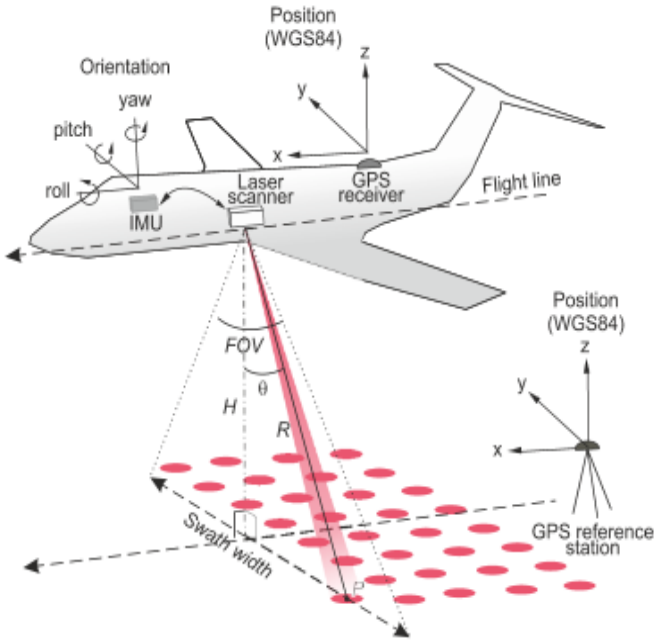

Figure 2.1. Airborne LIDAR system; points on surface represent at which laser is reflected back
Source: (Gallay, 2013)

The principle in the airborne LiDAR is to measure the time travel of the emitted laser signal from the target and back. As shown in Figure 2.2, LiDAR can be classified as discrete-return and waveform returning pulse signals. Discrete-return measures either single-return or multiple-return system. Usually one to five of height signals with peak returns and characterized with small footprint of mostly from 20-80 cm diameter. While waveform-return recording device records complete waveform returning pulses and produce multiple returns between the first and the last returns (Lefsky et al., 2002).

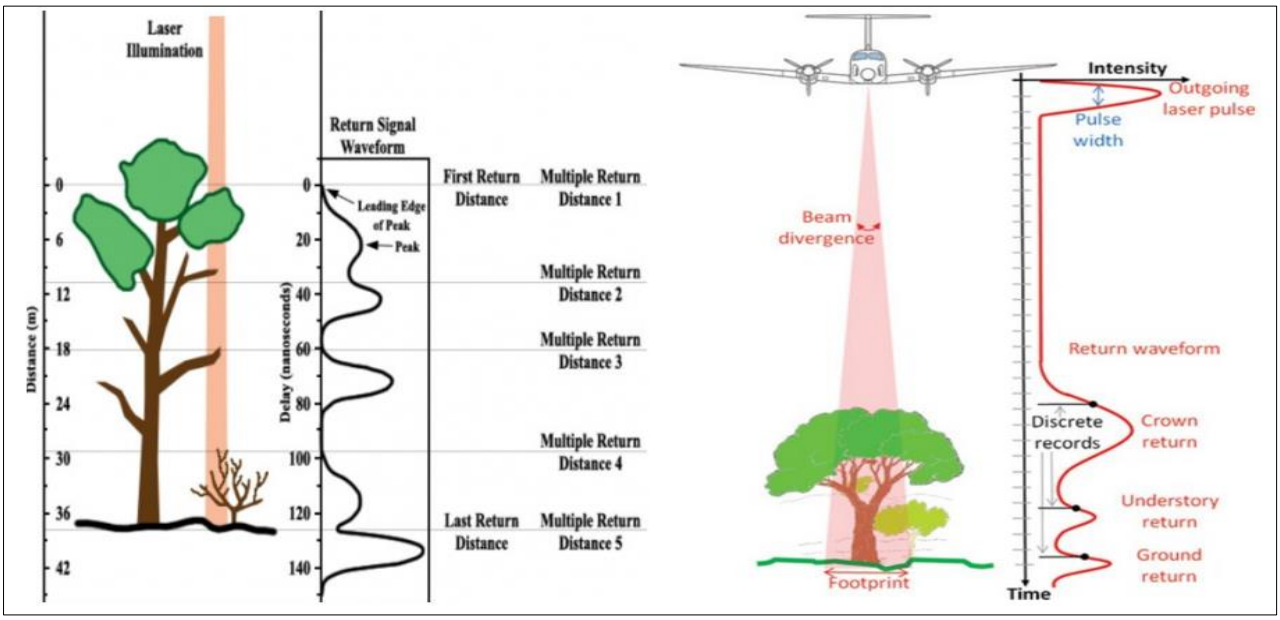

Figure 2.2. Discrete-return and waveform returning pulse signals
Source: (Lefsky et al., 2002)

Through recognizing the first and last return of the LiDAR pulses, digital surface model (DSM) which represents height value of first surface on the ground (including terrain and other objects), and digital elevation/terrain model (DEM) representing 3D presentation of terrain surfaces are executed (Figure 2.3). Absolute height of the objects or canopy height model (CHM) can be found by subtracting DTM from DSM. Hence, ALS measures vertical and horizontal structure of vegetation which enable to extract height of the tree with higher accuracy than traditional field-based measurements (Maltamo et al., 2004).

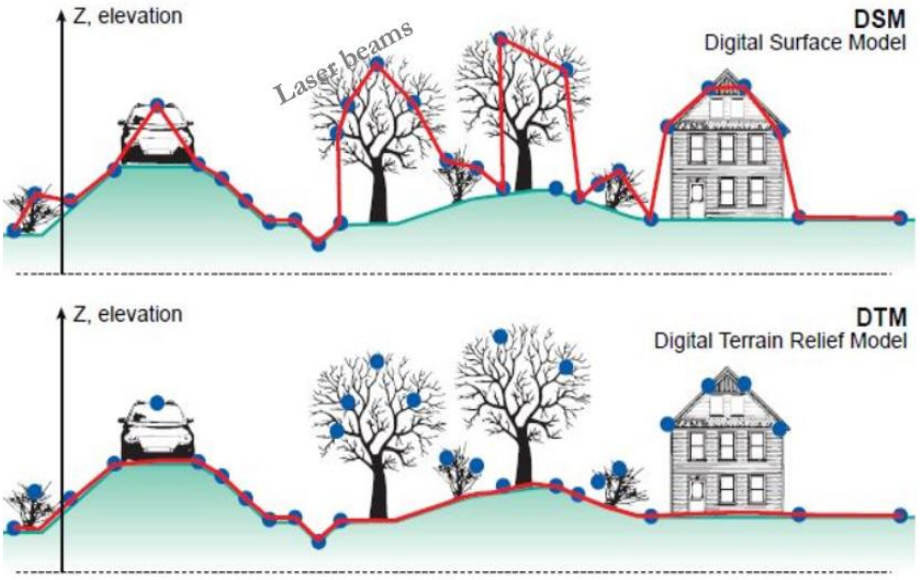

Figure 2.3. Airborne LiDAR digital surface and elevation model
Source: (GFDRR, 2016)

2.2. Terrestrial Laser Scanning

Terrestrial laser scanner (TLS) is ground based laser scanning technology enables to collect 3D point clouds data composed of millions of points of the surface of the scanned object (Dassot et al., 2011). The high point cloud

data acquired by TLS provides accurate 3D digital model of the object. As shown in Figure 2.4, the device has mounted on a tripod and takes hemispherical scanning by rotating a complete horizontal rotation and the rotating mirror scanning in the vertical plane. Some scanners have digital single lens reflex cameras (DSLR) which provide color images to display the point cloud in RGB colors.

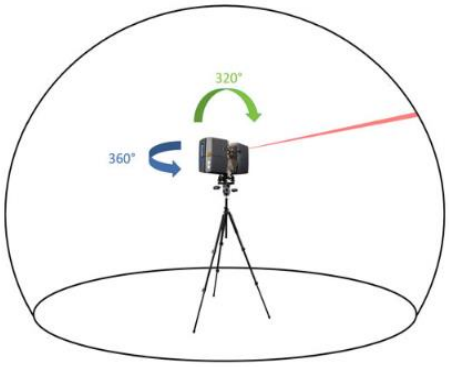

Figure 2.4. Operating system of terrestrial laser scanning
Source: (Dassot et al., 2011)

Two methods of scanning system can be applied; single scanning and multiple scanning (Bienert et al., 2006). In single scanning, the scanner placed in a single place and so only one dimension or side of the object can be scanned. In multi-scanning, the scanning can be done from different positions usually 3 or 4 positions and so provides 3D structure of a single object (Figure 2.5).

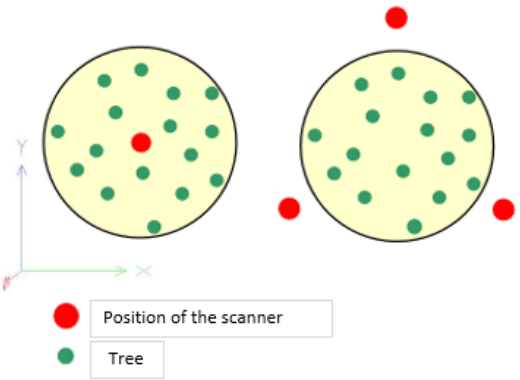

Figure 2.5. Single and multiple scanning methods
Source: (Bienert et al., 2006)

Terrestrial laser scanner can provide accurate 3D object ranges relative to the scanning position (Lemmens, 2011). Tree height and DBH can be easily acquired in TLS point cloud data. Studies showed that tree DBH can be acquired with vary high accuracy as comparable with field-based diameter tape measurements (Maas et al. 2008). Calders et al. (2015) confirmed that TLS tree height measurement is also very accurate when it is validated with destructively measured height.

2.3. Tropical Lowland Rainforest Structure

Tropical lowland rainforests generally are composed mainly broad-leaved trees found in wet tropical upland and lowlands of the equator (WTMA, 2016). As shown in Figure 2.6 , tropical rainforests have a complex pattern of distribution from ground to canopy described as a vertical structure of tropical rainforest; named emergent canopy, canopy, under canopy and Shrub layers (IG, 2016). The highest biomass or carbon density is found in tropical

rainforest. Thus, in the line of climate change mitigation tropical rainforests are the highest carbon reservoir of any terrestrial ecosystem of the planet, and play a significant role in the global carbon cycle (Clark, 2002).

Figure 2.6. Tropical Rainforest structure
(a)-Schematic diagram of topical forest structure; Source: (IG, 2016), (b)-Ayer Hitam tropical forest field picture

2.3.1. Tropical Forest Parameter Measurements

Biomass is the amount of live and inert organic matter found in above- and below-ground expressed as mass of dry matter per unit area (FAO, 1997). Forest carbon is found in three pools; above- and below-ground living vegetation, dead organic matter and soil organic carbon (IPCC, 2006). Use of allometric model derived from field measurements based on forest and site characteristics is a common way of above-ground biomass (AGB) estimation (Houghton et al., 2001). Tree height, DBH and crown diameter and/or area are the most important parameters used for biomass estimation input parameters (Figure 2.7). Tree height is a vertical distance from tree base to tree-top while DBH is diameter of tree stem at 1.30 m above-ground (GEOG, 2016). Crown projection area (CPA) is the extent covered by ground by vertical canopy projection (Rudiger, 2003), and is used for detection of individual tree.

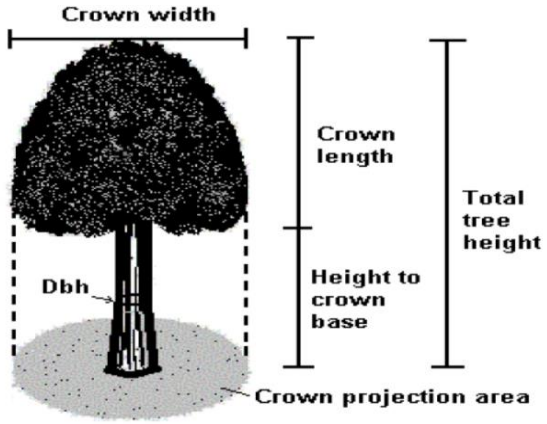

Figure 2.7. Individual tree parameter measurements (Tree height, DBH and crown diameter)
Source: (GEOG, 2016)

Direct traditional field-based measurement using hypsometer or handheld laser instruments are mostly used for tree height and DBH. Now a day's, ALS and TLS can give tree parameters with high accuracy. Studies showed that ALS provides highly accurate height (Heurich, 2008; Naesset & Gobakken, 2008; Leeuwen & Nieuwenhuis, 2010). Terrestrial laser scanner provides tree height and DBH measurements with very high accuracy. For instance in relatively open forest area, Srinivasan et al. (2015) showed TLS provides height measurement accuracy with R^2 of 0.92 and RMSE of 1.51 m, DBH of R^2 of 0.98 with RMSE of 1.08 cm of accurate compared to field measurements. However, in complex tropical rainforest, TLS can accurately measure height till a certain limit of height because of occlusion. Henning et al. (2006) obtained highly accurate tree height measurement with below < 2 cm for trees up to 13 m height. Lawas (2016) found a better accuracy of TLS height measurement for understory trees up to 15 m in tropical rainforest.

2.3.2. Remote Sensing Applications in Forest Biomass Estimation

Optical remote sensing images are accessible and affordable for a large area and so have been used for forest AGB assessment (Kajisa et al., 2009; Basuki et al., 2013). Radar which involves backscatter values also provides convenient biomass estimates as compared to field measurements (Ghasemi et al., 2011). Though this method gives accurate biomass estimates, saturation in radar wavelengths of C, L and P bands and polarization makes it difficult to apply in dense vegetation with complex structure forest areas having high biomass (Cutler et al., 2012). Lu (2006) demonstrated that using course spatial resolution images for AGB assessment in dense forests caused poor prediction due to a spectral mix of pixels.

The introduction of LiDAR technologies of ALS and TLS in biomass estimation improves the problem of saturation as these methods provide 3D tree geometry which allows direct extraction of forest parameters. Several studies demonstrated that ALS provides accurate biomass estimation with an R^2 value of more than 0.70 compared to field measurements (Naesset & Bjerknes, 2001; Patenaude et al., 2004; Naesset & Gobakken, 2008). TLS approach also provides forest parameters and biomass with high accuracy with above R^2 of 0.80 especially in temperate forests (Seidel et al., 2012; Olsoy et al., 2014).

2.3.3. Integrative use of ALS and TLS in AGB Estimation

Most studies in temperate and boreal plantations and natural open forests used ALS and TLS independently (Figure 2.8), and obtain accurate forest parameter measurements and acceptable AGB values (Popescu, 2007; Kankare et al., 2013). But, independent application of ALS and TLS for detection of all trees in tropical forest is very challenging since these forests are with multiple canopies, which makes it difficult for trees to be seen by single instrument (Figure 2.6). The ALS measures tree height and crown cover parameters of the top forest canopy in complex forest structure while it has limitation to detect lower canopy forest parameters and stem information of the trees. On the other hand, TLS measures height and DBH of trees with high accuracy with limitations of height and crown characteristics in trees of top forest canopies. Apostol et al. (2016) recommended that combination use of TLS and ALS technologies would have complementary effects in forest parameters extraction. One of the few studies where the combination of ALS and TLS has been used at tree level found out one-third of tree species were detected by TLS while the remaining detected by ALS in Estate forest of Sweden (Fritz et al., 2011).

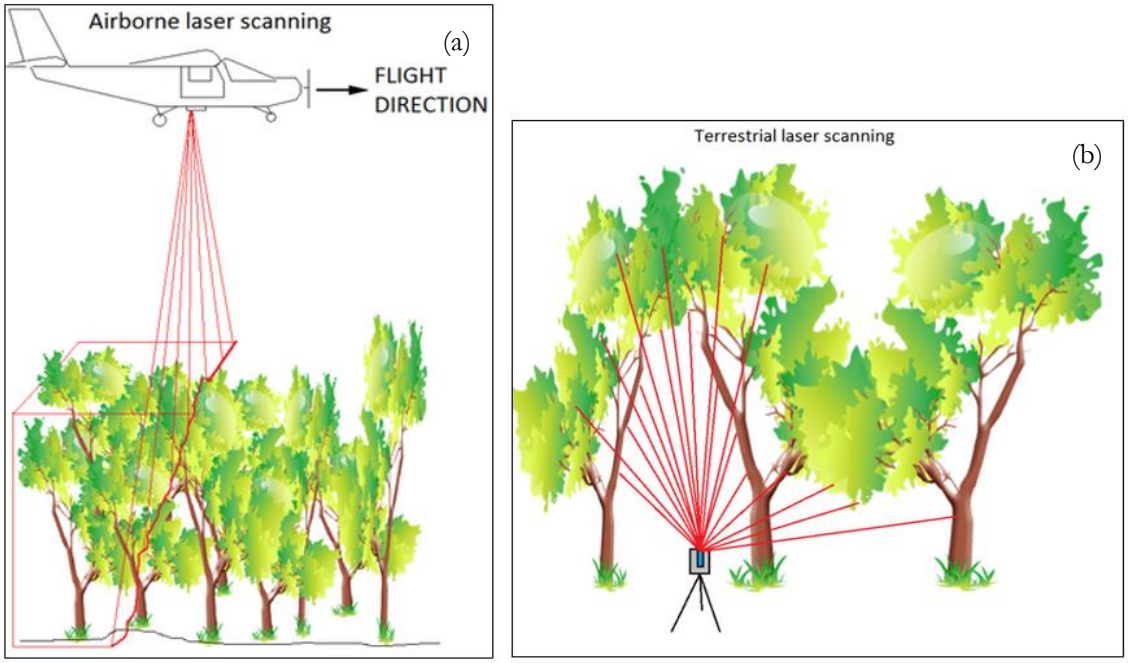

Figure 2.8. Independent application LiDAR in simple structure forests
(a)-ALS, (b)-TLS; Source: (AWF-WIKI, 2016)

3. MATERIALS AND METHODS

3.1. Materials

3.1.1. Study Area

Ayer Hitam tropical rainforest reserve is located in Selangor State of Malaysia. The forest is situated in southern Kuala Lumpur Capital City; 3º0'0" to 3º2'0" latitude and 101°38'0" to 101°40'0" longitude (Figure 3.1). Altitude of the forest ranges from 15 to 233 m a.s.l. and consists of tropical rainforest tree species (Nurul-Shida et al., 2014). Currently, the forest covers around 1248 ha. The forest is the only natural lowland forest left in Putrajaya district (UPM, 2016). The forest reserve is consists of complex multiple canopy rainforest species, and is leased by University of Putra Malaysia (UPM) since 1990 used for education and research purpose in the field of forestry. The multiple canopy structure of the forest has, therefore, complies with the objective of this study to develop an approach for accurate above-ground biomass (AGB) of the complex vertical structure of tropical forests. In addition, the study site was selected due to its accessibility, availability of data and support from UPM.

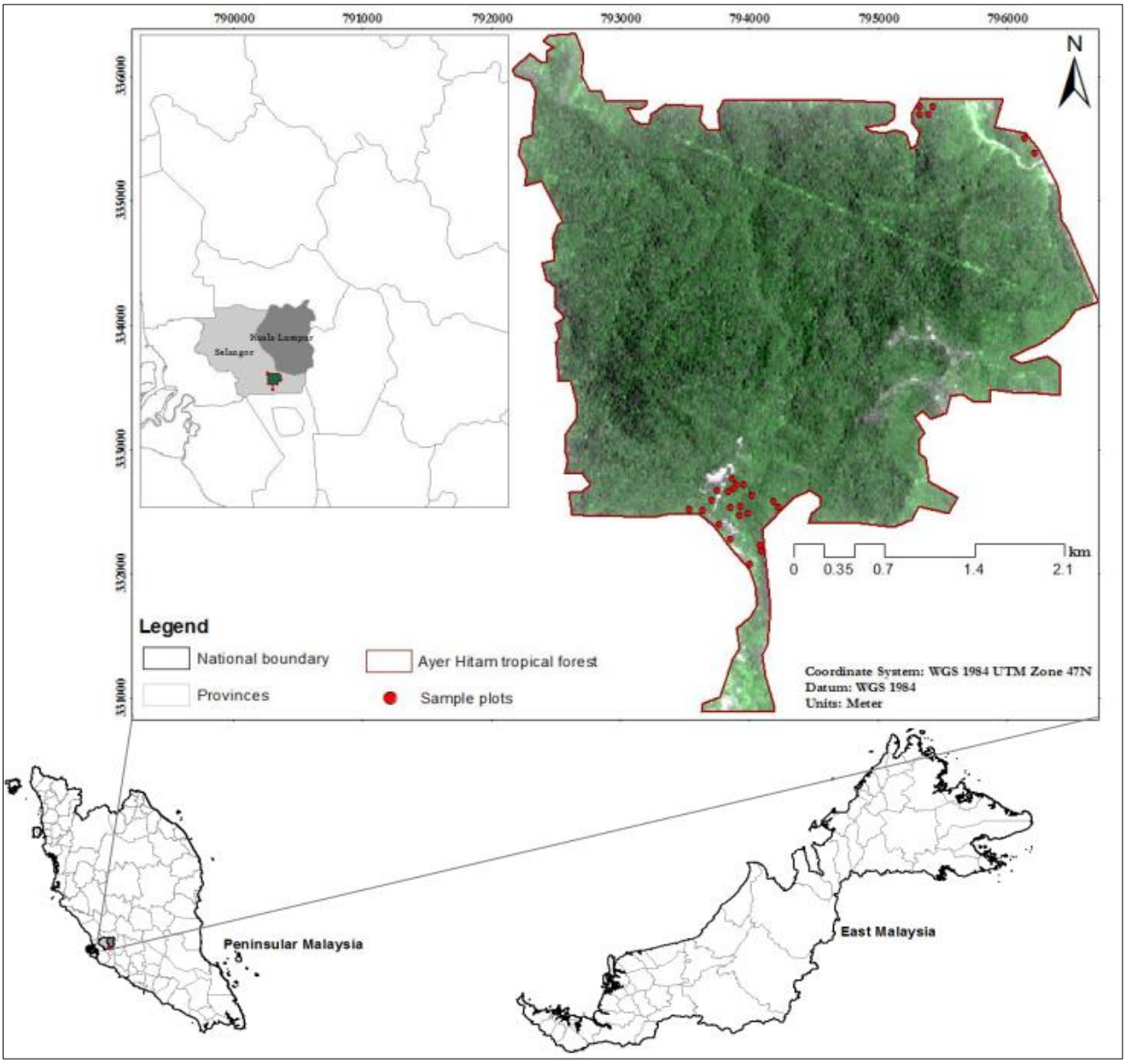

Figure 3.1. Study area location map

3.1.2. Climate

Ayer Hitam tropical forest reserve is characterized by average annual temperature ranges from 23 - 32 ℃ for 1980 to 2008 trend study. The area have high rainfall distribution throughout the year with annual average of 1, 765 mm and the precipitation is higher form October to February (Toriman et al., 2013). It is also characterized by relatively high avarage monthly humudity ranges from 94 - 97%.

3.1.3. Vegetation

Ayer Hitam is a secondary forest which was selectively logged form 1936 to 1965. It encompasses about 430 seed plant species with 203 genera and 72 families (Hunum, 1999). The forest is mainly dominated by dense small and medium sized trees with the lowest canopy of forest floor densely covered with saplings, herbs, ferns, climbers and palms. The forest is also characterized by its emergent, canopy and thick lower canopies, and the dominant tree species of this tropical rainforest are Dipterocarpaceae (Nurul-Shida et al., 2014).

3.1.4. Data

Airborne LiDAR scanner (ALS), Terrestrial Laser Scanner (TLS) and field-based forest parameter datasets were used for this study. The TLS and field-based parameter measurements were collected from September 30, 2016 to October 15, 2016. The ALS data provided by University Putra Malaysia (UPM) was acquired on July 23, 2013. The ALS data was used to derive a Canopy Height Model (CHM) which was used to acquire upper canopy trees height. The TLS data was used to acquire 3D point clouds of the trees for DBH of upper and lower canopy trees, and height measurement of lower canopy trees. Next to that tree height, DBH and crown diameter were measured in the field.

3.1.5. Field Instruments and Software

3.1.5.1. Field instruments

To design the sample plot and tree parameters measurement various field instruments were used. Details of field instruments used for this study are stated with their use in Table 3.1.

Table 3.1. Field instruments used for data collection

ID	Instrument	Purpose
1	RIEGL VZ-400	TLS for cloud points acquisition
2	Orthophoto image	Sampling design
3	Garmin GPSMAP 60CSx	Plot and tree location coordinate record
4	Leica DISTO D510	Tree height measurement
5	Suunto clinometer	Slope measurement and direction bearing
6	Diameter tape (3 m)	Tree DBH measurement
7	Measuring tape (30 m)	Plot layout
8	Densiometer	Canopy density measurement
9	iPad	Navigation
10	Plastic laminated paper with numbers,	Tree tagging and measurement
11	Datasheets	Field measurement recording

3.1.5.2. Software

Various software packages were used to process, extract, analyse and present ALS, TLS and field datasets. Details of the used software's are provided in Table 3.2.

Table 3.2. Software's used for the study

ID	Software	Purpose
1	ArcGIS 10.3.1	Data processing, Mapping, Visualization
2	LasTool	ALS data processing
3	RiSCAN PRO	TLS data processing
4	eCognition	Tree crown delineation
5	ENVI	ALS data processing and Image processing
6	ERDAS IMAGINE 2015	Image processing
7	SPSS	Statistical analysis
8	Microsoft excel	Data processing and analysis
9	Mendeley	Citation and reference writing
10	Microsoft Visio	Flowchart drawing
11	Microsoft word	Thesis writing
12	Microsoft power point	Presentation of thesis

3.2. Methods

The method used in this study consists of four (4) major parts (Figure 3.2).

1. ALS based upper canopy tree parameters and AGB assessment

The ALS point cloud data was used for extracting tree parameters of upper canopy emergent trees where crowns are detectable by airborne LIDAR. The point cloud data were rasterized and interpolated to produce Digital Terrain Model (DTM) and Digital Surface Model (DSM). Then Canopy Height Model (CHM) which represents absolute height of the trees was derived by subtracting DTM from DSM. To detect upper canopy trees crown, multi-resolution segmentation was done.

2. TLS based lower canopy tree parameters and AGB assessment

The TLS point cloud data was used to extract DBH of all trees, and height of the lower canopy trees which were not detected by ALS. The point cloud data acquired from multiple scan positions were registered and geo-referenced to create 3D of each trees. Then DBH and height of the trees were extracted manually using RISCAN PRO. DBH of the trees measured by TLS were validated using field based DBH measurement.

3. Traditional field based tree parameters and AGB Assessment

Field-based tree parameters measurement consists manual measurement of tree height, DBH, crown diameter, tree coordinate and canopy density. The height of upper and lower canopy trees were validated using ALS and TLS based tree height measurements, respectively.

4. Comparison of traditional field and remote sensing based AGB assessment methods.

The final part of the study was comparing AGB estimated from modern remote sensing (ALS and TLS) and traditional field based derived tree parameters. AGB derived from remote sensing represented the summation of AGB of upper canopy and lower canopies tree derived from ALS and TLS, respectively.

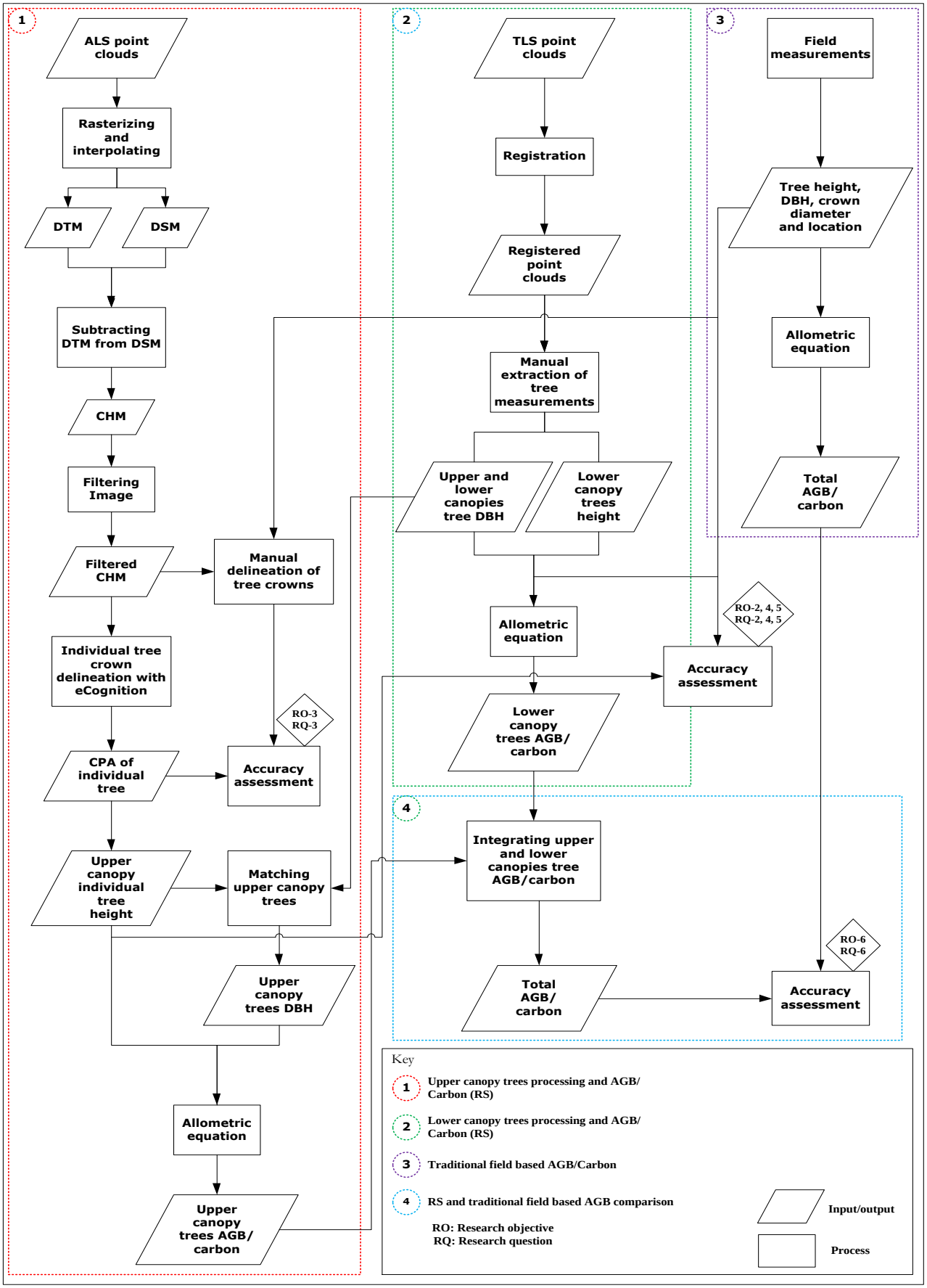

Figure 3.2. Flowchart of the study

3.2.1. Controlled Field Experiment

Prior to the actual fieldwork for this study, field experiment was conducted to investigate accuracy and error in height measurements between TLS and handheld laser instruments (Leica DISTO 510, TruPulse and Forestry Laser Rangefinder). The assessments were done in two ways (Figure 3.3)

1. ITC building windowsill's height measurements accuracy assessment with TLS and handheld laser instruments as compared to the actual height (see Figure 5.1).
2. Tree heights were measured with a Leica DISTO 510 at various distances in different stand conditions and different observers (see Figure 5.2).

The first assessment was used to assess and compare TLS and handheld laser instruments height measurement variation. Seven (7) observers were involved in measurement of ITC windowsills using handheld laser instruments. Besides, the building was scanned using TLS and the height of the windowsills was extracted from the scans. The accuracy of TLS and handheld laser instruments were validated using the actual height measured with a tape of the windowsills. Since the windowsills were at different heights and distances from the measuring point, the effect of distance on the accuracy could be also assessed.

The second part of the experiment was conducted to simulate various forest stands and assess the effect of distance to the tree, and the investigator dependant effect, if a Leica DISTO D510 handheld laser instrument is used. Seven (7) observers were involved in height measurements for 10 selected solitary and more complex stands of trees. The height of each tree was measured at 4 different measurement stand distances (5, 10, 20 and 30 m) to illustrate measurement variation along increasing distance from the tree and different observers.

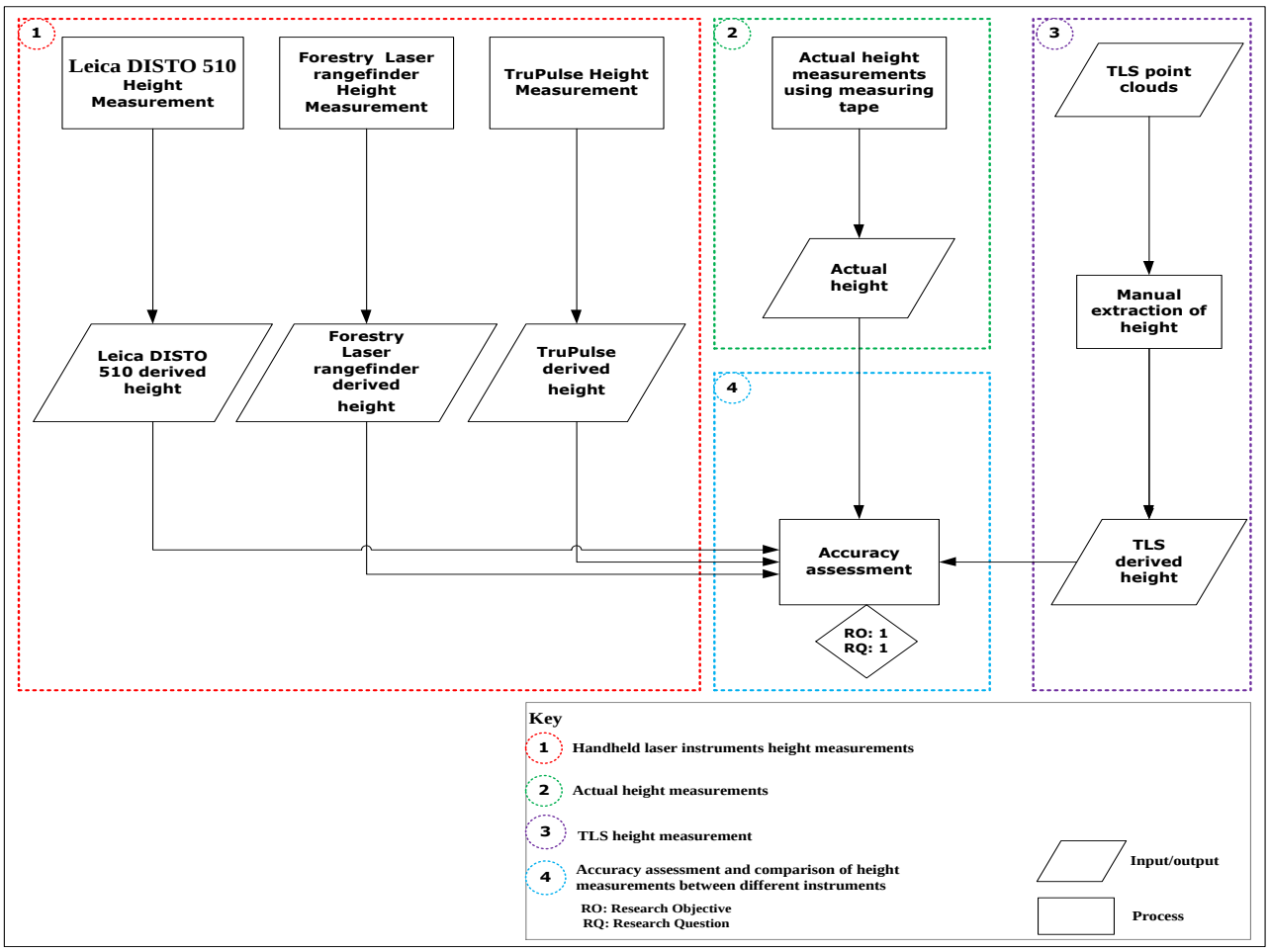

Figure 3.3. Flowchart of controlled field experiment for height accuracy assessment of different instruments

3.2.2. Fieldwork

Sampling design, identification of relevant data needed for the study, preparing data recording sheet, and testing and practicing with the instruments were done prior to the actual fieldwork.

3.2.3. Sampling Design and Plot Size

Considering terrain orientations and impenetrability of the forest in the field work area, a purposive sampling approach was used, aiming at covering the variation in forest structure types. Furthermore, the actual samples were selected based on slope steepness and distance to the road where it was possible to carry TLS equipment.

A total of 27 circular plots were selected; with a size of 500 m^2. A circular plot is relatively easy to set, and suitable for TLS multiple scan positions. This method also makes the tree measurement parameters more accurately captured since a circle minimizes the number of trees standing on the edge (Maniatis & Mollicone, 2010). In slopping areas, a slope correction factor was also applied to maintain an area of 500m^2 when vertically projected.

3.3. Data collection

3.3.1. Biometric Data Collection

Field work for biometric data collection was done in September and October 2016. The center of each circular plot of 500 m^2 (12.62 m radius), was assigned for field tree height and DBH measurements. Trees with DBH of < 10 cm were excluded based on their biomass contribution (Brown, 2002). DBH measurement was measured with diameter tape at 1.3 m from the ground, and tree height was also recorded with Leica DISTO D510. Next to that crown diameter of the dominant upper canopy trees, and canopy density were measured using measuring tape and a Densiometer, respectively.

3.3.2. Terrestrial Laser Scanner Data and Acquisition

For this study RIEGL VZ-400 was used and this scanner records multiple return up to four per emitted pulse (Table 3.3; Figure 3.4). The instrument can give measurement up to 600 m with wavelength of near infrared 1550 nm. The camera mounted on this scanner enabled to acquire images in RGB. The point cloud data from multiple scan was used to obtain 3D structure of the trees. Individual tree height of the lower canopy, and DBH of both upper and lower canopy trees were then extracted from the TLS point cloud data.

Figure 3.4. RIEGL VZ-400 Terrestrial laser scanning
Source: (Riegl, 2016)

Table 3.3. Specification of RIEGL VZ-400 Terrestrial laser scanner

Specification of RIEGL VZ-400 Terrestrial laser scanning	
Maximum range (m)	Up to 600
Minimum range (m)	1.5
Precision (mm)	3
Accuracy (mm)	5
Beam divergence (mrad)	0.35
Footprint size at 100m (mm)	30
Measurement (pulse) rate (kHz)	44 - 122
Line scan angle range (degree)	100
Laser wavelength	Near infrared (1550nm)
Weight (kg)	9.6

3.3.3. TLS Plot Layout and Scanning Positions

After identifying suitable sample area the plot was cleared from the undergrowth and palm trees and if necessary the plot radius was corrected for the slope.

Two approaches of scanning can be used; single and multiple scan (Bienert et al., 2006) (Figure 2.5). Single scan method uses only one position scan in the center of the plot and records only one side of the trees. In this study the multiple scan method with 4 scanning positions was applied (Figure 3.5). This scanning approach improves canopy height observation and enhance 3D representation of the trees (Srinivasan et al., 2015).

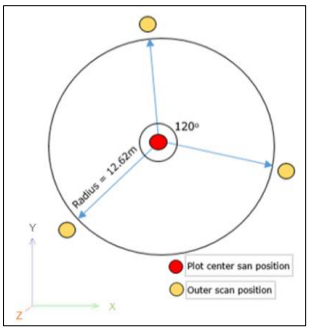

Figure 3.5. Terrestrial laser scanning positions applied in the field

3.3.3.1. TLS Scanning Process

After the plot was cleared, trees inside the plot with DBH ≥ 10 cm were labelled with A4 laminated numbers. The tree labels were placed on the stem of the tree facing to the direction of the center position (Figure 3.6). The labels were used to identify the trees on the scan and finding the corresponding tree on the ALS-CHM.

After labelling, 12 cylindrical and 4 circular retro-reflectors were placed in the plot for registration and georeferencing of the outer scan positions with the central scan position (Bienert et al., 2006). Cylindrical retro-reflectors were placed at near the outer scan positions. Circular retro-reflectors were placed in a way that were observable by center scan position and at least one of them was visible from each of outer scan position. Thus, it was insured that minimum of 5 retro-reflectors (4 cylindrical and 1circular retro-reflectors) were visible as tie point for registration and georeferencing. Figure 3.6 shows two types of retro-reflectors used for TLS.

Figure 3.6. Cylindrical retro-reflectors (with yellow color), circular retro-reflectors (with red color) and tree label numbers (Plot 13)

After mounting and levelling of the TLS scanner and camera on the tripod, the instrument records scanner own coordinate system (SOCS). Every position in the plot was scanned with Panorama 60 resolutions accompanied 13 overlapping digital camera images used to color the TLS point clouds. Figure 3.7 shows 2D view of the scanned plot

Figure 3.7. 2D view of scanned plot in true color (Sample plot 12)

3.4. Data Processing

3.4.1. Biometric Data

For each tree within a plot the biometric data (tree height, DBH, crown diameter and crown density) together with the coordinates and scientific species name were entered in Microsoft Excel sheet for the calculation of the traditional field-based AGB of the trees. A total of 786 trees in 27 plots were recorded. The coordinates of the individual trees were recorded with a handheld Garmin GPS which is later used for matching with the CPA of the corresponding tree on the Airborne LiDAR-CHM.

3.4.2. Terrestrial Laser Scanner Point Cloud Data

3.4.2.1. Registration of Multiple Scan Positions

Registration is the transformation of local systems into common reference system (Bienert & Mass, 2009). The points from the four scan positions were registered into common reference system using RISCAN PRO allowing the construction of a 3D point cloud. Marker based registration method using retro-reflectors was used to match the outer scan positions to the central scan (Theiler, 2015). This method matches common tie points (retro-reflectors) with the corresponding retro-reflectors on the central scan automatically. Thus, the 3 outer scan positions were matched to the central reference scan. To form 3D view of the plots with low standard deviation, multi-station adjustment (MSA) was then applied. Figure 3.8 shows the final registered 3D point cloud of the plot used for tree extraction and parameters measurement. The MSA accuracies were high for 27 plots obtained with standard deviation of < 0.03 m for most of plots (Table 3.4).

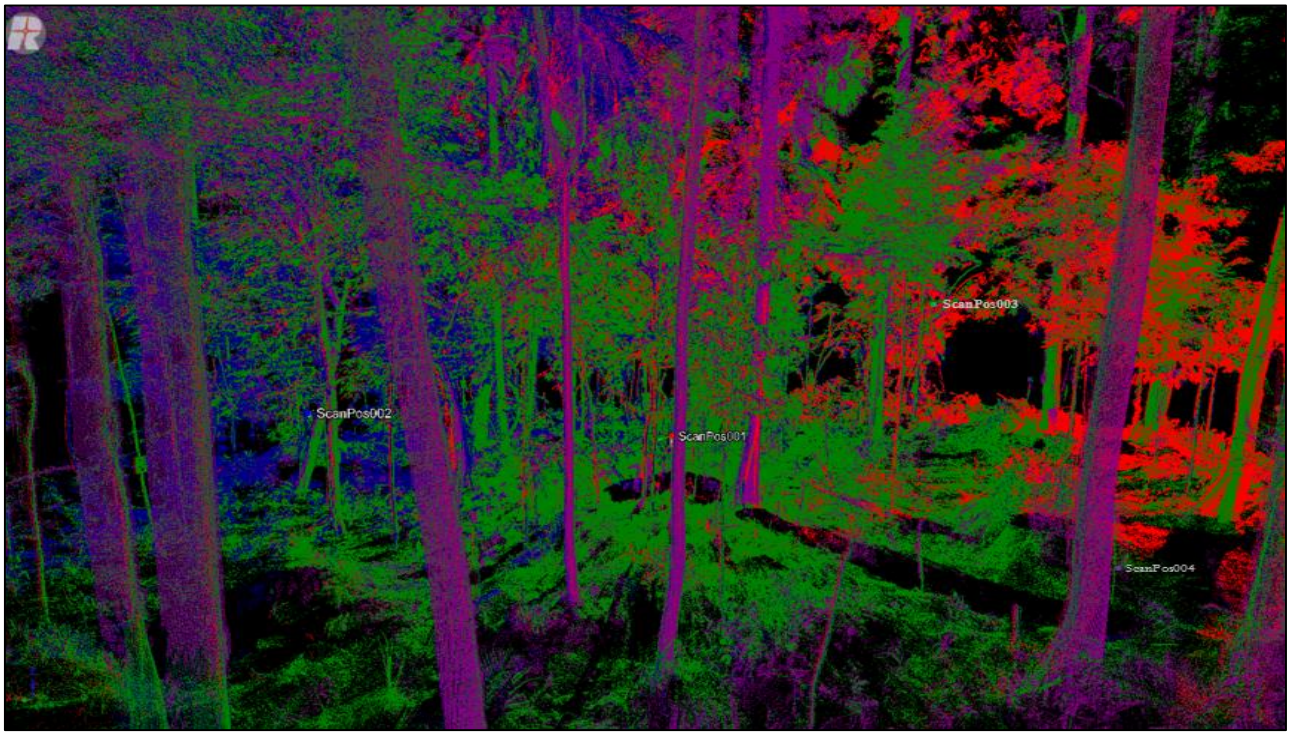

Figure 3.8. Registered point cloud data from multiple scan positions (Sample plot 15)

Table 3.4. Registration errors

Plot No.	1	2	3	4	5	6	7	8	9
Standard deviation (m)	0.0185	0.0229	0.0242	0.0221	0.0283	0.0253	0.0386	0.0233	0.0231
Plot No.	10	11	12	13	14	15	16	17	18
Standard deviation (m)	0.0198	0.029	0.021	0.025	0.022	0.021	0.023	0.026	0.0201
Plot No.	19	20	21	22	23	24	25	26	27
Standard deviation (m)	0.0248	0.0217	0.0244	0.028	0.024	0.026	0.021	0.024	0.022

3.4.2.2. Plot and Individual Trees Extraction

After registration of each plot scan positions, the point cloud of each plot was filtered to arrive at a 3D point cloud which exactly covers the circular area of the plot, viz. 500 m^2. Filtering method was done in RISCAN PRO by manually selecting the outer boundary using the position of the outer scan positions and excluding everything which does not fall within the outer boundary. Then, the extracted point cloud were saved to new Polydata object which was used as area of interest for parameter extraction. The Polydata was displayed in 3D true color linear scale to be able to identify the tags with tree numbers. The newly created Polydata of the plot was used to extract individual trees for height and DBH measurements. Individual trees were then selected from newly created Polydata point cloud using RISCAN PRO. Figure 3.9 shows extracted sample tree.

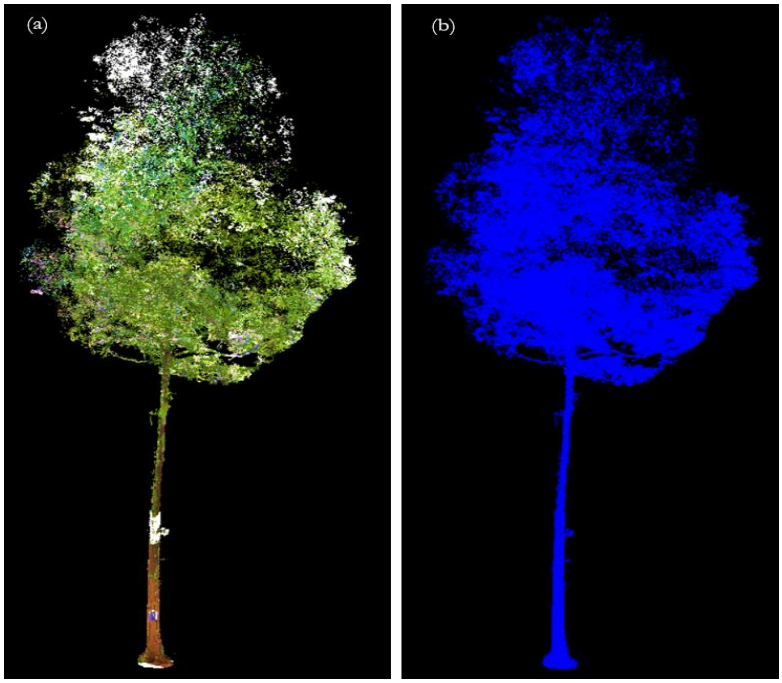

Figure 3.9. Extracted sample tree
Plot 15; Tree 39: (a)-True color, (b)-False color)

3.4.2.3. Measurement of Tree Parameters of DBH and Height

From the 3D point clouds of the individual trees the DBH was measured on the stem at 1.3 m height from the ground, using the distance measurement function tool in RISCAN PRO. Figure 3.10 shows measurement of DBH in RISCAN PRO.

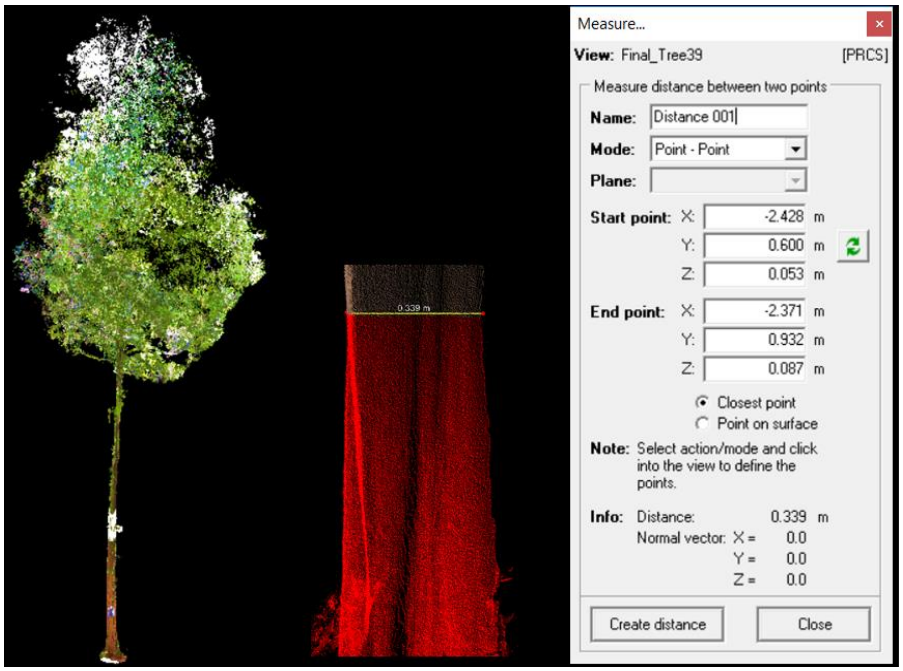

Figure 3.10. Tree DBH measurement (Plot 15, Tree 39)

Similarly also the height of individual trees was measured manually with distance measurement function tool in RISCAN PRO (Figure 3.11). The measurement records X, Y, Z values, and the difference of lowest and highest Z value was considered as the height of the tree. Manual measurement method provides high accuracy since the

most top and bottom of the identified manually by removing occlusions. This method has proven for its accuracy by (Prasad, 2015; Lawas, 2016; Sadadi, 2016).

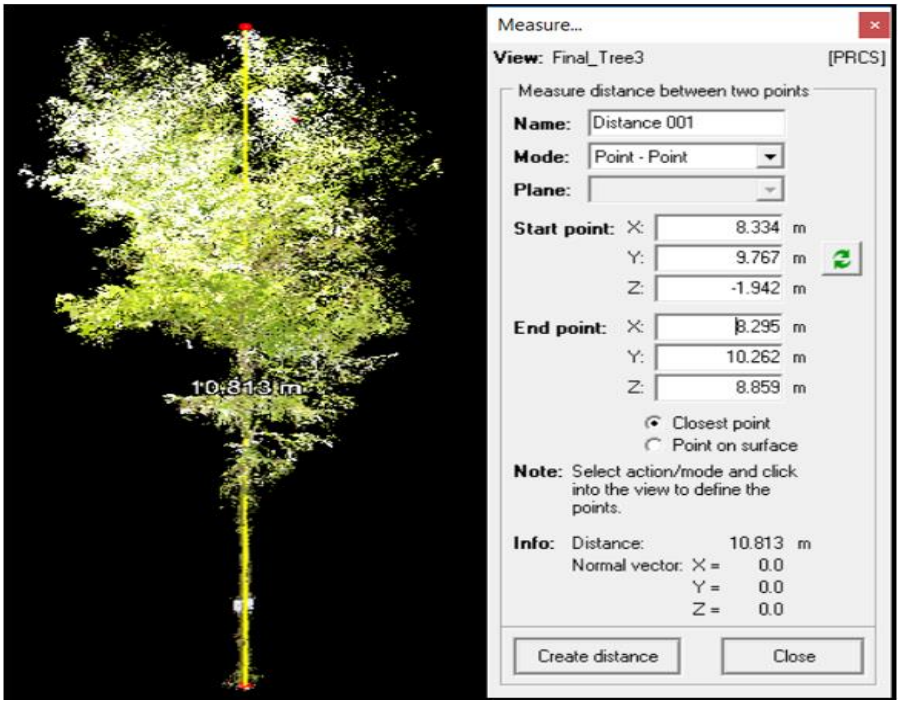

Figure 3.11. Tree height measurement (Plot 12, Tree 3)

3.4.3. Airborne LiDAR Scanner Point Cloud Data

The ALS point cloud density was 5-6 points/m². It was acquired by LiteMapper 5600 waveform-digitizing LiDAR system for terrain and vegetation mapping (IGI, 2016). The specification of the LiDAR system used for this study is provided below in Table 3.5.

Table 3.5. LiteMapper 5600 airborne system specification

Sensor feature	Description
Pulse rate	Range between 70 kHz and 240 kHz
Scan angle	60°
Scan pattern	Regular
Beam divergence	0.5 mrad
Line/sec	Max. 160
A/c ground speed	90 kts
Target reflectivity	20 – 60% (vegetation 30%, cliff 60%)
Flying height	700 – 1000 m
Laser points/m²	5 to 6 points with 808 m to 1155 m swath width
Spot diameter (laser)	0.35 – 0.50 m
Max (above ground level)	1040 m

Source: IGI (2016)

3.4.3.1. Airborne LiDAR Scanner Data Processing

From the ALS data a pit or hole free canopy height model (CHM) was constructed with a cell size of 1m, in "las" format. The cell size was determined by the point density (5 points/m²) of the original data (Sadadi, 2016). LasTool software has different algorithms to process the ALS Las file data. Lasview and Lasinfo were used to display and extract information of the point cloud data. Lasground and Lasheight algorithm were used to generate Digital Terrain Model (DTM) and Digital Surface Model

(DSM). The original CHM was contained pits and holes occurred from sub-layers which is mainly branches below the top of the trees. Thus, the pits were removed through CHM free algorithm (Khosravipour et al., 2014). Appendix 4 shows 3D view of ALS DSM, DTM and CHM.

3.4.3.2. Segmentation of ALS CHM

Segmentation is a technique of spatial clustering in which an image is subdivided into non-overlapping objects or segments (Moller et al., 2007). The method identifies relatively homogeneous areas, and grouping them into specific objects.

There are different methods of image segmentation approach, but multi-resolution image segmentation is the most recommended approach (Witharana & Civco, 2014). This method follows bottom-up algorithm where pixels are merged into real world large objects until no more adjacent pixels comply the algorithm setting (Definiens, 2009).

In region growing algorithm, setting different criteria are necessary to form the required "homogeneous" groups of pixels. The homogeneity criteria is based mainly on scale parameter, shape and compactness (Carleer et al., 2005). Determination of the best fitting scale parameters is a process of trial-and-error, until optimum scale parameter achieved (Yildiz et al., 2006; Kavzoglu & Yildiz, 2014). For this study, multi-resolution segmentation approach of Object Based Image Analysis (OBIA) was implemented. The segmentation was done in three phases: Segmentation, classification and accuracy assessment.

Setting appropriate algorithm parameters is required for multi-resolution segmentation. Scale parameter is used to determine the object size (Benz et al., 2004). It defines the maximum acceptable heterogeneity of the image object. Smaller scale parameter produces more homogenous objects. Weighing layers, setting shape and compactness are also important parameters considered in multi-resolution segmentation. Weighing layers for different bands is parameter routine used to give weight values for different layers. For instance, for plant identification giving more weight for infrared region band is good as plants has high reflectance in this region (Baral, 2011). Shape criterion are used to define the spectral value of the image layers affecting the heterogeneity of the segmented objects. Increasing the value makes the segment image objects have more meaningful spatial uniformity than spectral information. Additionally, the compactness value used to create compact segments (Definiens, 2009). Figure 3.12 shows process of multi-resolution segmentation.

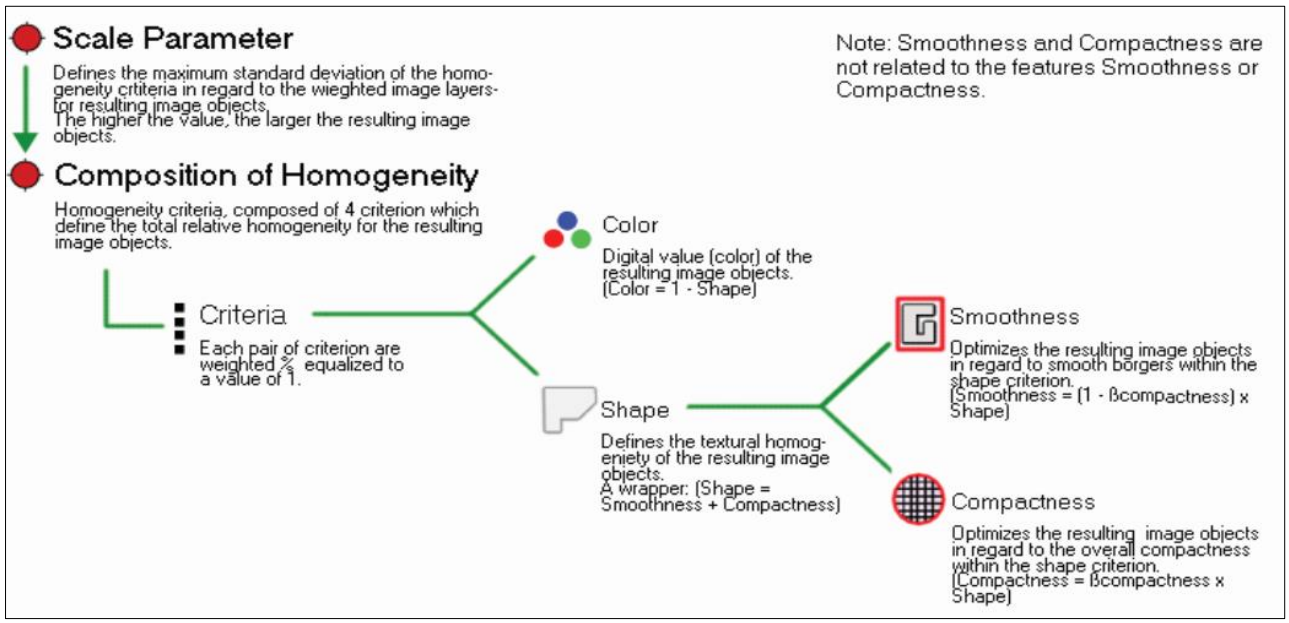

Figure 3.12. Multi-resolution segmentation process

3.4.3.3. Segmentation and Its Accuracy Assessment

Airborne LiDAR CHM segmentation was executed to delineate individual tree crown which used for individual tree and canopy delineation. Through segmentation, the minimum height of the trees detected by ALS was identified. In a subset, a number of parameters were set in eCognition for multi-resolution segmentation; rule set of scale parameter, shape, compactness, watershed transformation and tree morphology were applied. This rule set then was applied to the whole study area.

Accuracy assessment was conducted to recognize the number of trees identified by Airborne LiDAR for tree matching; assuming each image segment was a single tree as stated by Yao et al. (2014). Manual delineation was done on Airborne LiDAR CHM based on visually identified trees and crown diameter of reference trees recorded in the field. A number of computations were executed in order to assess the accuracy of segmentation (Equation 3.1 – 3.3).

Equation 3.1. Calculation of over segmentation

$$\textbf{Over segmentation} = 1 - \frac{Area(xi \cap yi)}{Area\ (xi)} \quad \ldots\ldots\ldots\ldots \textbf{eq. 3.1}$$

Equation 3.2. Calculation of under segmentation

$$\textbf{Under segmentation} = 1 - \frac{Area(xi \cap yi)}{Area\ (yi)} \quad \ldots\ldots\ldots\ldots \textbf{eq. 3.2}$$

Equation 3.3. Calculation of segmentation goodness

$$\mathbf{D} = \sqrt{(Over\ Segmentation_{ij}^2 + Lower\ segmentation_{ij}^2)/2} \quad \ldots\ldots\ldots\ldots \textbf{eq. 3.3}$$

Where;
xi: Manually delineated reference crowns
yi: Segments form automatic segmentation
D: Segmentation goodness

Segmentation goodness (D) result shows error ocured in authomatic segmentation. Zhan et al. (2005) also indicated segmented polygone considered to be 1:1 matched if it is overlaped with the reference polygone by at least 50%, and matching considers position, shape and size, completeness and correctness of an object. Figure 3.13 shows different example of one to one matching.

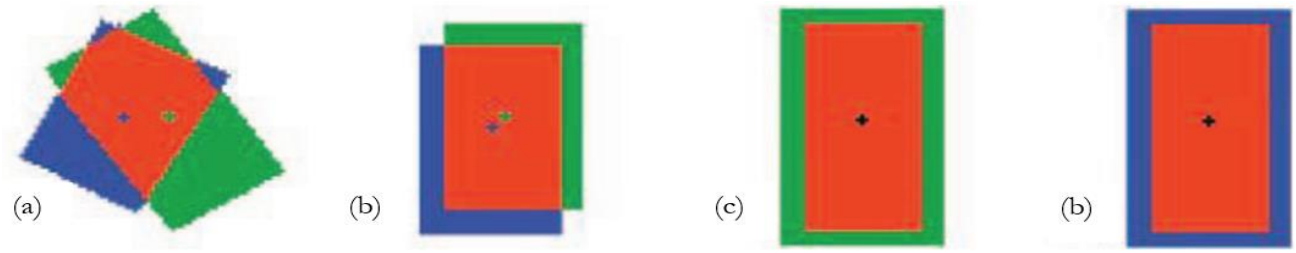

Figure 3.13. One to one matching in different conditions
Source: Zhan et al. (2005)
(a)->50% matched between reference and segmented object, (b)-The same size and shape of object but difference in location matched each other, (c) and (d)-Reference and segmented objects matched each other at same positional context but different in spatial extent.

3.4.4. Canopy Separation and Height Extraction

Accurate measurment of forest parameters of all trees was challenging in tropical forest due to natural complexity character of the forests. Thus, it is dificult to cupture all trees parameter with single independent remote sensing technology. Studies confirmed that in forests with multiple canopy layers, tree parameter extraction using ALS is effective in detecting upper canopy trees (Jung et al., 2011; Lawas, 2016). On the other hand, TLS-based height measurement in tropical forest is again challenging since multiple canopy, tall trees and dense interlocking crowns makes it difficult for the instrument to view the top canopy trees (Strahler et al., 2008).

In this study, two remote sensing technologies (ALS and TLS) were used for AGB estimation and the forest was separated in to two canopies; viz. upper and lower canopy. For upper canopy trees, the ALS-CHM was used to extract tree height while the TLS was used to measure DBH of upper and lower canopy trees, and height of lower canopy trees.

To separate upper and lower canopy, ALS-CHM segmented image was used. First, segmentation accuracy was assessed to establish appropriateness for tree crown identification. Then, the local maxima height value of each segment in the CHM was extracted for each plot to determine the minimum height of the complete tree crown that can be detected by airborne LiDAR. This minimum height was set as the lower boundary of the upper canopy. The trees with below the threshold was considered as lower canopy and tree parameters for those trees were extracted using TLS.

3.4.5. Tree Detection and Matching

Field recorded trees were matched with corresponding trees detected by the TLS. Based on the height threshold trees that were visible by ALS were classified as upper canopy trees. The upper canopy trees were matched with the segmented airborne LiDAR CHM, based on field GPS coordinates, and location of trees in TLS scan positions.

3.4.6. Above-ground Biomass and Carbon Estimation

Allometric equation can be used for AGB estimation, but in areas with a diverse species composition the use of species specific allometric equations is not feasible (Gibbs et al., 2007). Since the study area is a forest with mixed high diversity species, AGB was estimated based on generic allometric equation for tropical forest developed by Chave et al. (2014) (Equation 3.4). Field and TLS DBH, height derived from field, TLS and ALS, and wood density of each tree species was used as input parameters.

Equation 3.4. Allometric equation for AGB estimation

$$AGB = 0.0673 * (\rho D^2 H)^{0.976} \quad \text{eq. 3.4}$$

Where,
ABG-Above-ground biomass (kg); D-Diameter at breast height (DBH) (cm); H-height (m); and ρ-wood density (g/cm^3); Reyes et al. (1992) of wood density for tropical forest tree species.

Carbon content of the trees were also derived from AGB of the trees. Carbon amount is approximately 50% of the dry biomass of the tree (Dixon et al., 1994; Nizami et al., 2009). IPCC (2006) guideline for carbon stock estimation was used (Equation 3.5).

Equation 3.5. AGB carbon estimation

$$C = AGB \times CF \quad \text{eq. 3.5}$$

Where,
C-carbon stock (Mg); ABG-Above-ground biomass (Mg); CF-conversion factor which is 0.47 of AGB.

3.4.7. Data Analysis

The performance of ALS and TLS tree detection in tropical forest were performed based on comparison with number of trees recorded in the field. The performance was measured based the capability of the instruments in providing highly accurate tree height. Thus, it was assumed that ALS provided higher canopy trees height accurately while TLS was efficient and accurate for lower canopy trees height measurement (Equation 3.6 and 3.7).

Equation 3.6. Performance ALS tree detection

$$\textbf{ALS tree detection (Upper canopies) (\%)} = \frac{\textbf{No. of trees detected by ALS}}{\textbf{No. of field observed trees}} \textbf{ x 100} \ldots\ldots\ldots\ldots\ldots\ldots\ldots\ldots\ldots\ldots\ldots\ldots \textbf{eq. 3.6}$$

Equation 3.7. Performance TLS tree detection

$$\textbf{TLS tree detection (Lower canopies) (\%)} = \frac{\textbf{No. of trees detected by TLS}}{\textbf{No. of field observed trees}} \textbf{ x 100} \ldots\ldots\ldots\ldots\ldots\ldots\ldots\ldots\ldots\ldots\ldots\ldots \textbf{eq. 3.7}$$

Statistical analysis were used to assess the relationship between different tree parameters and AGB. Regression analysis for tree height, DBH and AGB derived from field and remote sensing methods were done for accuracy assessments and model validations. The coefficient of determination (R^2) and Pearson correlation (r) were used for accuracy assessment.

The relationship between field and remote sensing derived variables of DBH, height and AGB were also evaluated for measurement and estimation deviations based on calculated Root Mean Square Error (RMSE), RMSE (%) and bias (Equation 3.8 – 3.10).

Equation 3.8. RMSE calculation formula

$$\textbf{RMSE} = \sqrt{\frac{\sum_{i=1}^{n}(y_i - \hat{y})^2}{n}} \ldots\ldots\ldots\ldots\ldots\ldots\ldots\ldots\ldots\ldots\ldots\ldots\ldots\ldots\ldots\ldots\ldots\ldots\ldots\ldots\ldots\ldots\ldots\ldots\ldots\ldots \textbf{eq. 3.8}$$

Equation 3.9. RMSE percentage

$$\textbf{RMSE (\%)} = \frac{\textbf{RMSE}}{\left(\frac{\sum_{i=1}^{n}(y_i)}{n}\right)} \textbf{x100} \ldots\ldots\ldots\ldots\ldots\ldots\ldots\ldots\ldots\ldots\ldots\ldots\ldots\ldots\ldots\ldots\ldots\ldots\ldots\ldots\ldots\ldots\ldots\ldots\ldots\ldots \textbf{eq. 3.9}$$

Equation 3.10. Bias

$$\textbf{Bias} = \frac{\sum_{i=1}^{n}(y_i - \hat{y})}{n} \ldots\ldots\ldots\ldots\ldots\ldots\ldots\ldots\ldots\ldots\ldots\ldots\ldots\ldots\ldots\ldots\ldots\ldots\ldots\ldots\ldots\ldots\ldots\ldots\ldots\ldots \textbf{eq. 3.10}$$

Where;
RMSE-Root Mean Square Error; yi-Measured value of dependant variable; ŷ-Predicted value of dependant variable; n- Number of observations.

To observe the significance difference among measurement means, t-Test and one-way single factor-ANOVA were also done.

4. RESULTS

4.1. Controled Field Experiment for Height Measurment Instruments

Before going to the field a controlled experiment was execute to assess the accuracy and observer dependant measurement variation of the TLS and handheld laser instruments was executed (see section 3.2.1). Measurement records are shown in Appendix 1 and 2.

4.1.1. TLS and Handheld Laser Instruments Height Measurement Accuracy Assessment

Twelve (12) ITC windowsills at various heights and distances to the observer were measured with measuring tape, the TLS and handheld laser instruments, viz. Leica DISTO 510, Forestry Laser Rangefinder, and TruPulse (see Figure 5.1) to assess measurement error due to instrument used, distances and observers. TLS height measurement was found to be almost one-to-one relationship between the actual heights of the windowsills (Figure 4.1a). The measurement error recorded was a cm error in which calculated Root Mean Square Error (RMSE) was 0.053 m. Height measurements were not influenced by the distance from the TLS.

Handheld laser instruments height measurement were also examined on the same windowsills'. Seven (7) observers measured the heights of windowsills using three different instruments: Leica DISTO 510, Forestry laser rangefinder, and TruPulse. From handheld laser instruments used a RMSE of 0.602, 0.734 and 0.848 m were found for Leica DISTO D510, TruPulse and Forestry Rangefinder, respectively. The measurement with the Leica DISTO D510 was the most accurate. The accuracy of the handheld instruments was lower in comparison to the TLS and the deviation of the handheld instruments from the height measured with a tape increased with increasing distance from the observer (Figure 4.1b, c and d).The ANOVA test result showed there was no significance difference in measurements between different observers. Details of the ANOVA test is shown in Appendix 3.

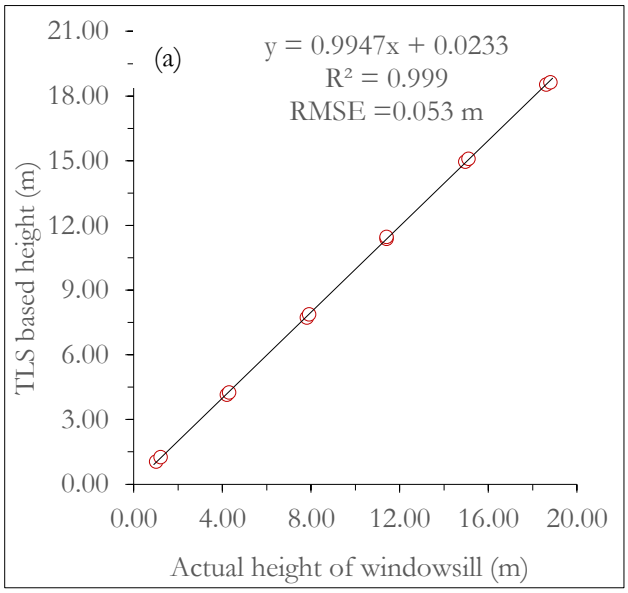

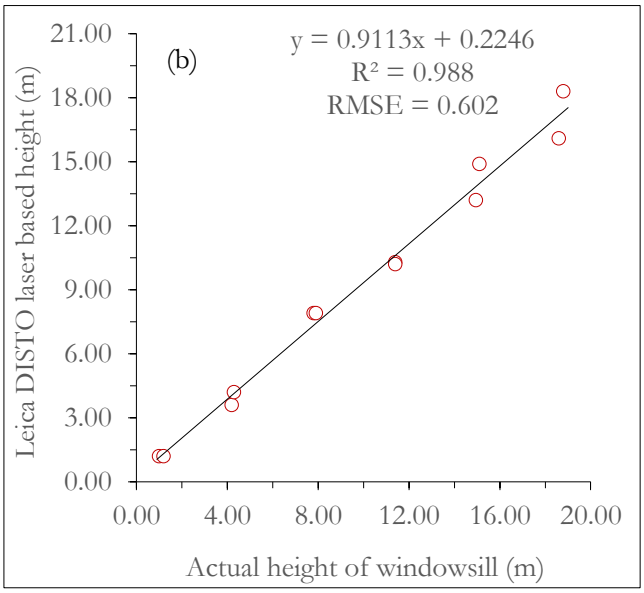

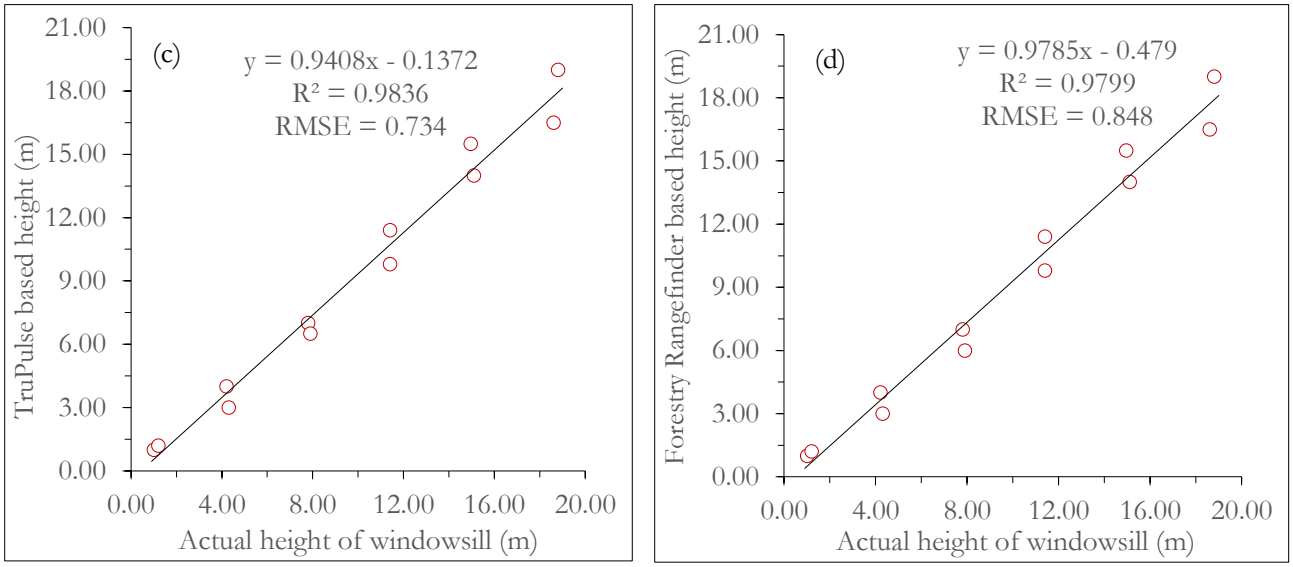

Figure 4.1. Scatter plot showing height measurements of windowsills
(a)-TLS measurement, (b)-Leica DISTO D510 measurement, (c)-TruPulse measurement, (d)-Forestry laser rangefinder measurement

4.1.2. Leica DISTO D510 Tree Height Measurements Variation Assessment

To illustrate measurement variability as a result of different observers and different stand conditions, seven (7) observers measured the height of ten (10) trees (solitary trees and trees in a more complex cluster of trees). Each tree was measured at 5, 10, 20 and 30 m distances. Resulting in a total of 280 observations.

Unlike the windowsills, the statistical analysis showed that there was significant difference in height measurements of the trees among different observers (Table 4.1). The height measurements were also significantly different at different measurement distances (Table 4.2).

Table 4.1. One way single factor ANOVA height measurement variation among different observers

Summary of single Factor ANOVA

Groups	Count	Sum	Average	Variance
Observer [1] (m)	40	371	9.275	16.91423077
Observer [2] (m)	40	551.67	13.79175	35.07482506
Observer [3] (m)	40	526.6	13.165	34.99771795
Observer [4] (m)	40	583.9	14.5975	43.39050641
Observer [5] (m)	40	486.4	12.16	35.18451282
Observer [6] (m)	40	484.9	12.1225	28.52230128
Observer [7] (m)	40	573.7	14.3425	38.95737821

ANOVA

Source of Variation	*SS*	*df*	*MS*	*F*	*P-value*	*F crit*
Between Groups	800.732083	6	133.455347	4.00867459	0.0007266	2.13186613
Within Groups	9088.61742	273	33.2916389			
Total	9889.34951	279				

Table 4.2. One way single factor ANOVA height measurement variation at different stand distances

Summary of single Factor ANOVA

Groups	Count	Sum	Average	Variance
At 5 m distance (m)	70	667.3	9.532857143	22.1622381
At 10 m distance (m)	70	924.87	13.21242857	37.10107373
At 20 m distance (m)	70	978.8	13.98285714	28.38086128
At 30 m distance (m)	70	1079.8	15.42571429	28.90628571

ANOVA

Source of Variation	*SS*	*df*	*MS*	*F*	*P-value*	*F crit*
Between Groups	1323.726981	3	441.242327	15.1433922	3.7618E-09	2.63731086
Within Groups	8041.981659	276	29.1376147			
Total	9365.70864	279				

The mean height of each tree measured by different observers is presented in Figure 4.2. This figure shows that there were considerable differences in mean height of individual tree among different observers; sometimes more than 10 m.

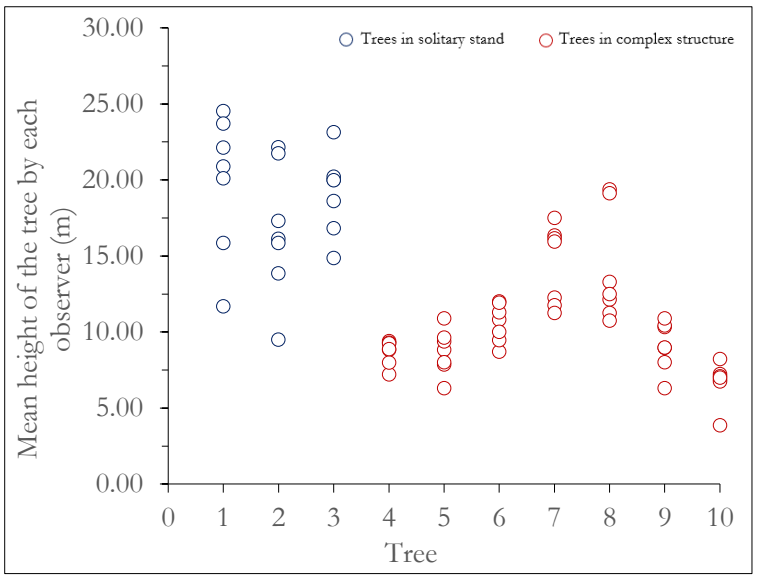

Figure 4.2. Mean height of each tree among observers at different stand distances

The standard deviation in mean height of the trees among observers and different distances from the tree is presented in Figure 4.3. The standard deviation for mean height of individual tree among observers decreased with increasing distance from the tree.

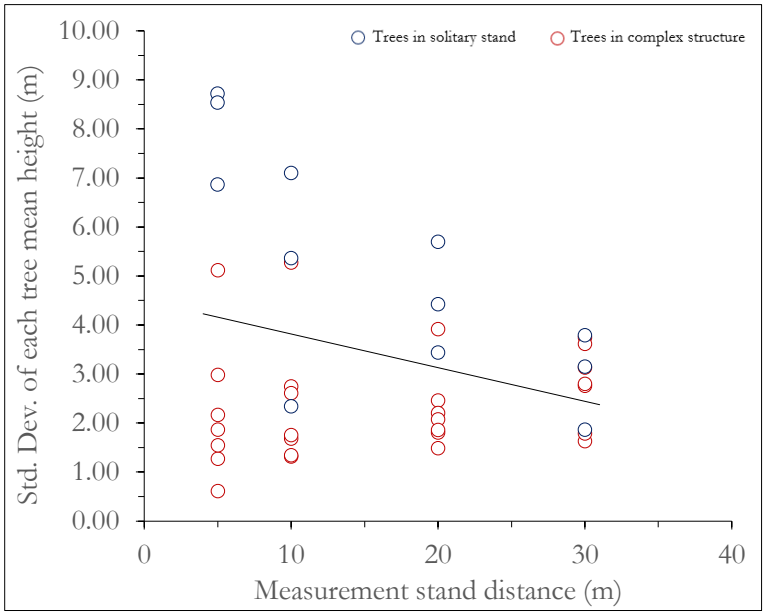

Figure 4.3. Standard deviation for the mean height of trees at different stand distances

4.2. Field Biometric Data of the Study

A total of 786 trees (163 different species) were recorded in the field. Diameter at breast height (DBH), height, top canopies crown diameter, and canopy density were recorded and entered into Microsoft Excel sheet. Based on the labels and location of each tree, field-measured trees were detected and matched with corresponding trees in the Terrestrial laser scanner (TLS) and Airborne LiDAR scanner (ALS) data. The measurements of tree parameters were checked for normality. The height measurements were normally distributed while DBH data showed positively skewness (Appendix 5)

4.2.1. DBH Measurements and Accuracy Assessment

Of 786 total trees recorded in the field, 735 (93.5%) trees were identified by the TLS and were used for DBH accuracy assessment. DBH was extracted from registered 3D point cloud TLS data (Figure 3.10).

Appendix 6 shows descriptive statistics of DBH for each sample plot. The extracted DBH from a 3D point cloud of TLS data was validated for its accuracy using field measured DBH. Table 4.3 shows a summary of matched trees used for analysis.

Table 4.3. Over all descriptive statistics of field and TLS DBH (cm)

Descriptive statistics	Field DBH (cm)	TLS DBH (cm)
Mean	19.98	19.93
Standard Deviation	10.8377	11.0640
Minimum	10.00	9.00
Maximum	84.00	83.60
Count	735	735

Accuracy assessment of TLS-based DBH showed that coefficient of determination (R^2) between the two variables was very high in which the model explained 98.9% of the independent variable measured with diameter tape (Figure 4.4).

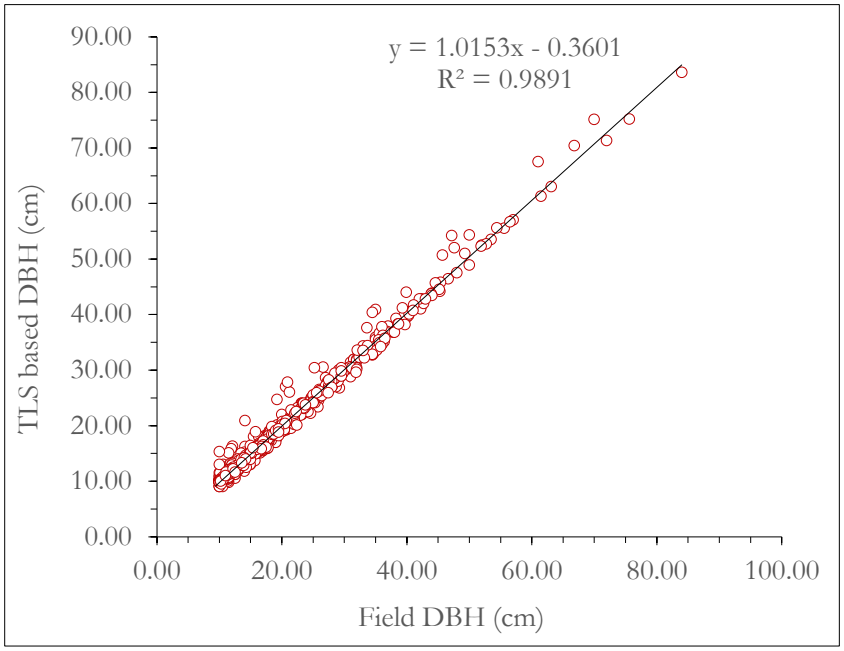

Figure 4.4. Scatter plot showing relationship between field and TLS DBH measurement

The RMSE of the model was found to be 1.30 cm (6.52%). The TLS method showed a small underestimation of DBH measurements with the measurement bias indicated in Table 4.4. Details of a linear regression statistics are found in Appendix 7.

Table 4.4. Relationship between field and TLS DBH (cm)

Tree parameter	No. of Observations	R^2	r	RMSE (cm)	RMSE (%)	Bias (cm)
DBH	735	0.989	0.994	1.30	6.52	– 0.52

As of the Pearson correlation coefficient (r) between field and TLS based DBH was very strong (Table 4.4), the t-Test statistics between field and TLS based DBH also showed there was no statistically significant difference between field and TLS DBH measurements (Table 4.5).

Table 4.5. t-Test between field and TLS based DBH (cm)

	Field DBH (cm)	TLS DBH (cm)
Mean	19.98129252	19.92680272
Variance	117.4566148	122.4123733
Observations	735	735
Pooled Variance	119.934494	
Hypothesized Mean Difference	0	
df	1468	
t Stat	0.09538318	
P(T<=t) one-tail	0.462011747	
t Critical one-tail	1.645892276	
P(T<=t) two-tail	0.924023493	
t Critical two-tail	1.961581284	

4.2.2. Tree Height Measurements and Accuracy Assessments

The height of the trees were derived from field measurements, Airborne LiDAR Canopy Height Model (CHM) (upper canopies) and TLS (lower canopies). The ALS-CHM was used to separate upper canopy trees from lower canopy. The provided pit free CHM was derived by subtracting Digital Terrain Model (DTM) from Digital Surface Model (DSM). The pit free CHM is displayed in 2D and 3D view (Figure 4.5a and b).

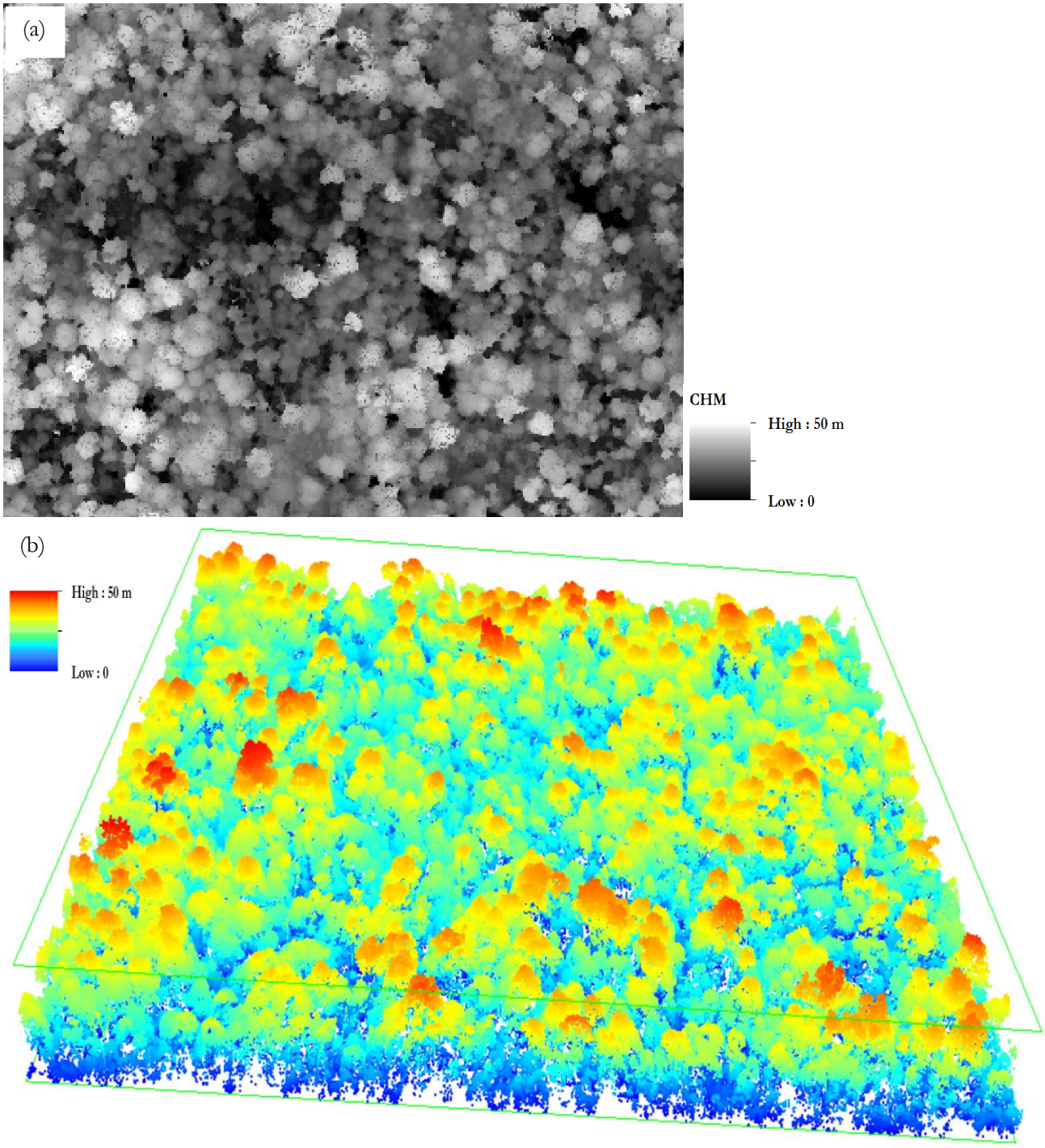

Figure 4.5. Airborne LiDAR point cloud CHM
(a)-2D view in ArcGIS, (b)-3D view in LAStools

4.2.2.1. Tree Crown Delineation using Airborne LiDAR CHM

Segmentation of the pit free ALS-CHM was done to identify individual tree crowns and separation of the higher canopies from the lower canopies. Appropriate values for parameters like scale, shape and compactness were established for segmentation in eCognition. Scale parameter 10, shape 0.7 and compactness of 0.5 were found to be reasonable accurate rule set for segmentation. The eCognition multi-resolution segmentation result is shown in Figure 4.6.

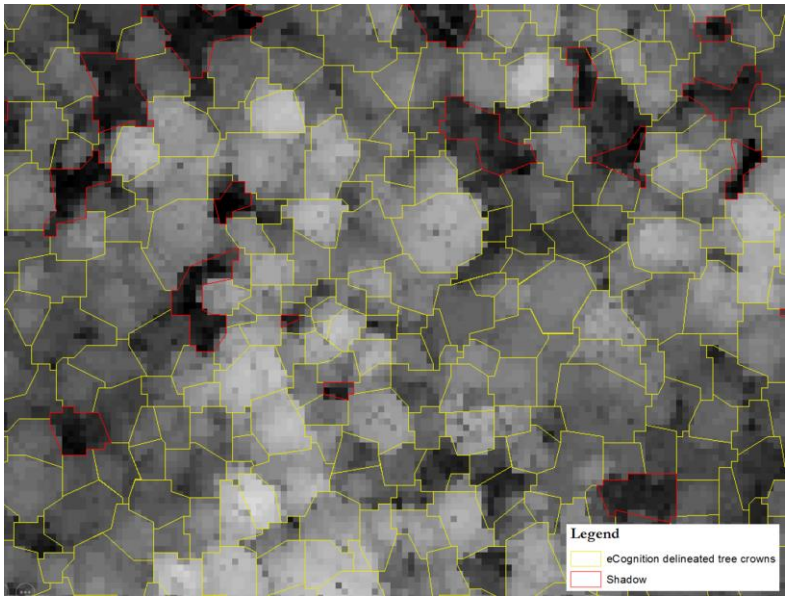

Figure 4.6. Individual tree crown delineation result with Multi-resolution segmentation

4.2.2.2. Segmentation Accuracy

The accuracy of segmentation was assessed by comparing with manual delineated crown polygons. Clearly visible crowns for which crown diameter measured in the field were digitized manually on screen in ArcMap. Manually digitized polygons were then compared with the automatically generated polygons of CHM image as shown in Figure 4.7.

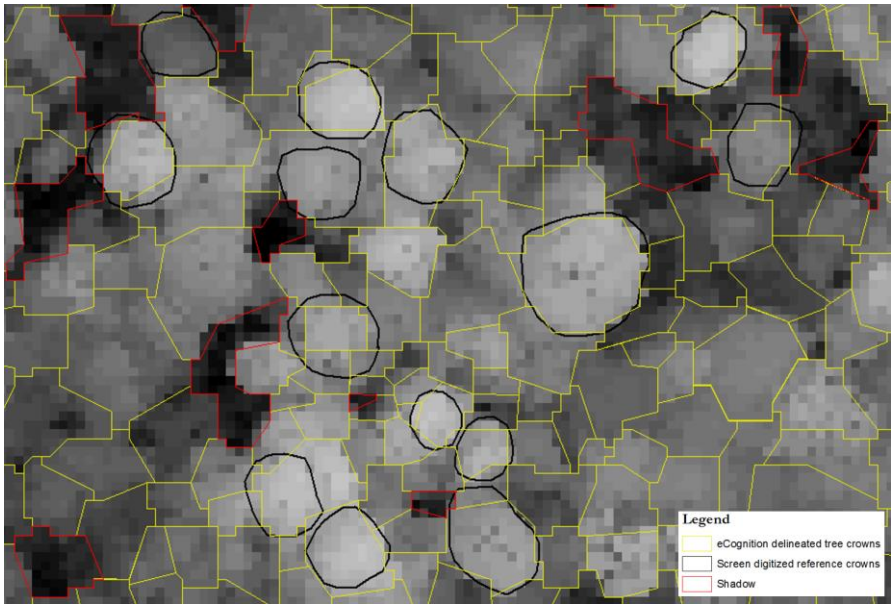

Figure 4.7. Sample showing comparison of manually and eCognition delineated tree crowns

The automatically segmented polygons were compared with manually delineated reference crowns and over and under segmentation was assessed. Accuracy assessment was done based on assesing segmentation goodness (D) as shown in Table 4.6. The segmentation error was 27%, and hence Airbone LiDAR-CHM of the study was accurate by 73% to delinate tree crowns in segmentation, while using 1:1 manual mateching of polygones resulted with 78% accuracy.

Table 4.6. Segmentation accuracy assessment result

	Total reference polygons	Total 1:1 matched polygons	Over Segmentation	Under Segmentation	Goodness of fit (D)
	132	103	0.24	0.30	0.27
Accuracy (%)		78			73

4.2.2.3. Canopy Separation and Tree Height Extraction

The segmentation result showed that the ALS-CHM had reasonable accuracy when it comes to identifying and mapping of Crown Projection Areas (CPA) of individual tree. The highest point in the ALS-CHM segment (the local maximum) was attributed to the corresponding tree in all plots.

Two approaches were used to set canopy separation threshold. One for plots with multiple and one for single upper canopy layers (Appendix 13). Multiple canopy layers were plots with many top emergent, medium and under canopy trees. For these plots, the minimum height of trees where the complete crown was visible on the ALS-CHM was 12 m. Thus, 12 m was used as threshold for the upper canopy. The remaining trees with height of ≤ 12 m were considered as lower canopy trees. On the other hand, single layer plots were higher top canopy trees have more or less the same height, a threshold of 8 m was applied to separate upper and lower canopy due to the fact that trees with height of > 8 m were identifiable on the ALS-CHM. Figure 4.8 shows the process of assessment of sample plots for separating upper and lower canopies from segmented CPA of Airborne LIDAR-CHM.

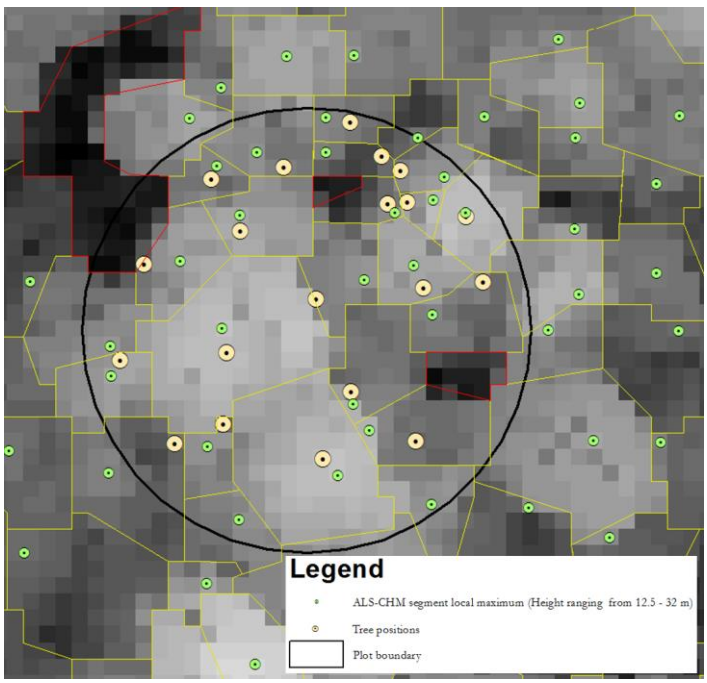

Figure 4.8. Method of setting threshold for canopy separation (sample plot 7)
(The green color shows the local maxima of segmented CPA while the yellow color is the field GPS location of the trees. The local maxima of CHM was considered for the corresponding field recorded trees).

4.2.3. Upper Canopy Trees Height Accuracy Assessment

Based on the threshold, trees height with > 12 and > 8 m with multiple and single upper canopy layers, respectively were detected by Airborne LiDAR. Of 786 trees, 486 (61.83%) trees were classified as upper canopy trees based on the height threshold. The descriptive statistics for field and ALS based trees of all sample plots were done as shown in Table 4.7.

Table 4.7. Summary of descriptive statistics of upper canopy field and ALS based height

		Field Height (m)				ALS Height (m)			
Plot	No. of trees	Mean	Std. Dev.	Min.	Max.	Mean	Std. Dev.	Min.	Max.
1	27	13.93	3.95	8.10	24.00	13.65	2.95	8.29	17.89
2	13	18.79	7.08	11.50	33.00	17.56	5.87	12.00	31.72
3	16	21.00	7.10	10.50	34.00	18.34	3.44	12.33	28.67
4	14	23.45	9.17	11.50	36.03	21.00	2.76	15.94	27.19
5	16	19.11	4.77	12.70	31.60	21.26	3.17	17.34	30.84
6	10	17.96	5.44	8.80	25.60	19.70	3.95	12.30	24.67
7	20	19.29	6.11	11.30	33.20	23.27	5.09	12.51	31.86
8	17	15.78	4.61	7.90	29.40	16.66	2.52	12.94	20.56
9	11	18.81	6.43	10.24	28.70	19.31	5.40	12.21	27.42
10	14	20.11	4.65	12.12	29.20	19.79	4.08	12.10	27.00
11	10	13.48	4.58	8.60	24.20	16.13	4.30	12.35	23.53
12	11	19.67	6.72	10.50	32.80	19.27	5.37	12.23	28.94
13	23	14.82	3.86	10.40	23.00	15.19	3.28	12.26	22.92
14	19	15.09	3.57	10.60	22.40	16.41	3.48	12.29	22.88
15	20	17.98	7.81	9.50	37.80	18.88	4.66	12.61	30.00
16	14	15.35	6.43	8.10	32.00	17.42	4.99	13.00	30.91
17	18	17.35	4.40	10.80	27.70	18.27	4.06	12.14	28.30
18	18	17.16	5.89	10.30	29.80	18.37	7.30	12.69	40.34
19	22	15.35	3.46	10.00	25.40	17.81	1.73	15.04	20.97
20	22	15.06	4.88	8.40	30.10	20.86	2.36	16.64	26.00
21	26	15.11	4.26	8.50	26.20	19.14	2.03	14.76	23.31
22	24	15.68	5.70	7.20	37.80	18.25	5.15	12.21	34.84
23	17	14.35	4.67	8.40	30.30	19.86	3.76	12.36	25.19
24	14	25.26	4.70	7.90	22.50	19.53	3.11	13.91	23.77
25	17	15.70	5.08	10.40	26.20	19.76	3.98	13.56	25.00
26	23	11.17	2.10	8.30	15.40	13.25	3.21	8.40	20.21
27	30	11.59	3.19	8.20	25.40	13.55	3.11	8.88	19.83

Of all upper canopy trees, 451 trees could be matched with corresponding trees in the field. Table 4.8 shows a descriptive summary of matched trees used for analysis.

Table 4.8. Over all descriptive statistics for trees identified as upper canopies (m)

Descriptive parameters	ALS height (m)	Field height (m)
Mean	18.04	16.09
Standard Deviation	4.529	5.190
Minimum	8.29	7.20
Maximum	40.34	37.80
Count	451	451

Field height was validated using ALS based height. Relationship between the two variables showed that field-based height explained 60.96% of the independent variable of ALS measured height (Figure 4.9). Summary of the linear regression model statistics is shown in Appendix 8.

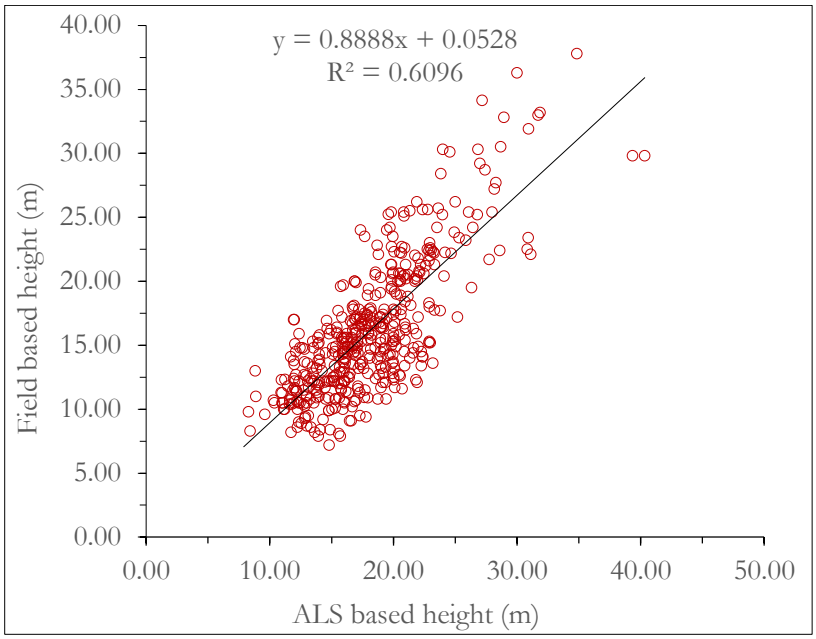

Figure 4.9. Scatter plot between field and ALS based height

Field based height was found to be underestimated the height of the tree by the calculated mean bias indicated in Table 4.9, and RMSE was 3.24 m (20.18%).

Table 4.9. Relationship between field and ALS based upper canopy trees height (m)

Tree parameter	No. of Observations	R^2	r	RMSE (m)	RMSE (%)	Bias (m)
Upper canopy trees height	451	0.61	0.78	3.24	20.18	– 1.20

The t-Test statistics between field derived and ALS height measurement showed that there was significant difference between the two methods (Table 4.10).

Table 4.10. t-Test for ALS and field based upper canopy trees height (m)

	ALS Height (m)	Field Height (m)
Mean	18.026711	16.075099
Variance	20.851891	27.02174
Observations	451	451
Pooled Variance	23.936816	
Hypothesized Mean Difference	0	
df	900	
t Stat	5.990092046	
P(T<=t) one-tail	1.51465E-09	
t Critical one-tail	1.646548458	
P(T<=t) two-tail	3.0293E-09	
t Critical two-tail	1.96260333	

4.2.4. Lower Canopy Trees Height Accuracy Assessment

Trees not detected by ALS were considered as lower canopy trees, and height was extracted using TLS (Figure 3.11). Of all trees recorded in the field, 300 (38.17%) trees were considered as lower canopy trees for TLS height measurement. The descriptive statistics of field and TLS based height are shown in Table 4.11.

Table 4.11. Summary of descriptive statistics of lower canopy field and TLS based heights

		Field Height (m)				TLS Height (m)			
Plot	No. of trees	Mean	Std. Dev.	Min.	Max.	Mean	Std. Dev.	Min.	Max.
1	3	6.77	0.28	6.48	7.03	6.46	0.61	5.79	8.00
2	13	9.38	2.80	5.00	14.00	9.42	2.15	5.10	11.90
3	14	11.42	5.12	7.00	15.70	9.23	1.76	6.45	12.00
4	14	13.24	5.05	7.50	16.70	9.50	1.70	6.09	11.91
5	15	13.44	3.06	10.10	16.30	10.67	0.91	9.26	12.00
6	10	11.34	2.92	6.97	16.50	10.12	1.38	8.09	12.00
7	6	10.58	3.55	6.40	13.00	9.15	2.52	6.08	12.00
8	10	11.51	3.40	6.20	17.80	10.00	1.60	8.09	11.94
9	16	11.18	2.26	7.29	14.57	9.96	1.35	6.78	11.72
10	13	10.69	2.81	6.00	14.40	9.80	1.78	6.94	12.00
11	13	8.44	2.06	5.90	12.70	8.73	2.02	5.20	12.00
12	12	11.47	3.83	6.40	16.90	10.37	1.60	7.30	11.90
13	8	11.22	1.20	8.80	12.80	10.20	1.10	8.60	11.70
14	13	9.00	1.62	7.00	12.30	8.58	1.65	6.70	12.00
15	3	9.03	3.26	5.60	12.10	8.83	2.70	5.80	11.00
16	15	8.95	2.97	5.00	17.00	8.90	1.45	6.00	12.00
17	9	10.73	2.34	6.70	14.20	10.94	1.47	7.30	12.00
18	10	10.99	2.76	7.90	16.00	10.60	1.55	8.10	12.00
19	7	10.02	3.32	6.20	14.50	9.84	2.45	6.00	12.00
20	11	9.11	1.88	5.70	12.20	9.63	1.90	6.00	12.00
21	9	9.10	2.82	5.50	15.90	8.69	2.16	5.80	12.00
22	9	10.77	2.42	7.80	14.70	10.30	1.65	7.10	11.90
23	12	9.10	2.63	6.40	14.90	9.60	1.80	7.20	12.00
24	14	9.74	2.23	6.80	15.20	9.70	1.60	7.10	12.00
25	10	8.94	1.10	7.20	10.60	9.16	1.00	6.90	11.40
26	10	7.00	0.98	5.30	8.00	7.80	0.86	5.30	8.00
27	15	7.56	0.67	6.20	8.80	7.50	0.55	6.00	8.00

A total of 290 trees were detected and matched with field identified trees for validation. Field based height was validated using TLS measured height. Table 4.12 shows a summary of descriptive statistics used for accuracy assessment.

Table 4.12. Over all descriptive statistics for trees identified as lower canopies (m)

Descriptive parameters	TLS height (m)	Field height (m)
Mean	9.42	9.83
Standard Deviation	1.775366	2.65310
Sample Variance	3.151924	7.03898
Minimum	5.1	5
Maximum	12	17
Count	290	290

The R^2 showed that the field based height explained about 68.99 the independent TLS based measured tree height (Figure 4.10).

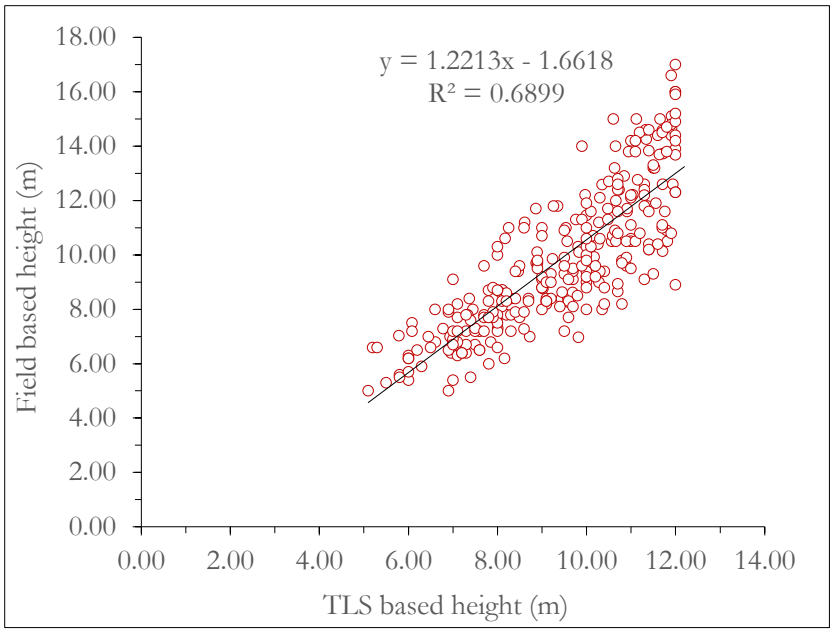

Figure 4.10. Scatter plot between lower canopy trees field and TLS based height

Height measurement assessment showed that field-based measurement overestimates the height of the lower canopy trees with the calculated bias shown in Table 4.13. The result indicated that field based height measurement had a higher correlation with TLS measurement as compared to upper canopy ALS measurements. Details of the regression statistics are found in Appendix 9.

Table 4.13. Relationship between field and TLS based lower canopy trees height (m)

Tree parameter	No. of Observations	R^2	r	RMSE (m)	RMSE (%)	Bias (m)
Lower canopy trees height	290	0.69	0.83	1.45	14.77	0.42

The t-Test statistics showed as there was statistically significant difference between field and TLS based height measurements (Table 4.14).

Table 4.14. t-Test for TLS and field based lower canopy trees height (m)

	TLS Height (m)	Field Height (m)
Mean	9.416724	9.838448276
Variance	3.161717	6.834787549
Observations	290	290
Pooled Variance	4.998252	
Hypothesized Mean Difference	0	
df	578	
t Stat	-2.27145	
P(T<=t) one-tail	0.011743	
t Critical one-tail	1.647494	
P(T<=t) two-tail	0.023486	
t Critical two-tail	1.964077	

4.3. Traditional Field and Remote Sensing based AGB Comparison

The AGB estimated from the field and modern remote sensing (ALS and TLS) based derived parameters were compared per plot. Total remote sensed based AGB was calculated by adding lower and upper canopies tree AGB derived from TLS and ALS, respectively. Table 4.15 shows the distribution of AGB within sample plots by different methods.

Table 4.15. Proportion of AGB estimated by remote sensing (RS) and traditional field based

	RS based AGB (Mg)		Field based AGB (Mg)		Combination of upper and lower canopies AGB (Mg)	
Statistics	Upper canopy trees (ALS)	Lower canopy trees (TLS)	Upper canopy trees	Lower canopy trees	RS method	Field method
Mean/Plot	8.445011	0.708560	7.408448	0.76778	9.1536	8.1762
Std. Dev.	3.271395	0.376738	2.989925	0.41520	3.3146	3.0655
Min.	3.431590	0.091633	3.283845	0.02466	3.9807	3.9390
Max.	17.89105	1.621062	15.56155	1.92615	18.2316	16.0022
Sum	228.0153	19.13112	200.0281	20.7302	247.146	220.758
Sample plots	27	27	27	27	27	27

Of a total of 247.15 Mg AGB calculated from remote sensing derived parameters, 228.02 Mg (92%) were accounted as upper canopy ALS based AGB, while 19.13 Mg (8%) was reserved in lower canopy TLS based AGB. Mean AGB of 8.44 and 0.71 Mg.plot^{-1} was estimated in upper and lower canopies tree, respectively (Table 4.15). Thus, 0.71 Mg.plot^{-1} of undetected AGB by ALS was captured through the complimentary use of TLS.

Based on traditional field-based parameters, a total of 218.33 Mg AGB was estimated with mean upper and lower canopies AGB of 7.41 Mg.plot^{-1} and 0.77 Mg.plot^{-1}, respectively (Table 4.15).

With remote sensing, 183.07 Mg.ha-1 of AGB was calculated. On the other hand, 163.52 Mg.ha^{-1} of AGB was estimated with traditional field-based method. Traditional field method was underestimated the AGB by 19, 547 Kg.ha^{-1} (19.547 Mg.ha^{-1}) which accounted 10.70% ha^{-1}. Thus, Traditional field-based estimated 89.3% of AGB.

Figure 4.11a and b shows the proportion of AGB estimated by remote sensing and traditional field methods AGB.

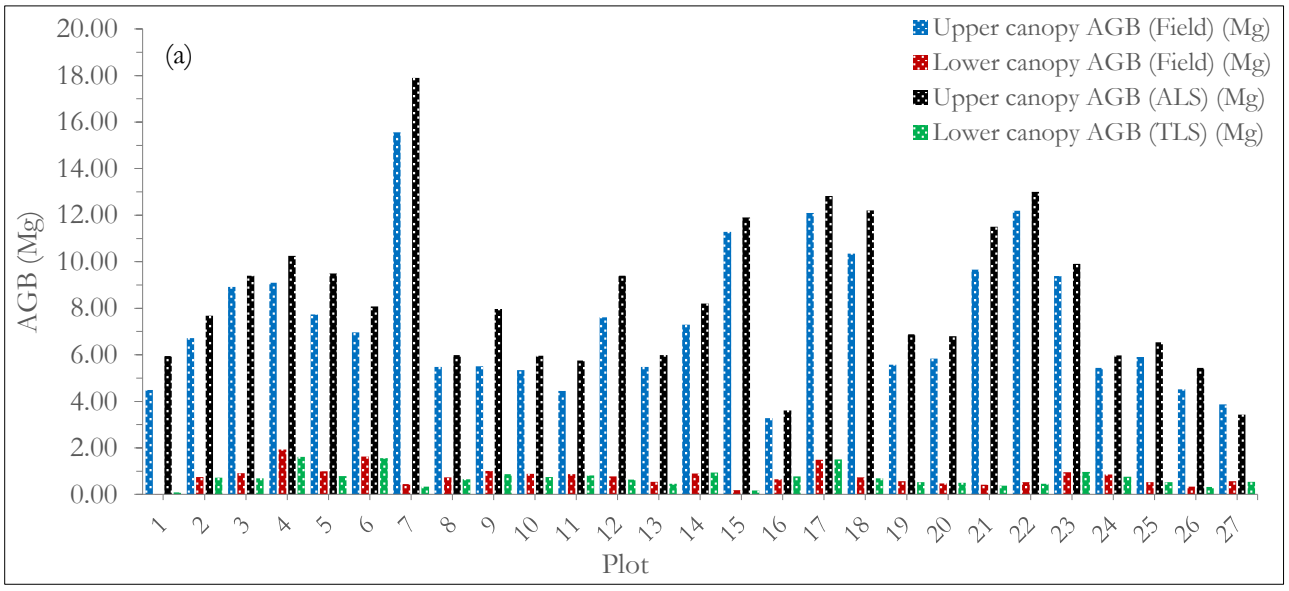

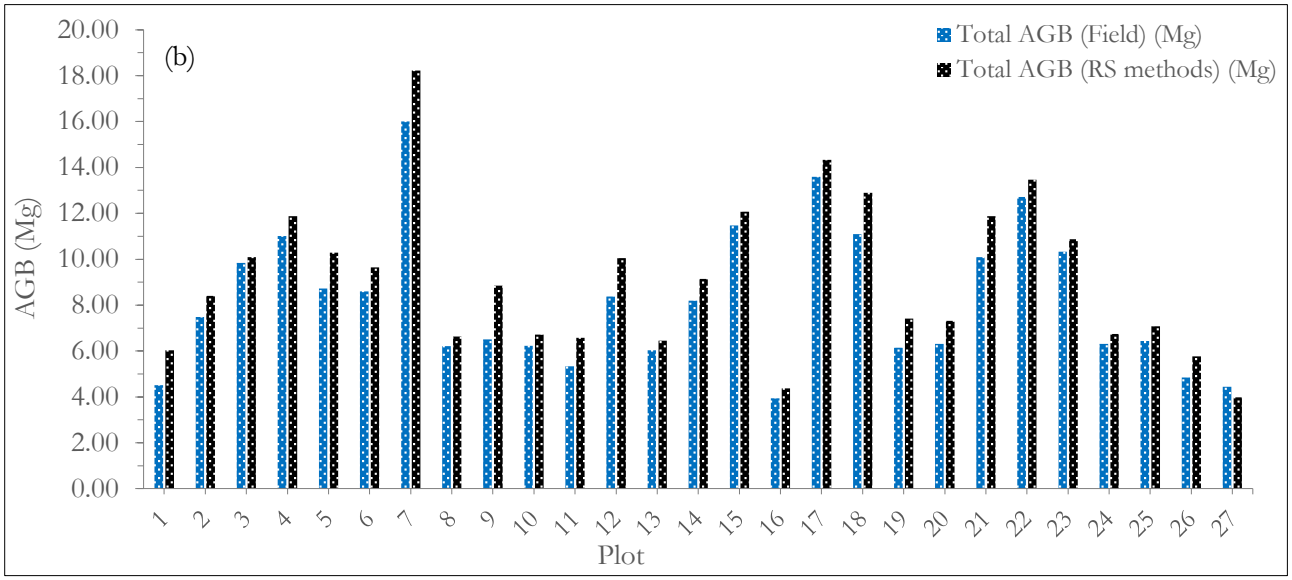

Figure 4.11. Estimated AGB per plot
(a)-AGB proportion based forest canopies; (b)-Traditional field and remote sensing methods total AGB

4.3.1. Accuracy Assessments of Above-ground Biomass

The effect field and remote sensing derived parameters on AGB estimations were recognized. First, the effect of using TLS DBH on remote sensing based AGB calculation was evaluated. The TLS derived DBH used for upper and lower canopies tree was highly accurate as shown in Figure 4.4 and Table 4.4. The error occurred in TLS extracted DBH was examined. By using common height of ALS, the effect of error of TLS-based DBH on calculated AGB was done. The result showed that TLS DBH had no significant effect in estimated AGB (Figure 4.12).

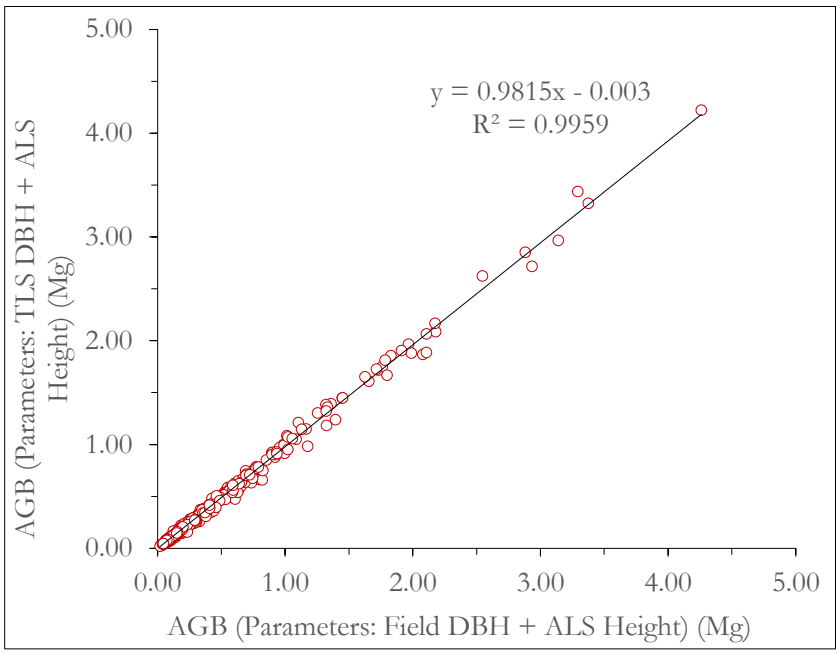

Figure 4.12. Effect of TLS extracted DBH on estimated AGB

Another comparison was done between on one hand the AGB estimated from modern remote sensing based on ALS and TLS height and TLS DBH and on the other hand the traditional AGB estimated from field DBH and

field height using Leica DISTO D510. The results is presented in Figure 4.13. The R^2 of 0.966 was achieved between the AGB with remote sensing technologies and traditional field methods.

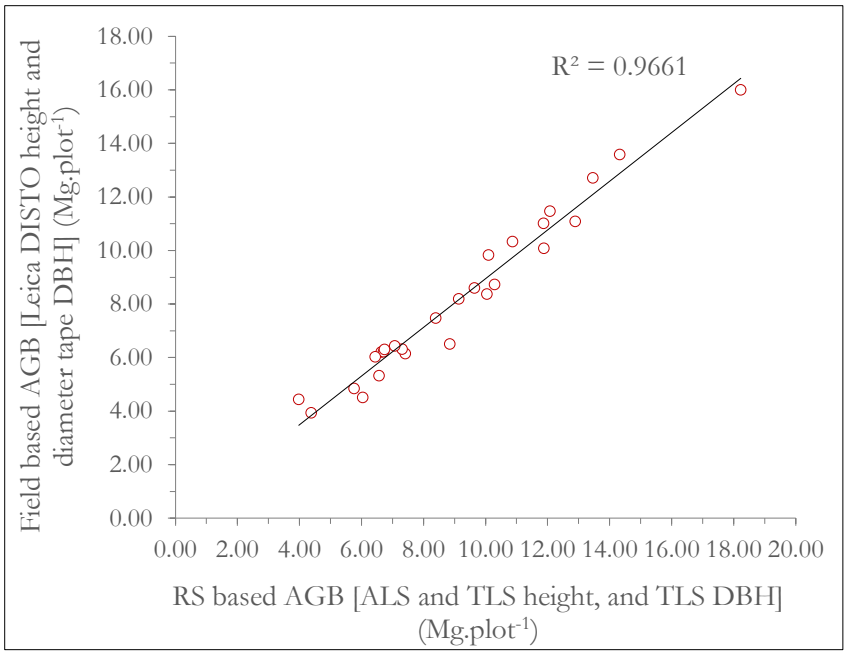

Figure 4.13. Scatter plot of field and remote sensing based AGB

RMSE of 0.62 Mg (7.64%) was found in which traditional field method underestimated the AGB with the bias of 0.2888 Mg (Table 4.16). Summary of the linear regression model statistics is found in Appendix 10.

Table 4.16. Relationship between field and Remote sensing method AGB (Mg)

Parameter	No. of Observations	R^2	r	RMSE (Mg)	RMSE (%)	Bias (Mg)
AGB	27	0.96	0.98	0.62	7.64	– 0.2888

The statistical t-test showed that there was no significant difference between plot AGB calculated with traditional field methods and remote sensing based methods (combination of ALS and TLS) (Table 4.17).

Table 4.17. t-Test for remote sensing (RS) and field based total AGB

	RS method AGB (Mg)	Traditional field based AGB (Mg)
Mean	9.153571	8.17623197
Variance	10.98716	9.397326303
Observations	27	27
Pooled Variance	10.19224	
Hypothesized Mean Difference	0	
df	52	
t Stat	1.124805	
P(T<=t) one-tail	0.132918	
t Critical one-tail	1.674689	
P(T<=t) two-tail	0.265837	
t Critical two-tail	2.006647	

4.3.2. Above-ground Biomass Carbon Stock Estimation

Above-ground biomass carbon (AGBC) was calculated based on IPCC (2016); 0.47 of AGB. The variation of AGBC derived with field and remote sensing method was compared (Table 4.18). A total amount of 116.159 and 103.756 Mg of AGBC were obtained with remote sensing and field method, respectively. The statistical t-test showed that there was no significant difference in AGBC per plot between RS and field based methods (Appendix 11).

Table 4.18. Proportion of AGBC estimated by remote sensing (RS) and traditional field based

Statistics	RS based AGBC (Mg)		Field based AGBC (Mg)		Combination of upper and lower canopies AGBC (Mg)	
	Upper canopy trees (ALS)	Lower canopy trees (TLS)	Upper canopy trees	Lower canopy trees	RS method	Field method
Mean/Plot	3.969155	0.333023	3.481971	0.360857	4.30219	3.84281
Std. Dev.	1.537556	0.177067	1.405265	0.195144	1.55786	1.44078
Min.	1.61285	0.043068	1.543407	0.011590	1.87093	1.85133
Max.	8.40879	0.761899	7.313928	0.905290	8.568852	7.52103
Sum	107.16719	8.991626	94.01321	9.74319	116.15860	103.75626
Sample plots	27	27	27	27	27	27

5. DISCUSSION

5.1. Source of Tree Height Measurements Errors in Controlled Field Experiment

This study shows that height measurements of windowsills using Terrestrial Laser Scanner (TLS) and handheld laser instruments are not significantly different from the results obtained with a measuring tape (Figure 4.1a, b, c and d), indicating height measurement errors in clearly visible objects are very low (Figure 5.1). However, the experiment also reveals that handheld laser instruments height measurement show increasing deviation from the true height with increasing distance between observer and object. This is because missing of the target due to hand movements increases with distance and height of the objects. On the contrary, TLS height measurements are not affected by distance and height of the windowsills, which means that the TLS provides highly accurate height measurements. Bienert et al. (2006), Lindberg et al. (2012) and Apostol et al. (2016) have also proved as TLS provides highly accurate height measurements up to a vertical field of view in less occluded areas.

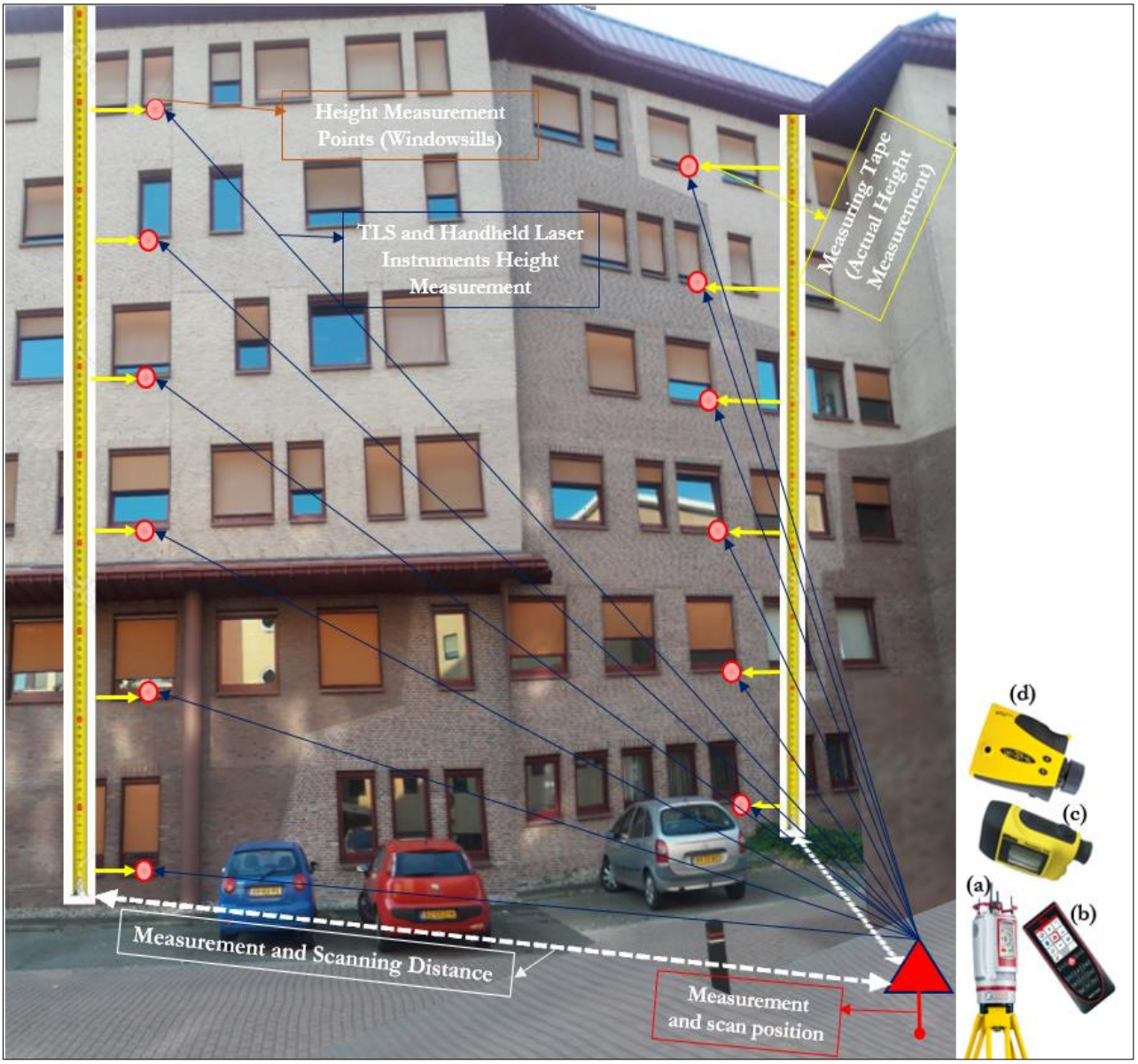

Figure 5.1. ITC windowsill's height measurements with different laser instruments
(a)-TLS, (b)-Leica DISTO D510, (c)-Forestry Laser Rangefinder, and (d)-TruPulse

On the other hand, tree height measurements with handheld laser instruments are sensitive to distance to the tree, complexity of the forest structure and the observer (Figure 4.3). Up to 10 m height differences have been recorded (Figure 4.2). Figure 5.2 and 5.3 illustrates the sources of errors in tree height measurements in the forest. For tree height measurements with handheld instruments it is pivotal to have a clear view of the top of the tree and a considerable distance from the tree (20 - 30 m). In reality, for a secondary tropical forest however it is challenging to get enough free space to comply with this requirement, due to occlusions of branches and forest density.

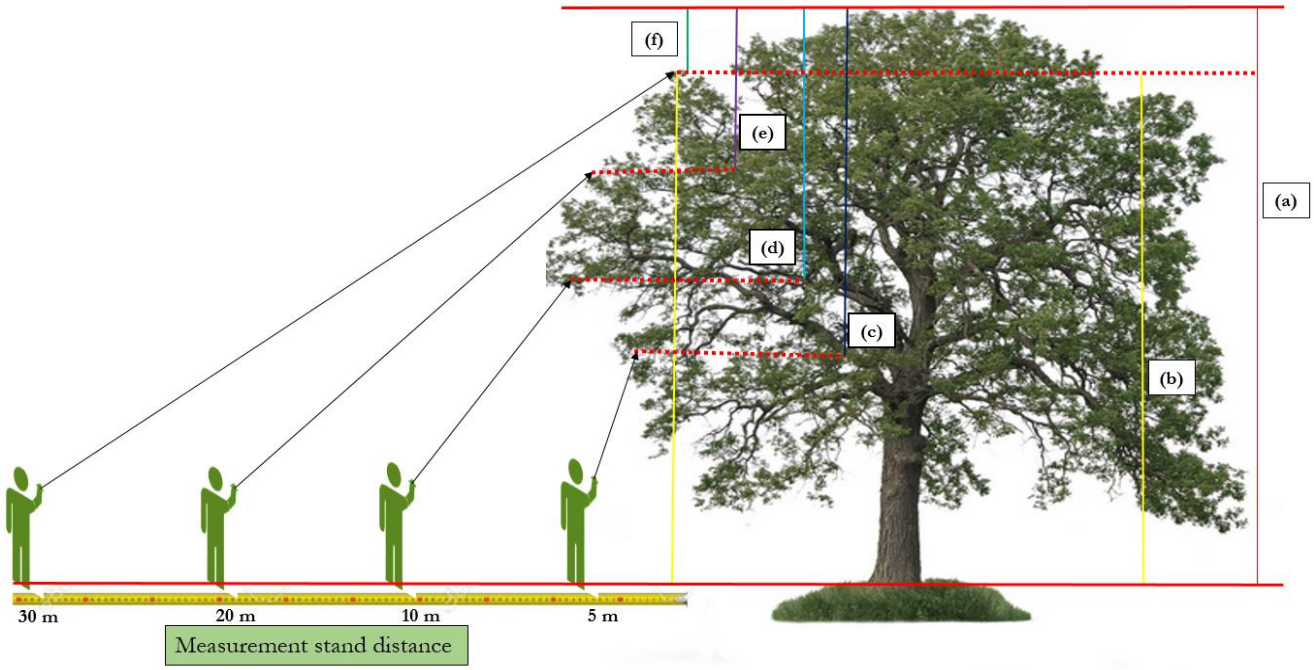

Figure 5.2. Effect of stand distances in measurement of trees height with handheld laser instruments
(a)-Actual tree height, (b)-Maximum measured height, (c)-Missed tree height at 5 m stand distance, (d)-Missed tree height at 10 m stand distance, (e)-Missed tree height at 20 m stand distance and (f)-Missed tree height at 30 m stand distance

Figure 5.3. In complex forest structure it is difficult to see tree tops.

The tree height measurements with a handheld laser instrument show high variation among different observers. This variation decreases with an increase in distance from the tree. This is due to the fact that the top is more clearly to be seen from a farther distance (Figure 5.2). Occlusions due to branches, tall trees, dense forest structure and multiple complex canopies contribute to the low accuracy of height measurements in forests. Larjavaara & Muller-Landau (2013) also pointed out using handheld laser instruments is ambiguous in providing accurate measurements in large trees and closed-stands where the tree tops are not easily visible.

5.2. Terrestrial Laser Scanner Tree Extraction

About 735 (93.5%) of trees has been identified and extracted from registered 3D point cloud data (Figure 5.4). Studies have shown that the TLS can detect more than 90% of the tree trunks depending on the method of extraction. Maas et al. (2008) detect 97.5 % of trees in an Austrian forest. In areas with less undergrowth, for instance the riparian forest in France, 100% of the tree trunks could be detected (Antonarakis, 2011). The result of this study showed that considerably lower number of trees were detected compared to those studies. This is because the complex forest structure of the study area contributes to some trees having lower point cloud density which makes difficult to extract individual tree. However, the result has been comparable to similar studies of tropical rainforest (Ghebremichael, 2015; Lawas, 2016).

Figure 5.4. 3D view of registered sample plot used for extraction of tree parameters

5.3. Terrestrial laser scanning DBH Accuracy assessment

The accuracy of TLS-based DBH achieved in this study was very high (Table 4.4). The accuracy achieved is comparable with tropical forest studies of Lawas (2016) with R^2 of 0.99 and RMSE of 1.03 cm, and Ghebremichael (2015) with R^2 of 0.986 and RMSE of 1.7 cm. The accuracy obtained was higher than studies in forest sites of Texas; R^2 ranged from 0.91 to 0.97 (Srinivasan et al., 2015), and in Eucalyptus forest of Victoria, Australia with R^2 of 0.97 (Calders et al., 2015) depends on the number of scanning position and instrument used. However, the RMSE of the study is higher as compared to Norway spruce dominated forest which is 0.38 cm (Lindberg et al., 2012). Plots with complex dense forest structure contribute to some tree trunks having lower point cloud density. Besides, in trees growing together also contributes to uncertainty in DBH measurements (Figure 5.5).

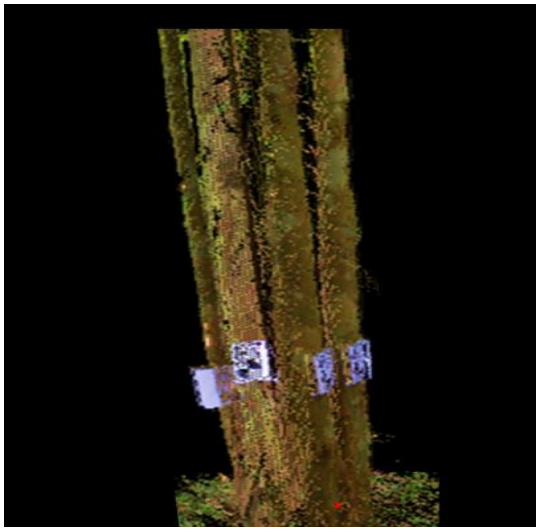

Figure 5.5. Trees growing together affect TLS DBH measurement

5.4. Airborne LiDAR CHM Segmentation Accuracy Assessment

The segmentation accuracy (goodness of fit) in this study was 73 % for the 78% of the 1:1 matching polygons (Table 4.6) which is slightly higher than studies of the subtropical forest of Nepal (Asmare, 2013), and tropical forest of Malaysia (Ghebremichael, 2015) with an accuracy of 69.0 and 68.6%, respectively. Similar studies of Airborne LiDAR CHM segmentation in the tropical forest of Malaysia provide 78.0% of 1:1 match and 75.0% of segmentation accuracy (Lawas, 2016), which is comparable with the current result.

On the other hand, the accuracy is lower in comparison to Airborne LiDAR CHM segmentation in Bois-Noir, France with 79.0% of segmentation accuracy (Hatami, 2012) and 84.0% of accuracy on similar study site of Bois-Noir, France (Kumar, 2012). This is due to high point cloud of LiDAR CHM, the structure and homogeneous species composition of the forest.

The ALS point cloud of 5-6 points/m^2 used for this study potentially contribute to the effectiveness of tree delineation of dense forest crown overlapping tropical forest to be relatively lower. Hatami (2012) indicated the decrease in point cloud density from 164 to 4 points/m^2 results in an accuracy of tree detection decline from 79.0% to 66.1%.

The effect of investigator dependant selected rule sets could also be contributed to the variation for the accuracy of the segmentation achieved.

5.5. Canopy Separation of Tropical Forest

In Ayer Hitam tropical forest with a complex vertical layer of trees, it is challenging to see all trees with single remote sensing technology. Airborne LiDAR has been effective to see emergent trees since the laser pulses of LiDAR cannot penetrate to the lower canopy trees. Jung et al. (2011) studies also confirm the overlapping effect of the top canopies crown in the forest prevented for lower canopy trees to be seen by ALS (Figure 5.6).

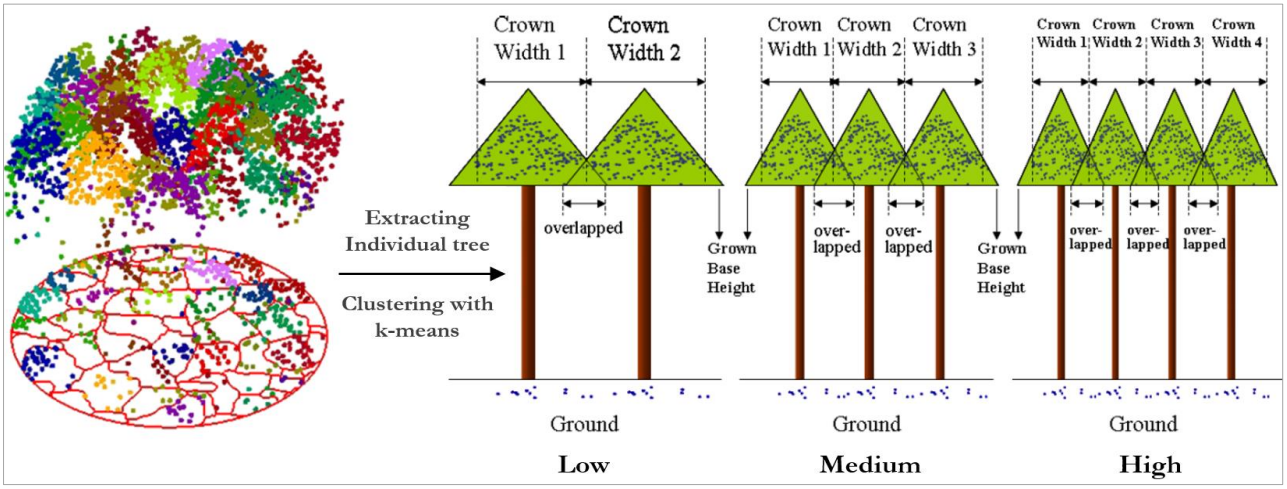

Figure 5.6. Crown overlapping effect in detecting lower canopy trees by using ALS
Source: (Jung et al., 2011)

To overcome crown overlapping effect in multiple canopy structure of the tropical forest, TLS has been used as a complementary tool with ALS. Canopy separation has been done by considering the missed trees from segmented Airborne LiDAR Canopy Projection Area (CPA). Trees not detected by Airborne LiDAR have been extracted with TLS.

Of 786 trees recorded in the field, 486 (61.83%) trees were identified with ALS-CHM, and these trees have been considered as upper canopy trees. Based on the height threshold on the detectability of ALS-CHM, about 300 (38.17%) trees have been considered as lower canopy trees. There are a few studies where the combination of TLS and ALS is used. In Karlsruhe municipal forest of Germany showing that one-third of 831 trees has been accurately detected with TLS for height parameter measurement and linked with ALS identified trees (Fritz et al., 2011). Norway spruce tree dominated forest of Romania, 40-61% of field-measured trees in different plots have been matched with Airborne LiDAR (Apostol et al., 2016). On the other hand, Solberg et al. (2006) studied the assessment in heterogeneous simple vegetation structure of open spruce forest identifies from 93% of top canopy dominant trees to 19% of understory trees. Hence, studies confirm that TLS is effective for understory trees extraction while Airborne LiDAR is for upper canopy trees.

5.6. Tree Height Measurements and Accuracy Assessment

5.6.1. Upper Canopy Trees Height Accuracy Assessment

Tree height is a key parameter in estimating forest biomass. Leica DISTO D510 laser technology with 360° tilt sensor give a measurement of both angles and distances. The instrument records the height information of the topmost point where the laser marks. Thus, it measures the height of the trees at any point of the crown or branch where the laser hits (Figure 5.2).

The relationship achieved in this study (Table 4.9) indicates that field-based height measurement underestimates tree height when compare to the ALS-CHM. A deviation up to 11 m has been recorded (Figure 4.9). The statistical test shows the relationship between field and ALS based height is statistically different.

Study of Airborne LiDAR and field data in four tropical regions forest of Hawaii Island, Amazonian Peru, and Central Panama showed that the relationship between ALS and field height is R^2 of 0.77, 0.82 and 0.84, respectively (Asner et al., 2012). Karna et al. (2015) found R^2 of 0.76 in Kayar Khola watershed forest of Nepal. The study in isolated agroforestry trees in tropical studies of Atlantic lowlands, east Costa Rica with no occlusion, field height

measurement and Airborne LiDAR has shown a high relationship between the two measurements with R^2 of 0.95 and RMSE of 2.5 m (Andersen et al., 2006).

Most of the studies in temperate open natural and plantation forests reported that Airborne LiDAR and conventional field-based tree heights have a high correlation. For instance, the study of Naesset & Okland (2002) in Norway spruce dominated boreal forest, and Heurich (2008) in the Bavarian forest of Germany achieves high correlation between field and Airborne LiDAR based height with R^2 of 0.91 and 0.98, respectively.

The correlation between traditional field and ALS based tree height measurement in this study show a lower accuracy compared to those findings. The study area is secondary tropical rainforest with complex vertical and horizontal structure which makes it difficult to get a clear view of the tree tops. Figure 5.2 and 5.3 demonstrate that large crowns, tall trees, and dense forest affects field height measurements. Getting a clear view of the tree tops at sufficient distance is challenging in a secondary tropical forest of Ayer Hitam. Occlusion under these field conditions contribute to the field height measurement error. Larjavaara & Muller-Landau (2013) and Hunter et al. (2013) also pointed out tree parameter extraction in tall trees, wide crowns, dense canopies and interlocking branches of tropical forest studies produce errors in tree height measurements.

The results obtained in this study are comparable with similar studies in the tropical rainforest of Malaysia who achieve R^2 of 0.65 and RMSE of 3.50 m (Ghebremichael, 2015), and R^2 of 0.61 and RMSE of 4.20 m (21.45%) (Sadadi, 2016).

In this study, Airborne LiDAR-CHM was used as reference to validate Leica DISTO D510 based field measurement since the field measured height is not accurate due to the complex vertical and horizontal structure of tropical rainforest which has been experienced in the field. Development of Airborne LiDAR technology provides accurate forest parameters of tree height. Andersen et al. (2006) study show Airborne LiDAR data with 6 points/m^2 reveals a high correlation with actual tree height as compared to conventional field measurement where accuracy of tree height mean error is $\pm$ Std. Dev. of 0.73 $\pm$ 0.43 m. The study also indicates the error in tree top detection due to the influence of Digital Terrain Model (DTM). It contributes only 10-20 cm in a flat area of Fort Lewis forest of Washington which might actually increase in dense and varied topographic area. Ginzler & Hobi (2015) have been also used Airborne LiDAR-CHM through matching stereo-image as ground-truth reference height to validate field-measured tree height in Swiss national forest inventory and provide a correlation coefficient (r) of 0.83.

5.5.3. Lower Canopy Trees height Accuracy Assessment

TLS has been used as a complimentary tool to extract height of lower canopy trees that are not observable with Airborne LiDAR. The TLS with multiple scan positions (4 positions) applied in this study provides 3D point cloud of trees for individual tree height extraction. The standard deviation of the desirable accuracy of multi-station adjustment (MSA) for registration of multiple scan positions provides highly accurate 3D of an individual tree (Table 3.4). The accuracy achieved is comparable with Prasad (2015) and Sadadi (2016). The MSA accuracy variation comes from a number of perfectly viewed tie points or retro-reflectors in each scan position which can be influenced by occlusions and slope in the field.

Manual tree height measurement tool was used in RiSCAN PRO, which provides highly accurate tree heights compared to automatic height measurements; which has been also achieved in Prasad (2015) study.

To investigate the measurement accuracy of TLS and handheld laser instruments, a controlled field experiment has been conducted. The experiment shows that TLS measurement has been highly correlated with the actual reference

height (Figure 4.1a, b, c and d). On the other hand, tree height measurements with handheld laser instruments showed substantial variation in height depending on distances from the tree and observers. The conventional field measurement method is affected by occlusions of tree branches which made difficult to see tree tops. Calders et al. (2015) also approve that TLS height measurement is more accurate (with $R^2 = 0.98$ and RMSE = 0.55 m) than conventional field-based approach (with $R^2 = 0.94$ and RMSE = 1.28 m) when both measurements validated against destructively measured reference tree heights.

Despite the fact that occlusion has an effect in both TLS and handheld laser instruments, TLS has a potential to provide a full 3D structure of the lower canopy trees. TLS provides highly accurate height measurement for the lower canopy trees since the laser pulse reaches the tree tops with minimal occlusion. But, field-based handheld laser instruments measurement is still affected by many branch leaves which block the laser to mark the tree tops in the tropical rainforest of the study area.

Due to the fact that TLS is highly accurate it was used to validate the corresponding lower canopy field-based height measurement with Leica DISTO D510. Relatively better accuracy has been achieved compared to upper canopy trees (Table 4.13) since the tree tops are more visible in understory trees. Height differences up to 5 m has been recorded in individual tree observation where conventional field-based measurement tend to overestimate by bias of 0.42 m.

The correlation between TLS and field based height found in this study is higher when compared to similar studies of Ayer Hitam tropical rainforest with R^2 of 0.59 and RMSE of 3.40 m (Madhibha, 2016), and Sadadi (2016) with R^2 of 0.62 and RMSE of 3.07 m where TLS measurement taken as ground-truth reference. This is because this study has considered only lower canopy trees where there is less occlusions.

In open temperate natural and plantation forests with very little occlusions, the correlation between TLS and field based height is higher than the complex structure of tropical forests. For instance, Maan et al. (2014) achieve R^2 of 0.80 in Amravati district forest of India. Since the current study was in a tropical rainforest with dense and multiple canopy trees, the correlation was lower compared to one layer temperate forest studies with minimal occlusions.

5.7. Above-ground Biomass/Carbon Accuracy Assessment

This study integrated ALS and TLS derived tree parameters for AGB estimation. The ALS provides the accurate height of observable upper canopy trees while TLS has been used as complimentary for measurement of lower canopy trees height, and upper and lower canopies tree DBH.

This integration appears to be the most reliable way to estimate above-ground biomass (AGB). Since DBH cannot be extracted directly from ALS, the predicted DBH using CPA as proxy has to be very strong in order to arrive at accurate AGB estimates. Due to the fact that tropical forest of Ayer Hitam is a complex structure with multiple canopies, individual tree crown diameter or CPA delineation achieved (Table 4.6) could not be used to predict DBH accurately. Similar study of Ghebremichael (2015) in Ayer Hitam tropical forest of Malaysia, ALS CHM with 5-6 points/m^2 also show a weak DBH prediction.

DBH can be predicted from Airborne LiDAR with the acceptable result in open plantation and natural forests where individual tree crown has clearly differentiated. For instance, Popescu (2007) and Yao et al. (2014) predicted DBH from Airborne LiDAR CHM with R^2 of 0.80 in temperate forest studies, but in tropical forest with a complex structure like Ayer Hitam, tree crowns would not be accurately delineated. Hence, predicted DBH from CPA is found to be far away from the ground-truth. DBH measurement based on TLS data (Table 4.4) were very accurate and were used for upper and lower canopies tree.

The AGB and carbon estimated from the traditional field and remote sensing based derived parameters have been compared (Table 4.15 and 4.18; Figure 4.11). The correlation between the AGB derived from traditional-field and remote sensing (ALS + TLS) parameters was high (Table 4.16). The correlation found in this study has been found to be higher compared to many of other studies described in (Table 5.1).

Table 5.1. Overview of estimated biomass from ALS and TLS derived parameters

Forest location	Remote sensing method	Accuracy	Source
Norway spruce dominated boreal forest of Norway	Airborne LiDAR	$R^2 = 0.88$	(Naesset & Gobakken, 2008)
Pine plantation of Houston National forest, USA	Airborne LiDAR	$R^2 = 0.88$	Popescu (2007)
Turkey lakes watershed forest of Canada	Airborne LiDAR	$R^2 = 0.80$	Fritz et al. (2011)
Tropical forest of Hawaii, Island Amazonian Peru, central Panama and moist forest of Madagascar	Airborne LiDAR	$R^2 = 0.84, 0.83, 0.85, 0.68$	Asner et al. (2012)
Tropical forest of Gola rainforest national park of Sierra Leone	Airborne LiDAR	$R^2 = 0.70$	Vaglio et al. (2014)
Tropical rainforest of northern Borneo, Malaysia	Airborne LiDAR	$R^2 = 0.78$	Ioki et al. (2014)
Central Panama of old growth tropical forest	Airborne LiDAR	$R^2 = 0.70, 0.75$	Meyer et al. (2013)
Northern basin and range forest, USA	Terrestrial LiDAR	$R^2 = 0.83, 0.92$	Olsoy et al. (2014)
Ayer Hitam tropical rainforest, Malaysia	Combination of Airborne and Terrestrial LiDAR	$R^2 = 0.98$	Lawas (2016)
Ayer Hitam tropical rainforest, Malaysia	Combination of Airborne and Terrestrial LiDAR	$R^2 = 0.96$	**Present study**

The reason for higher correlation achieved in this study is because of the complementary effect of ALS and TLS contribute to capturing trees of all canopy layers. Comparable number of field recorded trees have been detected through combination of ALS and TLS. Besides, the use of highly accurate TLS derived DBH has contributed to highly accurate estimation of ALS and TLS based AGB. The RMSE of 1.30 cm (6.52%) achieved in TLS-based DBH contributes very low uncertainty on calculated AGB (Figure 4.12). The difference in field and remote sensing (ALS + TLS) based calculated AGB in this study has been originated mainly from tree height measurement error. Hunter et al. (2013) have been reported that height error ranging from 3-20% of the total height results about 5-6% of uncertainty in estimated biomass. The RMSE of 3.24 m (20.18%) and 1.45 m (14.77%) for upper and lower canopies tree height measurement, respectively achieved in this study contributes up to RMSE of 0.62 Mg (7.64%).

5.8. Relevance of the Study to REDD+

Efficient and accurate computing of forest carbon is emphasized to be very important. Reduced Emission from Deforestation and Forest Degradation (REDD+) has been initiated to ensure for truthful Measurement, Reporting and Verification (MRV) of forest carbon stock of many countries.

Therefore, REDD+ MRV requires accurate way forest biomass assessment and currently has been implementing in tropical forests. On the other hand, accurate assessment of tropical forest biomass has been challenging as these forests are trees with complex multiple canopies. Currently, most of the studies used to estimate AGB is based on either:

1. Tree parameters derived from conventional traditional field-based measurements or
2. Using single remote sensing technology.

Using tree parameters derived from traditional field-based handheld laser measurements bears uncertainty in estimated AGB since field-based tropical forest tree height measurements incurred errors. Implementing only a single remote sensing technology in tropical forests also seems not a prominent method as these forests are with multiple canopies which make difficult to detect all trees. Thus, using the approach followed in this study would likely provide accurate forest parameter measurements and carbon stock.

5.9. Limitation of the Research

Matching of some trees recorded in the field with trees detected in Airborne LiDAR-CHM was challenging. This is because an errors in field GPS affects the actual positions of trees. To recognize the shifting direction of trees location and minimize the matching problem, information on tree height, DBH, and position of the trees in TLS scan positions were used.

Canopy separation was a challenging process. Since tropical rainforest of Ayer Hitam is complex with different layers, applying single threshold has not been enough. Two different thresholds have therefore implemented based on the capability of Airborne LiDAR-CHM tree detection within sample plots with different forest structures.

Ayer Hitam tropical rainforest is rolling to hilly, with steep slope. These terrain condition poses a limitation for sample plot distribution. The area has dense understory which required substantial clearance to reduce occlusion. On top of that, the TLS weighs about 30 kg which makes it difficult to transfer it from one to another sample plot if it has to be carried through areas with steep slopes.

6. CONCLUSION AND RECOMMENDATIONS

6.1. Conclusion

1. *How accurate is tree height measurement of TLS and field handheld laser instruments in controlled field experiment?*

The experiment of TLS and hand held laser instruments (Leica DISTO D510, TruPulse and Forestry Laser Rangefinder) were done with clearly identifiable objects (windowsills) with a known height and trees in different site conditions (solitary and complex stands).

The experiment showed that the TLS height measurement of the windowsills is very accurate (RMSE of 5.3 cm) and almost the same as the actual height. The accuracy of the handheld laser instruments was slightly less (RMSE 60, 73 and 85 cm for Leica DISTO D510, TruPulse and Forestry Laser Rangefinder, respectively), with an increasing deviation from the actual height at farther distances.

Handheld laser instruments height measurement for selected trees showed that there were significant differences in height measurements among observers and distance to the tree. The experiment revealed that trees height measurement with handheld laser instruments in situations where the tree top cannot clearly be seen are a significant source of error. Accordingly, TLS height measurement was used as ground-truth reference for validation of field height measurements of lower canopy trees.

Based on the statistical test in height measurement of the windowsills, the null hypothesis (**Ho**) stated as "There is no significant difference between the accuracy of tree height measured from TLS and handheld laser instruments" was accepted.

2. *How accurate are trees DBH of upper and lower canopies tropical forest derived from TLS as compared with field measured DBH?*

The TLS measured DBH was validated with field measured DBH. The R^2 of 0.989 and RMSE of 1.30 cm (6.52%) were achieved which indicted there was high correlation between the two measurements. The statistical result showed that there was no significant difference between the two measurements. Therefore, the null hypothesis (**Ho**) stated as 'There is no significant difference between the accuracy of tropical forest trees DBH derived from TLS and field' was accepted.

3. *How accurate are individual trees CPA segmented from Airborne LiDAR image?*

The study showed that Airborne LiDAR CHM segmentation was accurate by 78% in one-to-one matching and the goodness of fit was 73%. These results are in line with existing literatures and indicate that Airborne LiDAR is suitable for upper canopy crown detection in tropical forest.

4. *How accurate is trees height of upper canopies tropical forest derived from the field as compared with ALS measured height?*

Field-based height measurement of upper canopy trees was validated with ALS measured height of trees. R^2 of 0.60 and RMSE of 3.25 m (20.18%) were achieved. The statistical result showed that there was a significant difference between the two measurements. The null hypothesis (**Ho**) stated as 'There is no significant difference between the accuracy of upper canopies tree height derived from ALS and field' has therefore rejected.

5. *How accurate is trees height of lower canopies tropical forest derived from the field as compared with TLS measured height?*

Field based height measurement was validated with TLS derived height. R^2 of 0.69 and RMSE of 1.45 m (14.77%) were achieved. The result showed that there was significant difference between the two methods. Thus, the null hypothesis (**Ho**) stated as 'There is no significant difference between the accuracy of lower canopies tree height derived from TLS and field' was rejected.

6. *What are the amount and the difference between estimated AGB derived from integrating ALS and TLS forest parameters compared to field based AGB per plot?*

The AGB calculated from field and remote sensing derived parameters was compared at a plot level. The study revealed that there was high correlation between field and remote sensing based estimated AGB (R^2 of 0.96 and RMSE of 0.62 Mg or 7.64%). The error was originated mainly from field height measurement error. This study showed that it was achieved highly accurate AGB through combination of TLS and ALS derived parameters. The statistical result showed that there was no significant difference between the two measurements at plot level. Hence, the null hypothesis (**Ho**) stated as 'There is no significant difference between remote sensing method of integrating ALS and TLS and field based AGB per plot' was accepted.

6.2. Recommendations

- Since Ayer Hitam was dense tropical rainforest, the GPS receiver used for this study had error which made shifting of the actual location of some trees beyond their crown. It's recommended to use highly accurate GPS for future other studies in tropical forests.

- Since the TLS is a heavy instrument (approx. 30 kg), number and distribution of samples had to be selected depending on distance to the road and slope steepness. If purposive field sampling aims at covering all variation in the study area, or if a (stratified) random sampling scheme is required, the transportability and accessibility in the terrain have to be taken into consideration during fieldwork planning.

LIST OF REFERENCES

Andersen, H. E., Reutebuch, S. E., & McGaughey, R. J. (2006). A rigorous assessment of tree height measurements obtained using Airborne LiDAR and conventional field methods. *Canadian Journal of Remote Sensing*, *32*(5), 355–366. doi.org/10.5589/m06-030

Antonarakis, A. S. (2011). Evaluating forest biometrics obtained from ground LiDAR in complex riparian forests. *Remote Sensing Letters*, *2*(1), 61–70. doi.org/10.1080/01431161.2010.493899

Apostol, B., Lorent, A., Petrila, M., Gancz, V., & Badea, O. (2016). Height extraction and stand volume estimation based on fusion Airborne LiDAR data and Terrestrial measurements for a Norway Spruce. Notulae Botanicae Horti Agrobotanici Cluj-Napoca, *44*(5), 313–323. Retrieved from http://search.proquest.com/openview/64d47310f934b10229dd270937c6e1fc/1?pq-origsite=gscholar&cbl=1246351

Asmare, M. F. (2013). Airborne LiDAR data and VHR WorldView satellite imagery to support community based forest certification in Chitwan, Nepal. *MSc. Thesis*. University of Twente, Faculity of Geo-information Science and Earth Observation (ITC). Enschede, The Netherlands. Retrieved from http://www.itc.nl/library/papers_2013/msc/nrm/asmare.pdf

Asner, G. P., Mascaro, J., Muller-Landau, H. C., Vieilledent, G., Vaudry, R., Rasamoelina, M., … van Breugel, M. (2012). A universal Airborne LiDAR approach for tropical forest carbon mapping. *Oecologia*, *168*(4), 1147–1160. doi.org/10.1007/s00442-011-2165-z

AWF-WIKI. (Forest Inventory and Remote sensing). (2016). Field manual for national forest inventory. Retrieved August 13, 2016, from http://wiki.awf.forst.uni-goettingen.de/wiki/index.php/Category:Single_tree_variables

Baral, S. (2011). Mapping carbon stock using high resolution satellite images in sub-tropical forest of Nepal. *MSc. Thesis*. University of Twente, Faculity of Geo-information Science and Earth Observation (ITC). Enschede, The Netherlands. Retrieved from http://www.itc.nl/Pub/Home/library/Academic_output/AcademicOutput.html?p=11&y=11&l=20

Basuki, T. M., Skidmore, A. K., Hussin, Y. A., & Van Duren, I. (2013). Estimating tropical forest biomass more accurately by integrating ALOS PALSAR and Landsat-7 ETM+ data. *International Journal of Remote Sensing*, *34*(13), 4871–4888. doi.org/10.1080/01431161.2013.777486

Benz, U. C., Hofmann, P., Willhauck, G., Lingenfelder, I., & Heynen, M. (2004). Multi-resolution, object-oriented fuzzy analysis of remote sensing data for GIS-ready information. *ISPRS Journal of Photogrammetry and Remote Sensing*, *58*(3–4), 239–258. doi.org/10.1016/j.isprsjprs.2003.10.002

Bienert, A., Scheller, S., Keane, E., Mullooly, G., & Mohan, F. (2006). Application of Terrestrial laser scanners for the determination of forest inventory parameters. *Remote Sensing and Spatial Information Science*, *36*, 1–5. Retrieved from http://citeseerx.ist.psu.edu/viewdoc/download?doi=10.1.1.222.3218&rep=rep1&type=pdf

Boudreau, J., Nelson, R. F., Margolis, H. A., Beaudoin, A., Guindon, L., & Kimes, D. S. (2008). Regional above-ground forest biomass using Airborne and Spaceborne LiDAR in Québec. *Remote Sensing of Environment*, *112*(10), 3876–3890. doi.org/http://dx.doi.org/10.1016/j.rse.2008.06.003

Brown, S. (2002). Measuring carbon in forests: Current status and future challenges. *Environmental Pollution*, *116*(3), 363–372. doi.org/10.1016/S0269-7491(01)00212-3

Calders, K., Newnham, G., Burt, A., Murphy, S., Raumonen, P., Herold, M., … Kaasalainen, M. (2015). Nondestructive estimates of above-ground biomass using Terrestrial laser scanning. *Methods in Ecology and Evolution*, *6*(2), 198–208. doi.org/10.1111/2041-210X.12301

Canadell, J. G., & Raupach, M. R. (2008). Managing forests for climate change mitigation. *Science*, *320*(5882), 1456–1457. doi.org/10.1126/science.1155458

Carleer, A.P, Debeir, O., & Wolff, E. (2005). Assessment of very high spatial resolution satellite image segmentations. *Photogrammetric Engineering & Remote Sensing*, *11*(10), 1285–1294. doi.org/https://doi.org/10.14358/PERS.71.11.1285

Chave, J., Rejou-Mechain, M., Burquez, A., Chidumayo, E., Colgan, M. S., Delitti, W. B. C., … Vieilledent, G. (2014). Improved allometric models to estimate the aboveground biomass of tropical trees. *Global Change Biology*, *20*(10), 3177–3190. doi.org/10.1111/gcb.12629

Clark, D. A. (2002). Are tropical forests an important carbon sink? Reanalysis of the long-term plot data. *Ecological Applications*, *12*(1), 3–7. doi.org/10.1890/1051-0761(2002)012[0003:ATFAIC]2.0.CO;2

Clark, M. L., Clark, D. B., & Roberts, D. A. (2004). Small-footprint LiDAR estimation of sub-canopy elevation

and tree height in a tropical rain forest landscape. *Remote Sensing of Environment*, *91*(1), 68–89. doi.org /10.1016/j.rse.2004.02.008

Crowley, T. (2000). Causes of climate change over the past 1000 years. *Science*, *289*(5477), 270–277. doi.org/ 10.1126/science.289.5477.270

Cutler, M. E. J., Boyd, D. S., Foody, G. M., & Vetrivel, A. (2012). Estimating tropical forest biomass with a combination of SAR image texture and Landsat TM data: An assessment of predictions between regions. *ISPRS Journal of Photogrammetry and Remote Sensing*, *70*, 66–77. doi.org/10.1016/j.isprsjprs.2012.03.011

Dassot, M., Constant, T., & Fournier, M. (2011). The use of Terrestrial LiDAR technology in forest science: Application fields, benefits and challenges. *Annals of Forest Science*, *68*(5), 959–974. doi.org/10.1007/ s13595-011-0102-2

Definiens, A. G. (2009). Definiens eCognition developer 8 user guide. Advanced image analysis software for fast, accurate geo-spatial information extraction from any kind of remote sensing imagery. Retrieved from http://www.ecognition.com/sites/default/files/eCognition%20v8_Datasheet.pdf

Dengsheng, L. (2006). The potential of and challenge of remote sensing based biomass estimation. *International Journal of Remote Sesnsing,* 27(7), 1297–1328. doi.org/10.1080/01431160500486732

Dixon, R. K., Solomon, A. M., Brown, S., Houghton, R. A., Trexier, M. C., & Wisniewski, J. (1994). Carbon pools and flux of global forest ecosystems. *Science*, *263*, 185–190. doi.org/10.1126/science.263.5144.185

Dong, J., Kaufmann, R. K., Myneni, R. B., Tucker, C. J., Kauppi, P. E., Liski, J., … Hughes, M. K. (2003). Remote sensing estimates of boreal and temperate forest woody biomass: carbon pools, sources, and sinks. *Remote Sensing of Environment*, *84*(3), 393–410. https://doi.org/http://dx.doi.org/10.1016/S0034-4257(02)00130-X

FAO. (1997). Estimating Biomass and Biomass Change of Tropical Forests: *A Primer, FAO Forestry Paper - 134*. Rome, Italy: A Forest resources assessment publication. Retrieved from http://www.fao.org/docrep/ w4095e/w4095e00.htm

Ferraz, A., Saatchi, S., Mallet, C., & Meyer, V. (2016). LiDAR detection of individual tree size in tropical forests. *Remote Sensing of Environment*, *183*, 318–333. doi.org/10.1016/j.rse.2016.05.028

Foody, G. M. (2003). Remote sensing of tropical forest environments: Towards the monitoring of environmental resources for sustainable development. *International Journal of Remote Sensing*, *24*(20), 4035–4046. doi. org/10.1080/0143116031000103853

Fritz, A., Weinacker, H., & Koch, B. (2011). A method for linking TLS and ALS derived trees. Retrieved from http://www.locuscor.net/silvilaser2011/papers/009_Fritz.pdf

Gallay, M. (2013). *Direct Acquisition of Data: Airborne laser scanning*. Jesenna, Slovakia: British Society for Geomorphology. Retrieved from http://www.geomorphology.org.uk/assets/publications/subsections/ pdfs/OnsitePublicationSubsection/10/2.1.4_lidar.pdf

Garcia, M., Riano, D., Chuvieco, E., & Danson, F. M. (2010). Estimating biomass carbon stocks for a Mediterranean forest in central Spain using LiDAR height and intensity data. *Remote Sensing of Environment*, *114*(4), 816–830. doi.org/10.1016/j.rse.2009.11.021

GEOG. (Topographic Mapping with LiDAR). (2016). Typical individual tree measurements. Retrieved December 15, 2016, from https://www.e-education.psu.edu/geog481/l8_p4.html

GFDRR. (Global Facility for Disaster Reduction and Recovery). (2016). Difference in Airborne LiDAR digital surface and elevation model. Retrieved August 15, 2016, from http://www.charim.net/datamanagement/32

Ghasemi, N., Sahebi, M. R., & Mohammadzadeh, A. (2011). A review on biomass estimation methods using synthetic aperture radar. *International Journal Ofgeomatics and Geosciences*, *1*(4), 776–788. Retrieved from http://search.proquest.com/openview/8ee75213440ca50596f81bf366d9ea47/1.pdf?pq-origsite=gscholar& cbl=616552

Ghebremichael, Z. M. (2015). Airborne LiDAR and Terrestrial laser scanner (TLS) in assessing above-ground biomass/ carbon stock in tropical rainforest of Ayer Hitam forest reserve, Malaysia. *MSc. Thesis*. University of Twente, Faculity of Geo-information Science and Earth Observation (ITC). Enschede, The Netherlands. Retrieved from http://www.itc.nl/library/papers_2016/msc/nrm/ghebremichael.pdf

Gibbs, H. K., Brown, S., Niles, J. O., & Foley, J. A. (2007). Monitoring and estimating tropical forest carbon stocks: making REDD a reality. *Environmental Research Letters*, *2*(2007), 45023. doi.org/10.1088/1748-9326/ 2/4/045023

Ginzler, C., & Hobi, M. (2015). Countrywide stereo-image matching for updating digital surface models in the framework of the Swiss National Forest Inventory. *Remote Sensing*, *7*(4), 4343–4370. doi.org/10.3390/ rs70404343

Gupta, J., Grijp, N. V., & Kuik, O. (2013). Climate change, forests and REDD*: Lessons for institutional design* (10th

ed.). New York, NY: Taylor and Francis. Retrieved from http://ezproxy.utwente.nl:2200/patron/FullRecord.aspx?p=1125204

Hatami, F. (2012). Carbon estimation of individual trees using high laser density of Airborne LiDAR: A case study in Bois-Noir, France. *MSc. Thesis*. University of Twente, Faculty of Geo-Information and Earth Observation Science (ITC). Enschede, The Netherlands. Retrived from https://www.itc.nl/library/papers_2012/msc/nrm/hatami.pdf

Henning, J. G.; & Radtke, P. J. (2006). Detailed stem measurements of standing trees from ground-based scanning LiDAR. *Forest Science*, *52*(14), 67–80. Retrieved from http://www.ingentaconnect.com/content/saf/fs/2006/00000052/00000001#expand/collapse

Heurich, M. (2008). Automatic recognition and measurement of single trees based on data from Airborne laser scanning over the richly structured natural forests of the Bavarian Forest National Park. *Forest Ecology and Management*, *255*(7), 2416–2433. doi.org/10.1016/j.foreco.2008.01.022

Houghton, R. A, Lawrence, K. T., Hackler, J. L., & Brown, S. (2001). The spatial distribution of forest biomass in the Brazilian Amazon: A comparison of estimates. *Global Change Biology*, *7*(7), 731–746. doi.org/DOI 10.1046/j.1365-2486.2001.00426.x

Hunter, M. O., Keller, M., Victoria, D., & Morton, D. C. (2013). Tree height and tropical forest biomass estimation. *Biogeosciences*, *10*(12), 8385–8399. doi.org/10.5194/bg-10-8385-2013

Hunum, I. F. (1999). Plant diversity and conservation value of Ayer Hitam forest, Selangor, Peninsular Malaysia. *Pertanika Journal of Tropical Agricultural Science*, *22*(2), 73–83. Retrieved from http://psasir.upm.edu.my/3795/

Hyde, P., Dubayah, R., Walker, W., Blair, J. B., Hofton, M., & Hunsaker, C. (2006). Mapping forest structure for wildlife habitat analysis using multi-sensor (LiDAR, SAR/InSAR, ETM+, Quickbird) synergy. *Remote Sensing of Environment*, *102*(1–2), 63–73. doi.org/10.1016/j.rse.2006.01.021

Hyyppa, J., Holopainen, M., & Olsson, H. (2012). Laser scanning in forests. *Remote Sensing*, *4*(10), 2919–2922. doi.org/10.3390/rs4102919

IGI. (Integrated Geospation Inovation). (2016). Airborne LiDAR system: LiteMapper-5600-A waveform-digitizing LiDAR terrain and vegetation mapping system. Retrieved November 30, 2016, from http://www.igi-systems.com/downloads.html

Ioki, K., Tsuyuki, S., Hirata, Y., Phua, M. H., Wong, W. V. C., Ling, Z.-Y., … Takao, G. (2014). Estimating above-ground biomass of tropical rainforest of different degradation levels in Northern Borneo using Airborne LiDAR. *Forest Ecology and Management*, *328*, 335–341. doi.org/10.1016/j.foreco.2014.06.003

IPCC. (2006). IPCC Guidelines for national greenhouse gas inventories, Volume 4. Agriculture, Forestry and Other Land Use. In N. H. Aalde, P. Gonzalez, M. Gytarsky, T. Krug, W.A. Kurz, S. Ogle, J. Raison, D. Schoene (Ed.), (pp. 15–83). Institute for Global Environmental Strategies (IGES), Hayama, Japan. Retrieved from http://www.ipcc-nggip.iges.or.jp/public/2006gl/pdf/4_Volume4/V4_04_Ch4_Forest_Land.pdf

IG. (Internate Geography) (2016). Tropical rainforest structure. Retrieved August 16, 2016, from http://www.geography.learnontheinternet.co.uk/topics/rainforest.html

Jung, S.-E., Kwak, D.-A., Park, T., Lee, W.-K., & Yoo, S. (2011). Estimating crown variables of individual trees using Airborne and Terrestrial laser scanners. *Remote Sensing*, *3*(12), 2346–2363. doi.org/10.3390/rs3112346

Kaasalainen, S., Krooks, A., Liski, J., Raumonen, P., Kaartinen, H., Kaasalainen, M., … Makipaa, R. (2014). Change detection of tree biomass with Terrestrial laser scanning and quantitative structure modelling. *Remote Sensing*, *6*(5), 3906–3922. doi.org/10.3390/rs6053906

Kajisa, T., Murakami, T., Mizoue, N., Top, N., & Yoshida, S. (2009). Object-based forest biomass estimation using Landsat ETM+ in Kampong Thom Province, Cambodia. *Journal of Forest Research*, *14*(4), 203–211. doi.org/10.1007/s10310-009-0125-9

Kankare, V., Holopainen, M., Vastaranta, M., Puttonen, E., Yu, X., Hyyppa, J., … Alho, P. (2013). Individual tree biomass estimation using Terrestrial laser scanning. *ISPRS Journal of Photogrammetry and Remote Sensing*, *75*, 64–75. doi.org/10.1016/j.isprsjprs.2012.10.003

Karna, Y. K., Hussin, Y. A., Gilani, H., Bronsveld, M. C., Murthy, M. S. R., Qamer, F. M., … Baniya, C. B. (2015). Integration of WorldView-2 and Airborne LiDAR data for tree species level carbon stock mapping in Kayar Khola watershed, Nepal. *International Journal of Applied Earth Observation and Geoinformation*, *38*, 280–291. doi.org/10.1016/j.jag.2015.01.011

Kavzoglu, T., & Yildiz, M. (2014). Parameter-based performance analysis of object-based image analysis using aerial and Quikbird-2 images. *ISPRS Annals of Photogrammetry, Remote Sensing and Spatial Information Sciences*, 2(*7*),

31–37. doi.org/10.5194/isprsannals-II-7-31-2014

Khosravipour, A., Skidmore, A. K., Isenburg, M., Wang, T., & Hussin, Y. A. (2014). Generating pit-free canopy height models from Airborne LiDAR. *Photogrammetric Engineering & Remote Sensing*, *80*(9), 863– 872. doi.org/10.14358/PERS.80.9.863

Kumar, V. (2012). Forest inventory parameters and carbon mapping from Airborne LiDAR. *MSc. Thesis*. University of Twente, Faculity of Geo-information Science and Earth Observation. Enschede, The Netherlands. Retrieved from https://www.itc.nl/library/papers_2012/msc/nrm/vinodkumar.pdf

Larjavaara, M., & Muller-Landau, H. C. (2013). Measuring tree height: A quantitative comparison of two common field methods in a moist tropical forest. *Methods in Ecology and Evolution*, *4*(9), 793–801. doi.org/10.1111/2041-210X.12071

Lawas, C. J. C. (2016). Complementary use of Airborne LiDAR and Terrestrial laser scanner to assess above ground biomass/carbon in Ayer Hitam tropical rain forest reserve. *MSc. Thesis*. University of Twente, Faculity of Geo-information Science and Earth Observation (ITC). Enschede, The Netherlands. Retrieved from http://www.itc.nl/library/papers_2016/msc/nrm/lawas.pdf

Lefsky, M. A., Cohen, W. B., Parker, G. G., & Harding, D. J. D. (2002). LiDAR Remote sensing for Ecosystem Studies. *BioScience*, *52*(1), 19–30. doi.org/10.1641/0006-3568(2002)052[0019:LRSFES]2.0.CO;2

Lemmens, M. (2011). Geo-information technologies, applications and the environment. In R. R. J. Jay & D. Gatrell, Eds.), *Terrestrial and Airborne LiDAR scanning* (pp. 101–165). New York, NY: Springer International Publishing.

Lim, K., Treitz, P., Wulder, M., St-Onge, B., & Flood, M. (2003). LiDAR remote sensing of forest structure. *Progress in Physical Geography*, *27*(1), 88–106. doi.org/10.1191/0309133303pp360ra

Lindberg, E., Holmgren, J., Olofsson, K., & Olsson, H. (2012). Estimation of stem attributes using a combination of Terrestrial and Airborne laser scanning. *European Journal of Forest Research*, *131*(6), 1917–1931. doi.org/10.1007/s10342-012-0642-5

Lu, D. (2006). The potential and challenge of remote sensing-based biomass estimation. *International Journal of Remote Sensing*, *27*(7), 1297–1328. doi.org/10.1080/01431160500486732

Maan, G. S., Singh, C. K., Singh, M. K., & Nagarajan, B. (2014). Tree species biomass and carbon stock measurement using ground based-LiDAR. *Geocarto International*, *6049*(July), 1–18. doi.org/10.1080/10106049.2014.925003

Maas, H.-G., Bienert, A., Scheller, S., & Keane, E. (2008). Automatic forest inventory parameter determination from Terrestrial laser scanner data. *International Journal of Remote Sensing*, *29*(5), 1579–1593. doi.org/10.1080/01431160701736406

Madhibha, T. P. (2016). Assessment of above-ground biomass with Terrestrial LiDAR using 3D quantitative structure modelling in tropical rain forest of Ayer Hitam forest reserve, Malaysia. *MSc. Thesis*. University of Twente, Faculity of Geo-information Science and Earth Observation (ITC). Enschede, The Netherlands. Retrieved from http://www.itc.nl/library/papers_2016/msc/nrm/madhibha.pdf

Maltamo, M., Mustonen, K., Hyyppa, J., Pitkanen, J., & Yu, X. (2004). The accuracy of estimating individual tree variables with Airborne LiDAR laser scanning in a boreal nature reserve. *Canadian Journal of Forest Research*, *34*(9), 1791–1801. doi.org/10.1139/x04-055

Maniatis, D., & Mollicone, D. (2010). Options for sampling and stratification for national forest inventories to implement REDD+ under the UNFCCC. *Carbon Balance and Management*, *5*(9), 1–14. doi.org/10.1186/1750-0680-5-9

Meyer, V., Saatchi, S. S., Chave, J., Dalling, J. W., Bohlman, S., Fricker, G. A., … Hubbell, S. (2013). Detecting tropical forest biomass dynamics from repeated Airborne LiDAR measurements. *Biogeosciences*, *10*(8), 5421–5438. doi.org/10.5194/bg-10-5421-2013

Moller, M., Lymburner, L., & Volk, M. (2007). The comparison index: A tool for assessing the accuracy of image segmentation. *International Journal of Applied Earth Observation and Geoinformation*, *9*(3), 311–321. doi.org/10.1016/j.jag.2006.10.002

Naesset, E., & Bjerknes, K. O. (2001). Estimating tree heights and number of stems in young forest stands using Airborne laser scanner data. *Remote Sensing of Environment*, *78*(3), 328–340. doi.org/10.1016/S0034-4257(01)00228-0

Naesset, E., & Gobakken, T. (2008). Estimation of above- and below-ground biomass across regions of the boreal forest zone using Airborne laser. *Remote Sensing of Environment*, *112*(6), 3079–3090. doi.org/10.1016/j.rse.2008.03.004

Naesset, E., & Okland, T. (2002). Estimating tree height and tree crown properties using Airborne scanning laser

in a boreal nature reserve. *Remote Sensing of Environment*, *79*(1), 105–115. doi.org/10.1016/S0034-4257(01)00243-7

Nizami, S. M., Mirza, S. N., Livesley, S., Arndt, S., Fox, J. C., Khan, I. A., & Mahmood, T. (2009). Estimating carbon stocks in sub-tropical pine (*Pinus roxburghii*) forests of Pakistan. *Pakistan Journal of Agricultural Sciences, 46*(4), 266–270. Retrieved from http://pakjas.com.pk/papers/78.pdf

NOAA. (Earth System Research Laboratory). (2016). Trends in atmospheric carbon dioxide. Retrieved May 23, 2016, from http://www.esrl.noaa.gov/gmd/ccgg/trends/monthly.html

NRE. (Ministry of Natural Resources and Environment). (2014). REDD+ framework for Malaysia. Retrieved May 31, 2016, from http://www.nre.gov.my/en-my/Environment/Pages/default.aspx

Nurul-Shida, S., Faridah-Hanum, I., Wan Razali, W.M. I., & Kamziah, K. (2014). Community structure of trees in Ayer Hitam forest reserve, Puchong,. *The Malaysian Forester*, *77*(1), 73–86. Retrieved from https://www.researchgate.net/publication/270106458_Community_structure_of_trees_in_Ayer_Hitam_Forest_Reserve_Puchong_Selangor_Malaysia

Olsoy, P. J., Glenn, N. F., Clark, P. E., & Derryberry, D. R. (2014). Above-ground total and green biomass of dryland shrub derived from Terrestrial laser scanning. *ISPRS Journal of Photogrammetry and Remote Sensing*, *88*, 166–173. doi.org/10.1016/j.isprsjprs.2013.12.006

Pan, Y., Birdsey, R. A., Fang, J., Houghton, R., Kauppi, P. E., Kurz, W. A., … Hayes, D. (2011). A large and persistent carbon sink in the world's forests. *Science*, *333*(6045), 988–993. doi.org/10.1126/science.1201609

Parresol, B. R. (1999). Assessing tree and stand biomass: A review with examples and critical comparisons. *Forest Science*, *45*(4), 573–593. Retrieved from http://www.ingentaconnect.com/content/saf/fs/1999/00000045/00000004/art00014#expand/collapse

Patenaude, G., Hill, R. A., Milne, R., Gaveau, D. L. A., Briggs, B. B. J., & Dawson, T. P. (2004). Quantifying forest above-ground carbon content using LiDAR remote sensing. *Remote Sensing of Environment*, *93*(3), 368–380. doi.org/10.1016/j.rse.2004.07.016

Popescu, S. C. (2007). Estimating biomass of individual pine trees using Airborne LiDAR. *Biomass and Bioenergy*, *31*(9), 646–655. doi.org/10.1016/j.biombioe.2007.06.022

Popescu, S. C., Wynne, R. H., & Nelson, R. F. (2003). Estimating plot-level tree heights with LiDAR: Local filtering with a canopy-height based variable window size. *Computers and Electronics in Agriculture*, *37*(1–3), 71–95. doi.org/10.1016/S0168-1699(02)00121-7

Prasad, O. M. P. (2015). Derivation of forest plot inventory parameters from Terrestrial LiDAR data for carbon estimation. *MSc. Thesis.* University of Twente, Faculity of Geo-information Science and Earth Observation. Enschede, The Netherlands. Retrieved from https://www.itc.nl/library/papers_2015/msc/nrm/kalwar.pdf

Ramirez, F. A., Armitage, R. P., & Danson, F. M. (2013). Testing the application of Terrestrial laser scanning to measure forest canopy gap fraction. *Remote Sensing*, *5*(6), 3037–3056. doi.org/10.3390/rs5063037

Reyes, G., Brown, S., Chapman, J., & Lugo, A. E. (1992). Wood densities of tropical tree species (General technical report No. 88). New Orleans, LA: U.S. Department of Agriculture, Forest Services, Southern Forest Experiment. Retrieved from https://www.fs.fed.us/global/iitf/pubs/gtr_so088_1992.pdf

Rudiger, G. (2003). Estimation of crown radii and crown projection area from stem size and tree position. *Annals of Forest Science*, *60*(5), 393–402. doi.org/10.1051/forest:2003031

Sadadi, O. (2016). Accuracy of measuring tree height using Airborne LiDAR and Terrestrial laser scanner and its effect on estimating forest biomass and carbon stock in Ayer Hitam tropical rain forest reserve, Malaysia. *MSc. Thesis.* University of Twente, Faculity of Geo-information Science and Earth Observation. Enschede, The Netherlands. Retrieved from http://www.itc.nl/library/papers_2016/msc/nrm/ojoatre.pdf

Segura, M., & Kanninen, M. (2005). Allometric models for tree volume and total above-ground biomass in a tropical humid forest in Costa Rica. *Biotropica*, *37*(1), 2–8. doi.org/10.1111/j.1744-7429.2005.02027.x

Seidel, D., Albert, K., Fehrmann, L., & Ammer, C. (2012). The potential of Terrestrial laser scanning for the estimation of understory biomass in coppice-with-standard systems. *Biomass and Bioenergy*, *47*, 20–25. doi.org/10.1016/j.biombioe.2012.10.009

Sileshi, G. W. (2014). A critical review of forest biomass estimation models, common mistakes and corrective measures. *Forest Ecology and Management*, *329*, 237–254. doi.org/http://dx.doi.org/10.1016/j.foreco.2014.06.026

Soares-Filho, B., Moutinho, P., Nepstad, D., Anderson, A., Rodrigues, H., Garcia, R., … Maretti, C. (2010). Role of Brazilian Amazon protected areas in climate change mitigation. *Proceedings of the National Academy of Sciences of the USA*, *107*(24), 10821–10826. doi.org/10.1073/pnas.0913048107

Solberg, S., Naesset, E., & Bollandsas, O. M. (2006). Single tree segmentation using Airborne laser scanner data in

a structurally heterogeneous spruce forest. *Photogrammetric Engineering & Remote Sensing*, *12*(10), 1369–1378. doi.org/10.14358/PERS.72.12.1369

Srinivasan, S., Popescu, S. C., Eriksson, M., Sheridan, R. D., & Ku, N. W. (2015). Terrestrial laser scanning as an effective tool to retrieve tree level height, crown width, and stem diameter. *Remote Sensing*, *7*(2), 1877–1896. doi.org/10.3390/rs70201877

Steininger, M. K. (2000). Satellite estimation of tropical secondary forest above-ground biomass: Data from Brazil and Bolivia. *International Journal of Remote Sensing*, *21*(6–7), 1139–1157. doi.org/10.1080/014311600210119

Strahler, A. H., Jupp, D. L. B., Woodcock, C. E., Schaaf, C. B., Yao, T., Zhao, F., … Boykin-Morris, W. (2008). Retrieval of forest structural parameters using a ground-based LiDAR instrument (Echidna). *Canadian Journal of Remote Sensing*, *34*(2), 426–440. doi.org/10.5589/m08-046

Theiler, P. W. (2015). Automated registration of Terrestrial laser scanner point clouds. PhD. Thesis. Newcastle University, England. Retrieved from https://www.ethz.ch/content/dam/ethz/special-interest/baug/igp/igp-dam/documents/PhD_Theses/117.pdf

Toriman, M. E., Er, A. C., Lee, Q. Y., Sharifah, M. S. A., Jali, F. M., Mokhtar, M., … Jusoh, H. (2013). Paddy production and climate change variation in Selangor, Malaysia. *Asian Social Science*, *9*(14), 55–62. doi.org/10.5539/ass.v9n14p55

UNFCCC. (2015). Paris agreement to the United Nations framework convention on climate change. Bonn, Germany. Retrieved from http://unfccc.int/files/essential_background/convention/application/pdf/english_paris_agreement.pdf

UPM. (University Putra Malaysia). (2016). Ayer Hitam forest reserve. Retrieved December 21, 2016, from http://www.upm.edu.my/sp/page/48/hutanayerhitam?LANG=en

Vaglio, L. G., Chen, Q., Lindsell, J. A., Coomes, D. A., Frate, F. Del, Guerriero, L., … Valentini, R. (2014). Above-ground biomass estimation in an African tropical forest with LiDAR and hyperspectral data. *ISPRS Journal of Photogrammetry and Remote Sensing*, *89*, 49–58. doi.org/10.1016/j.isprsjprs.2014.01.001

Van Leeuwen, M., & Nieuwenhuis, M. (2010). Retrieval of forest structural parameters using LiDAR remote sensing. *European Journal of Forest Research*, *129*(4), 749–770. doi.org/10.1007/s10342-010-0381-4

Watt, P. J., & Donoghue, D. N. M. (2005). Measuring forest structure with Terrestrial laser scanning. *International Journal of Remote Sensing*, *26*(7), 1437–1446. doi.org/10.1080/01431160512331337961

Wehr, A., & Lohr, U. (1999). Airborne laser scanning: An introduction and overview. *ISPRS Journal of Photogrammetry and Remote Sensing*, *54*(2), 68–82. doi.org/Doi: 10.1016/s0924-2716(99)00011-8

Witharana, C., & Civco, D. L. (2014). Optimizing multi-resolution segmentation scale using empirical methods: Exploring the sensitivity of the supervised discrepancy measure Euclidean distance 2 (ED2). *ISPRS Journal of Photogrammetry and Remote Sensing*, *87*, 108–121. doi.org/10.1016/j.isprsjprs.2013.11.006

WTMA. (Wet Tropics Management Authority). (2016). Structure of tropical rainforest. Retrieved August 15, 2016, from http://www.wettropics.gov.au/rainforest-structure

Yao, W., Krull, J., Krzystek, P., & Heurich, M. (2014). Sensitivity analysis of 3D individual tree detection from LiDAR point clouds of temperate forests. *Forests*, *5*(6), 1122–1142. doi.org/10.3390/f5061122

Yildiz, M., Kavzoglu, T., Colkesen, I., & Sahin, E. K. (2006). An assessment of the effectiveness of segmentation methods on classification performance. In *10th international symposium on spatial accuracy assessment in natural resources and environmental sciences*. Florianopolis, Brazil. Retrieved from http://www.spatial-accuracy.org/system/files/YildizAccuracy2012.pdf

UN-REDD. (2016). The United nations program in developing countries for Reducing Emisssion from Deforestation and Forest Degradation. Retrieved August 10, 2016, from http://www.un-redd.org/

Zhan, Q., Molenaar, M., Templfi, K., & Shi, W. (2005). Quality assessment for geo-spatial objects derived from remotely sensed data. *International Journal of Remote Sesnsing,* 26(14), 2953–2974. doi.org/10.1080/01431160500057764

LIST OF APPENDICES

Appendix 1. ITC windowsill's height measurement records with TLS and handheld instruments

ID	Windowsills No.	Actual height	TLS height	Height meaurments (m)																				
				Obs. 1			Obs. 2			Obs. 3			Obs. 4			Obs. 5			Obs. 6			Obs. 7		
				1	2	3	1	2	3	1	2	3	1	2	3	1	2	3	1	2	3	1	2	3
1	2	18.6	18.5	18.40	18.00	18.90	18.60	18.60	18.30	16.80	18.10	16.10	18.60	18.10	18.50	17.00	18.60	15.50	17.20	18.90	18.00	18.20	18.30	18.50
2	4	15.0	15.0	14.80	14.20	14.40	14.80	15.00	14.30	13.40	14.60	13.20	14.40	14.90	13.60	15.00	11.10	9.60	15.00	14.90	14.10	14.60	14.60	14.30
3	6	11.4	11.4	11.60	11.80	11.20	11.20	11.40	11.20	11.00	11.00	10.30	10.80	11.00	10.20	11.20	10.00	10.50	11.40	11.10	10.50	11.00	11.20	11.10
4	9	7.8	7.7	7.00	7.30	7.20	7.20	7.60	7.60	7.60	7.50	7.90	7.60	6.10	7.60	7.80	7.00	7.40	7.60	7.70	7.90	7.40	7.40	7.50
5	11	4.2	4.2	3.80	4.00	3.80	4.00	4.20	4.00	3.80	4.00	3.60	3.80	4.00	4.10	4.00	4.10	3.95	4.00	4.10	3.90	3.80	4.00	4.10
6	13	1.0	1.1	0.80	0.90	1.14	1.00	1.00	1.00	1.20	1.00	1.20	1.40	0.90	0.90	1.00	1.00	1.02	1.00	1.00	1.09	1.00	1.00	0.90
7	1	18.8	18.6	17.00	17.00	18.80	19.20	18.40	18.00	17.20	17.90	18.30	18.00	17.40	15.50	17.40	18.00	17.60	17.80	18.50	18.20	18.60	17.70	16.60
8	3	15.1	15.1	13.60	13.80	14.80	15.00	14.00	14.40	14.60	14.00	14.90	15.00	13.80	12.30	13.60	14.60	15.20	14.00	15.10	14.50	15.20	14.30	12.40
9	5	11.4	11.5	10.20	10.50	12.00	11.40	11.10	11.90	10.40	11.30	10.20	11.60	11.30	9.40	9.80	11.10	11.70	9.80	12.50	10.50	11.20	11.20	10.30
10	8	7.9	7.9	6.20	6.30	7.60	7.80	7.90	7.90	7.40	7.60	7.90	7.40	7.60	6.60	7.60	7.80	8.00	6.80	8.40	7.50	7.60	7.40	6.70
11	10	4.3	4.3	3.40	4.00	4.10	4.20	4.20	4.10	3.80	4.1.	4.20	3.40	4.10	3.70	4.60	4.00	4.20	3.00	4.30	4.00	4.00	4.00	3.60
12	12	1.2	1.3	0.80	0.80	1.20	1.20	1.20	1.10	0.20	1.20	1.20	0.80	1.00	1.10	0.80	0.60	1.10	1.20	1.10	1.10	1.00	1.10	0.80

Key: Obs.-Observer, 1-Forestry Rangefinder, 2-TruPulse, and 3- Leica DISTO 510

Appendix 2. Tree height measurement records among observers and different measurement stand distances

Tree stand	Leica DISTO 510 tree height measurment (m)																											
	Observer 1				Observer 2				Observer 3				Observer 4				Observer 5				Observer 6				Observer 7			
	Stand Distance (m)																											
	5	10	20	30	5	10	20	30	5	10	20	30	5	10	20	30	5	10	20	30	5	10	20	30	5	10	20	30
Solitary	8.30	23.20	20.00	21.00	12.00	29.60	20.10	21.80	10.00	12.10	18.80	22.50	29.00	24.00	21.10	24.00	12.30	27.70	22.60	25.90	9.40	25.00	22.00	24.00	27.00	20.50	22.30	25.00
Solitary	11.00	15.00	17.70	18.40	10.00	22.00	17.50	15.00	7.00	8.80	20.80	18.80	26.10	21.00	22.70	18.80	10.40	16.40	23.30	19.10	8.40	16.00	21.00	18.00	25.00	21.00	22.00	19.00
Solitary	13.00	15.00	20.00	21.00	20.00	16.40	22.60	21.00	15.00	23.20	20.60	22.00	29.10	20.90	19.50	23.00	14.00	18.50	19.00	22.30	14.00	17.00	21.40	22.00	13.00	19.90	20.00	27.00
Complex	5.00	7.00	10.00	11.00	8.00	9.60	10.00	10.00	5.80	7.70	8.00	13.80	10.00	8.70	9.20	9.30	7.00	6.00	9.50	9.40	11.00	7.00	9.00	10.00	7.00	9.50	10.00	9.00
Complex	7.00	8.00	10.30	10.50	4.60	10.00	10.30	10.40	5.20	7.80	11.80	18.80	8.40	7.90	9.70	11.50	6.00	8.90	7.00	9.50	7.00	8.00	7.00	10.00	6.00	7.00	11.00	14.50
Complex	6.00	11.00	8.00	9.00	9.80	11.70	12.70	9.00	8.00	10.50	12.00	14.70	11.00	14.00	10.00	13.00	7.00	10.50	8.20	12.10	8.00	11.00	9.00	12.00	10.50	14.20	10.00	13.00
Complex	9.00	17.00	18.00	18.00	10.80	18.40	18.00	18.20	18.40	17.20	16.20	18.20	17.20	15.20	15.40	16.80	8.00	14.00	13.00	12.00	7.00	12.00	14.00	12.00	18.40	13.00	12.40	20.00
Complex	15.00	18.00	19.00	19.00	19.20	19.27	20.00	19.00	15.00	22.00	20.00	19.50	14.90	10.60	13.70	14.00	12.00	8.00	12.00	13.00	10.00	9.00	11.00	13.00	14.35	14.48	15.95	16.25
Complex	4.00	6.00	10.00	9.00	7.50	8.20	10.30	9.80	5.00	7.70	8.20	8.00	8.70	8.00	10.00	9.20	6.00	13.00	10.30	12.00	6.24	8.58	9.76	9.60	6.00	12.60	9.00	16.00
Complex	4.00	7.30	8.00	11.00	3.00	7.00	8.90	10.00	4.00	5.00	9.00	9.50	4.40	6.70	8.00	9.20	4.00	5.00	8.00	10.00	3.88	6.20	8.38	9.94	4.40	5.00	9.50	14.00

Appendix 3. Summary of one way single factor ANOVA showing variation of measurements among observers

Groups	Count	Sum	Mean	Variance	Std. Dev.
Leica DISTO [Obs1]	12	115.14	9.595	40.4828454	6.362613
Leica DISTO [Obs2]	12	113.8	9.48333333	37.6160606	6.133193
Leica DISTO [Obs3]	12	109	9.08333333	33.5178787	5.789462
Leica DISTO [Obs4]	12	103.5	8.625	32.0275	5.659284
Leica DISTO [Obs5]	12	105.77	8.81416666	31.1207719	5.578599
Leica DISTO [Obs6]	12	111.29	9.27356666	36.8132810	6.067394
Leica DISTO [Obs7]	12	106.8	8.9	35.2	5.932958

ANOVA

Source of Variation	*SS*	*df*	*MS*	*F*	*P-value*	*F crit*
Between Groups	9.229240476	6	1.53820675	0.0436321	0.9996369	2.21881674
Within Groups	2714.561717	77	35.2540483			
Total	2723.790957	83				

Appendix 4. 3D view of Airborne LiDAR DSM, DTM and CHM

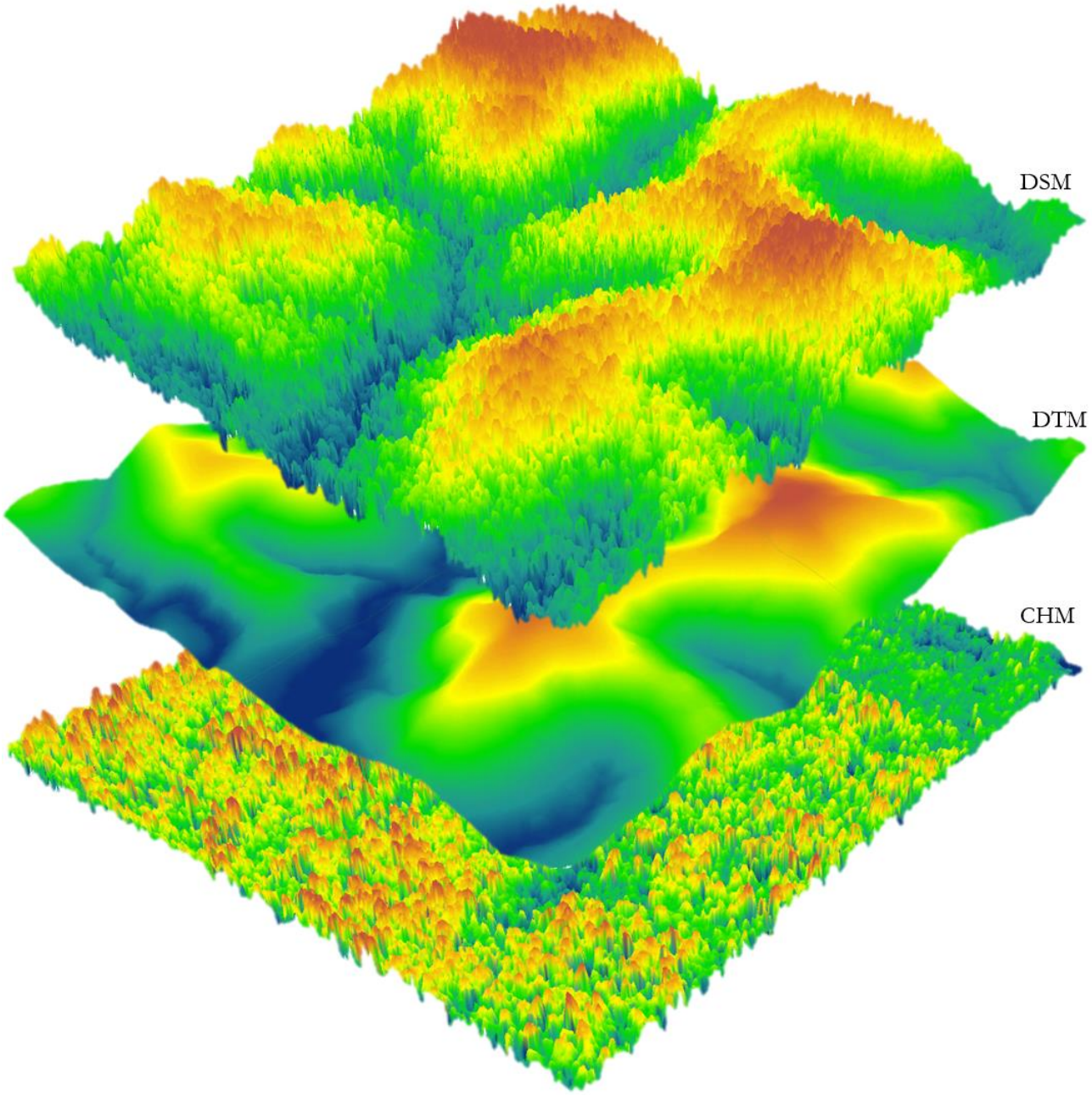

Appendix 5. Histogram showing distribution of tree parameters

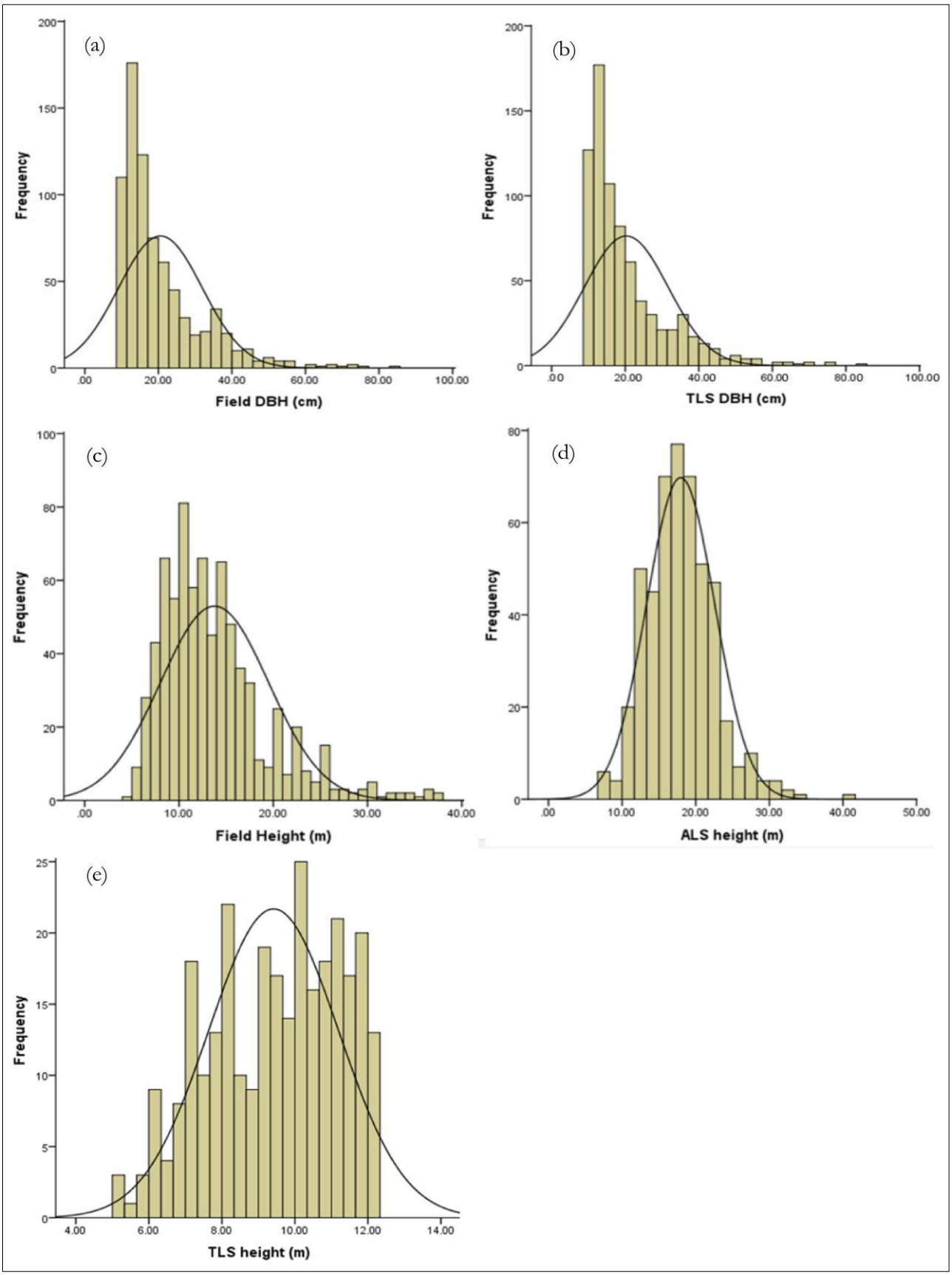

Appendix 6. Summary of descriptive statistics of field and TLS DBH

		Field based DBH (cm)				TLS based DBH (cm)			
Plot	No. of trees	Mean	Std. Dev.	Min.	Max.	Mean	Std. Dev.	Min.	Max.
1	28	19.17	8.34	10.00	42.20	19.88	8.22	10.10	41.30
2	25	20.68	12.41	11.00	66.00	20.28	12.25	10.80	64.10
3	27	19.83	11.36	10.00	50.00	19.36	11.34	9.90	49.30
4	26	21.25	13.12	10.00	53.10	21.10	12.69	10.30	53.50
5	29	22.69	12.84	10.10	55.60	22.70	13.00	10.30	55.50
6	19	22.99	12.58	10.50	48.00	22.84	12.57	10.00	47.50
7	25	28.69	15.92	10.00	64.70	27.39	15.37	11.20	62.20
8	25	20.59	8.20	10.50	42.70	20.10	8.00	10.00	42.00
9	26	19.00	12.56	10.00	72.00	18.96	12.50	10.00	71.30
10	25	19.70	9.18	10.00	42.00	19.66	9.20	10.10	42.80
11	22	18.77	12.82	10.00	70.00	18.65	13.08	9.00	71.10
12	22	20.98	12.17	10.00	54.40	20.78	12.57	9.20	55.60
13	30	19.72	8.56	10.00	47.20	19.35	8.33	9.00	45.20
14	32	21.23	9.66	12.20	47.60	20.77	9.62	11.20	48.00
15	22	28.80	12.10	11.00	52.00	28.18	12.24	11.20	52.50
16	26	17.07	6.92	10.00	40.00	16.59	6.42	9.90	39.60
17	25	25.20	16.09	10.00	75.60	25.00	15.98	10.00	75.20
18	26	23.29	14.37	10.00	66.80	23.23	14.30	10.00	66.40
19	27	20.19	6.74	12.30	34.50	20.15	6.72	12.20	34.40
20	30	19.33	10.93	10.10	57.00	19.26	10.92	10.10	57.00
21	34	21.43	11.18	10.00	50.70	21.28	9.90	9.90	50.40
22	31	22.13	15.48	10.20	84.00	21.64	15.35	10.00	83.60
23	27	21.66	13.19	10.00	73.20	21.49	13.43	10.20	74.40
24	27	20.61	10.67	10.00	49.00	19.85	10.69	9.80	49.40
25	26	21.10	12.15	10.30	51.90	20.42	12.09	9.50	52.30
26	31	18.13	10.77	10.40	56.50	17.88	10.78	10.00	56.70
27	42	14.70	4.76	10.00	33.00	14.60	4.87	10.00	33.50

Appendix 7. Relationship between field and TLS DBH (cm)

Summary of Regression Statistics	
Multiple R	0.99453
R Square	0.989089
Adjusted R Square	0.989075
Standard Error	1.156467
Observations	735

ANOVA

	df	*SS*	*MS*	*F*	*Significance F*
Regression	1	88870.36	88870.36	66449.35	0
Residual	734	980.3252	1.337355		
Total	735	89850.68			

	Coefficients	Standard Error	t Stat	P-value	Lower 95%	Upper 95%	Lower 95.0%	Upper 95.0%
Intercept	-0.36008	0.089516	-4.02248	6.36E-05	-0.53582	-0.18434	-0.53582	-0.18434
Field DBH (cm)	1.015294	0.003939	257.7777	0	1.007561	1.023026	1.007561	1.023026

Appendix 8. Relationship between field and ALS Height (m)

Summary of Regression Statistics	
Multiple R	0.779887757
R Square	0.608224914
Adjusted R Square	0.607352363
Standard Error	3.252235319
Observations	451

ANOVA

	df	*SS*	*MS*	*F*	*Significance F*
Regression	1	7372.888318	7372.8883	697.06573	2.0878E-93
Residual	449	4749.088523	10.577034		
Total	450	12121.97684			

	Coefficients	Standard Error	t Stat	P-value	Lower 95%	Upper 95%	Lower 95.0%	Upper 95.0%
Intercept	-0.03924	0.62967	-0.062315	0.95098	-1.276708	1.19823	-1.2767	1.19823
ALS Height (m)	0.893552	0.03384	26.402002	2.08E-93	0.8270398	0.96006	0.82704	0.96007

Appendix 9. Relationship between field and TLS Height (m)

Summary of Regression Statistics	
Multiple R	0.830625525
R Square	0.689938764
Adjusted R Square	0.688862162
Standard Error	1.458273301
Observations	290

ANOVA

	df	*SS*	*MS*	*F*	*Significance F*
Regression	1	1362.804028	1362.804	640.84878	3.313E-75
Residual	288	612.449574	2.126561		
Total	289	1975.253602			

	Coefficients	Standard Error	t Stat	P-value	Lower 95%	Upper 95%	Lower 95.0%	Upper 95.0%
Intercept	-1.66177	0.4623	-3.59469	0.00038	-2.5717	-0.7519	-2.5717	-0.75189
TLS Height (m)	1.221255	0.0483	25.31499	3.31E-75	1.12630	1.31621	1.12630	1.316207

Appendix 10. Relationship between field and RS method (Mg)

Summary of Regression Statistics	
Multiple R	0.982898837
R Square	0.966090123
Adjusted R Square	0.964733728
Standard Error	0.575681043
Observations	27

ANOVA

	df	*SS*	*MS*	*F*	*Significance F*
Regression	1	236.0452673	236.0453	712.24833	6.83E-20
Residual	25	8.285216589	0.331409		
Total	26	244.3304839			

	Coefficients	Standard Error	t Stat	P-value	Lower 95%	Upper 95%	Lower 95.0%	Upper 95.0%
Intercept	-0.144448	0.33087	-0.4365	0.66175	-0.8259	0.53700	-0.82589	0.53700
RS based AGB (Mg)	0.9090091	0.03406	26.6879	6.86E-20	0.83886	0.97915	0.838860	0.97916

Appendix 11. t-Test: Two-Sample Assuming Equal Variances between remote sensing and field based AGBC

	Total AGBC (RS methods) (Mg)	Total AGBC (Field method) (Mg)
Mean	4.302178405	3.842829026
Variance	2.42706347	2.07586938
Observations	27	27
Pooled Variance	2.251466425	
Hypothesized Mean Difference	0	
df	52	
t Stat	1.12480511	
P(T<=t) one-tail	0.132918464	
t Critical one-tail	1.674689154	
P(T<=t) two-tail	0.265836929	
t Critical two-tail	2.006646805	

Appendix 12. Field data collection sheet

Data sheet for AGB estimation in Ayer Hitam Tropical Rainforest reserve, Malaysia October, 2016

Name of recorder: …….. Date: ……..…….

Sample No.: ……..	GPS plot center location X: ……...….. Y: ……..……...….	Slope (%): ...……..	Plot radius: ……..…

No.	Tree No.	Species Name	Location		Field DBH (cm)	Field Height (m) Leica DISTO 510	Crown Diameter (m)	Crown Cover (%)
			Latitude	Longitude				
1								
2								
3								
4								
5								
6								
7								
8								
9								
10								
11								
12								
13								
14								
15								
16								
17								
18								
19								
20								
21								
22								
23								
24								
25								
26								
27								
28								
29								
30								
31								
32								
33								

Other observation

Appendix 13. Field photo showing single and multiple layers of upper canopies

Appendix 14. Upper canopy trees GPS location and tree parameter measurements

Plot No.	Tree No.	Long (Deg.)	Lat (Deg.)	Species	Field DBH (cm)	TLS DBH (cm)	Field Height (m)	ALS Height (m)
1	46	101.644870	3.001070	*Shorea leprosula*	22.00	21.50	9.80	8.29
	9	101.644760	3.001270	*Accacia mangium*	42.20	41.30	13.00	8.82
	72	101.644740	3.001090	*Accacia mangium*	29.20	26.80	8.20	11.73
	44	101.644780	3.001130	*Shorea leprosula*	16.10	15.70	17.00	11.92
	27	101.644850	3.001120	*Cinnamomum iners*	18.00	17.50	17.00	11.99
	45	101.644870	3.001130	*Cinnamomum iners*	20.20	20.80	15.10	12.02
	49	101.644880	3.001120	*Accacia mangium*	38.90	38.60	10.00	12.25
	28	101.644880	3.001120	*Cinnamomum iners*	25.80	25.40	9.50	13.13
	48	101.644920	3.001170	*Shorea hypochra*	12.10	11.00	15.10	13.90
	16	101.644870	3.001240	*Cinnamomum iners*	13.50	13.30	11.00	13.97
	25	101.644840	3.001190	*Syzgium grande*	11.50	11.20	14.40	14.52
	13	101.644780	3.001280	*Syzgium grande*	10.40	10.40	10.00	15.92
	10	101.644780	3.001230	*Cinnamomum iners*	20.60	20.30	14.00	16.00
	7	101.644710	3.001230	*Cinnamomum iners*	22.20	21.90	12.90	16.00
	2	101.644710	3.001180	*Cinnamomum iners*	15.00	14.90	13.60	16.09
	73	101.644710	3.001180	*Cinnamomum iners*	19.90	18.90	9.10	16.46
	4	101.644730	3.001190	*Accacia mangium*	36.20	36.80	13.50	16.71
	3	101.644780	3.001150	*Shorea parvifolia*	18.00	18.20	20.00	16.87
	1	101.644780	3.001140	*Cinnamomum iners*	21.40	21.10	15.05	16.89
	5	101.644830	3.001170	*Cinnamomum iners*	21.30	21.20	17.00	16.94
	26	101.644840	3.001190	*Cinnamomum iners*	20.70	19.20	24.00	17.34
	18	101.644870	3.001190	*Cinnamomum iners*	12.50	12.60	17.30	17.90
2	1	101.644050	3.004717	*Shorea leprosula*	66.00	64.10	11.50	12.89
	4	101.644083	3.004800	*Sandaricum koetjape*	16.00	15.60	14.50	12.10
	14	101.644167	3.004717	*Syzygium polyanthum*	35.20	35.40	11.50	13.76
	17	101.644150	3.004650	*Gironniera nervosa*	14.40	13.10	16.00	15.44
	18	101.644133	3.004667	*Artocarpus scortechinii*	20.20	19.70	12.00	15.53
	19	101.644083	3.004683	*Lithocarpus amygdalifolius*	14.00	13.60	14.50	16.00
	21	101.644067	3.004650	*Syzygium polyanthum*	29.40	28.80	16.20	16.93
	27	101.644067	3.004650	*Castanopsis acuminatissima*	36.10	36.50	19.40	18.00
	28	101.644050	3.004633	*Shorea leprosula*	35.00	34.80	16.90	18.17
	29	101.644017	3.004633	*Aquilaria malaccensis*	14.70	13.90	23.50	19.97
	30	101.644017	3.004683	*Sandaricum koetjape*	20.00	18.90	30.30	26.84
	40	101.643967	3.004717	*Litsea glutinosa*	36.00	36.40	33.00	31.72
3	70	101.644760	3.004890	*Streblus elongatus*	16.00	16.10	10.50	12.33
	67	101.644750	3.004850	*Endospermum diadenum*	26.00	26.50	12.50	15.10
	68	101.644740	3.004940	*Paropsia verruciformis*	15.00	14.50	13.40	15.24
	75	101.644680	3.004920	*Endospermum diadenum*	34.50	32.70	15.00	17.12
	42	101.644630	3.004930	*Paropsia verruciformis*	13.00	12.80	17.80	17.22
	41	101.644620	3.004870	*Endospermum diadenum*	23.50	22.60	18.90	17.90
	49	101.644610	3.004870	*Endospermum diadenum*	42.50	41.40	20.70	18.56
	54	101.644640	3.004880	*Streblus elongatus*	46.60	46.40	17.20	19.00
	51	101.644670	3.004890	*Terminalia subspathulata*	33.60	32.90	24.20	19.73
	64	101.644700	3.004850	*Arfocarpus scortechinis*	50.00	49.30	19.40	19.84
	60	101.644690	3.004780	*Paropsia verruciformis*	16.80	16.90	19.00	20.23

	58	101.644610	3.004780	*Nipperocapre venucolus*	28.00	27.70	30.50	28.68
4	3	101.643980	3.006970	*Endospermum diadenum*	37.00	34.40	15.50	19.35
	7	101.643880	3.006950	*Nyatoh tembaga*	53.10	53.50	13.70	15.94
	10	101.643910	3.006960	*Endospermum diadenum*	23.10	22.60	14.50	18.97
	16	101.643910	3.007050	*Endospermum diadenum*	34.70	33.00	14.71	19.32
	22	101.644000	3.007040	*Pouteria malaccensis*	27.10	27.20	15.40	20.16
	26	101.643980	3.007100	*Palaquium gutta*	50.00	48.90	20.63	20.44
	35	101.644010	3.006990	*Macaranga gigantea*	45.40	45.80	18.90	20.59
	1	101.643930	3.007040	*Spondias dulcis*	16.80	16.50	20.20	21.74
	2	101.644000	3.007010	*Sandaricum koetjape*	15.30	14.80	25.60	22.37
	4	101.643960	3.006930	*Metadina trichotoma*	19.70	19.20	34.13	27.19
5	67	101.643570	3.006670	*Sapium baccatum*	37.00	37.80	13.50	17.34
	59	101.643670	3.006740	*Endospermum diadenum*	49.30	51.00	16.00	17.99
	54	101.643710	3.006790	*Endospermum diadenum*	26.10	26.00	14.70	18.17
	56	101.643630	3.006790	*Monocarpia marginalis*	22.10	21.20	16.70	18.59
	74	101.643590	3.006650	*Sterculia foetida*	31.70	31.50	17.10	19.46
	70	101.643610	3.006680	*Elaeocarpus petiolatus*	21.60	21.40	21.30	19.80
	72	101.643530	3.006600	*Endospermum diadenum*	37.00	36.90	12.70	20.48
	66	101.643710	3.006590	*Sapium baccatum*	41.80	41.40	25.50	21.34
	33	101.643570	3.006600	*Endospermum diadenum*	40.00	39.50	18.13	21.42
	42	101.643560	3.006730	*Koompassia malaccensis*	12.70	13.20	20.40	21.89
	35	101.643550	3.006730	*Sapium baccatum*	20.20	20.90	17.20	22.00
	43	101.643500	3.006730	*Sapium baccatum*	37.00	37.90	18.30	22.88
	41	101.643570	3.006740	*Palaquium hispidum*	55.60	55.50	18.00	22.91
	61	101.643680	3.006660	*Pellacalyx axillaris*	14.40	14.10	22.20	23.30
	49	101.643600	3.006740	*Endospermum diadenum*	22.00	21.50	22.50	30.84
6	9	101.646870	3.005300	*Endospermum diadenum*	36.90	36.90	10.50	12.06
	10	101.646830	3.005320	*Endospermum diadenum*	45.30	44.20	16.40	15.42
	2	101.646770	3.005310	*Syzygium spp*	33.00	34.30	15.20	18.98
	14	101.646890	3.005410	*Artocarpus elasticus*	38.70	38.70	22.30	20.07
	18	101.646820	3.005400	*Lithocarpus celebicus*	23.20	23.10	20.00	20.59
	21	101.646850	3.005410	*Ochanostachys amentacea*	40.00	40.50	16.68	20.92
	27	101.646900	3.005440	*Xerospermum noronhianum*	24.90	24.00	25.60	22.78
	28	101.646870	3.005390	*Ochanostachys amentacea*	48.00	47.50	22.00	23.00
	6	101.646870	3.005280	*Atrocarpus odoratissimus*	23.20	22.00	22.19	24.68
7	67	101.646470	3.005640	*Artocarpus odoratssimus*	20.00	22.00	17.80	20.64
	65	101.646460	3.005700	*Elaeis guineensis*	24.90	24.00	12.80	13.51
	70	101.646470	3.005690	*Dipterocarpus crinitus*	15.00	13.00	15.10	16.02
	71	101.646430	3.005720	*Palaquium gutta*	27.00	24.20	11.30	17.30
	61	101.646450	3.005690	*Myristicaceae*	17.00	17.70	12.80	19.18
	60	101.646420	3.005730	*Shorea macroptera*	53.50	53.50	20.00	20.36
	58	101.646470	3.005760	*Dipterocarpus crinitus*	28.90	26.20	18.40	20.95
	57	101.646490	3.005880	*Aquilaria malaccensis*	54.50	51.40	21.30	21.00
	54	101.646530	3.005790	*Canarium granddifolium*	40.30	39.80	18.80	21.18
	75	101.646420	3.005790	*Baccaurea maingayi*	25.90	24.50	16.30	21.62
	22	101.646480	3.005810	*Shorea macroptera*	57.90	54.80	14.10	22.38
	42	101.646480	3.005860	*Shorea macroptera*	27.30	27.90	20.40	24.11

	47	101.646520	3.005870	*Lophopetalum javanicum*	25.80	23.40	19.50	26.33
	43	101.646580	3.005870	*Shorea macroptera*	64.70	62.20	24.20	26.43
	45	101.646450	3.005780	*Dipterocarpus crinitus*	50.80	48.00	21.70	27.76
	46	101.646510	3.005860	*Callophylum spp*	22.00	20.20	25.40	27.98
	68	101.646520	3.005790	*Dipterocarpus crinitus*	28.00	25.00	31.90	30.94
	38	101.646550	3.005810	*Ochanostachys amentacea*	42.20	41.00	33.20	31.86
	40	101.646530	3.005850	*Shorea macroptera*	24.60	22.20	22.10	31.11
8	4	101.642260	3.005900	*Ochanostachys amentacea*	37.80	36.80	12.60	12.94
	5	101.642170	3.005880	*Endospermum diadenum*	36.80	36.70	13.30	13.47
	29	101.642150	3.005900	*Pellacalyx axillaris*	21.60	21.30	16.93	14.60
	28	101.642090	3.005920	*Xylopia ferruginea*	24.20	24.10	12.20	15.00
	30	101.642100	3.005900	*Pellacalyx axillaris*	16.30	16.20	12.50	15.18
	27	101.642080	3.005880	*Palaquium gutta*	21.40	20.30	7.90	15.72
	11	101.642090	3.005800	*Gonystylus affinis*	42.70	42.00	17.20	15.85
	13	101.642110	3.005770	*Palaquium gutta*	21.60	20.00	12.20	15.96
	25	101.642270	3.005810	*Canarium littorale*	14.70	14.90	15.30	16.23
	26	101.642290	3.005870	*Arena obtusifolia*	23.20	22.30	17.80	16.75
	2	101.642200	3.005870	*Antidesma cuspidatum*	21.90	21.10	18.10	16.83
	3	101.642250	3.005890	*Sapium baccatum*	28.70	27.00	15.90	16.89
	21	101.642230	3.005760	*Syzygium spp*	21.30	20.30	17.20	18.14
	6	101.642140	3.005860	*Pellacalyx axillaris*	17.10	16.30	16.40	19.04
	10	101.642140	3.005860	*Pellacalyx axillaris*	22.00	22.30	13.19	20.05
	20	101.642200	3.005780	*Polylthia glauca*	25.30	24.10	20.10	20.56
9	48	101.642480	3.006570	*Castanopsis acuminatissima*	72.00	71.30	10.70	12.29
	1	101.642570	3.006630	*Sapium baccatum*	35.00	35.90	10.24	12.85
	7	101.642430	3.006530	*Pellacalyx axillaris*	13.40	13.10	15.89	14.81
	8	101.642430	3.006550	*Aquilaria malaccensis*	31.50	31.90	13.89	16.11
	40	101.642560	3.006540	*Endospermum diadenum*	24.70	24.30	16.86	17.48
	23	101.642590	3.006430	*Strombosia javanica*	20.80	20.40	15.80	20.47
	42	101.642580	3.006530	*Palaquium gutta*	23.50	23.80	22.03	21.74
	41	101.642530	3.006520	*Endospermum diadenum*	20.00	19.10	20.60	22.47
	37	101.642520	3.006490	*Pellacalyx axillaris*	15.60	15.90	28.40	23.84
	39	101.642540	3.006490	*Endospermum diadenum*	23.70	23.40	23.84	24.94
	49	101.642560	3.006580	*Litsea costalis*	24.80	24.90	28.70	27.43
10	46	101.641460	3.005110	*Streblus elongatus*	14.80	14.50	13.80	12.94
	40	101.641400	3.005100	*Elaeocarpus ganitrus*	35.00	35.50	12.12	14.46
	43	101.641450	3.005010	*Endospermum diadenum*	24.20	23.40	20.00	16.85
	45	101.641410	3.004990	*Endospermum diadenum*	18.40	18.20	15.50	18.17
	22	101.641510	3.005110	*Endospermum diadenum*	26.20	26.30	22.81	18.69
	55	101.641510	3.005100	*Sterculia foetida*	22.20	22.10	24.00	19.47
	52	101.641540	3.005040	*Cinnamomum iners*	42.00	42.80	19.58	19.85
	60	101.641560	3.005050	*Myristica maxina*	21.00	20.60	22.70	19.86
	65	101.641570	3.005160	*elateriospermum tapos*	19.20	20.10	17.40	20.00
	64	101.641530	3.005190	*Endospermum diadenum*	35.90	35.60	19.20	20.10
	69	101.641460	3.005170	*Campnosperma auriculatum*	35.40	34.80	22.26	20.53
	71	101.641380	3.005190	*Endospermum diadenum*	29.00	29.10	17.74	23.33
	5	101.641530	3.005060	*Syzygium spp*	20.50	19.20	25.20	26.79

	72	101.641380	3.005180	*Xylopia ferruginea*	12.80	12.60	29.20	27.00
11	16	101.664820	3.031010	*Nyatoh Nayke kuning*	23.20	24.00	11.26	12.01
	75	101.664740	3.031040	*Castanopsis acuminatissima*	39.60	39.90	11.67	12.50
	40	101.664750	3.031010	*Shorea macroptera*	70.00	71.10	14.80	12.63
	70	101.664730	3.031000	*Kurgkur spp*	22.90	22.00	9.30	12.85
	54	101.664820	3.031010	*Litsea costalis*	14.70	13.70	8.60	13.33
	61	101.664790	3.030990	*Macaranga Gigantea*	17.90	17.60	15.30	17.09
	71	101.664700	3.031000	*Syzygium spp*	29.10	30.00	12.10	19.36
	43	101.664700	3.031040	*Syzygium spp*	16.30	17.50	10.80	19.41
	48	101.664680	3.031020	*Koompassia excelsa*	19.10	17.60	16.80	20.09
	55	101.664690	3.030970	*Archidendron pauciflorum*	18.20	17.80	24.20	23.53
12	62	101.664050	3.032050	*Canarium Pseudodecumanum*	21.60	22.30	12.31	12.23
	42	101.663980	3.032090	*Dipterocarpus baudii*	21.80	21.00	10.50	12.99
	60	101.663970	3.032120	*Elaeocarpus ganitrus*	22.40	22.30	12.19	16.08
	18	101.664000	3.032130	*Elaeocarpus ganitrus*	19.50	19.10	18.00	16.69
	4	101.664030	3.032150	*Artocarpus scortechinii*	44.20	44.80	16.50	17.70
	57	101.664050	3.032150	*Canarium Pseudodecumanum*	41.10	41.70	20.50	18.53
	37	101.664090	3.032140	*Palaquium hispidum*	36.20	36.20	25.23	19.59
	33	101.664090	3.032130	*Artocapus odoratissimus*	28.10	27.10	20.70	19.98
	37	101.664080	3.032120	*Dipterocarpus crinitus*	54.40	55.60	22.26	24.17
	38	101.663990	3.032160	*Shorea macroptera*	22.50	23.20	25.40	26.10
	74	101.664000	3.032160	*Aidia densiflora*	20.20	19.40	32.80	28.95
13	43	101.640690	3.005170	*Xylotria javanica*	18.40	18.50	10.50	12.38
	27	101.640720	3.005140	*Xylopia ferruginea*	24.70	25.00	11.30	12.93
	54	101.640750	3.005080	*Macaranga triloba*	19.50	19.70	10.40	12.78
	36	101.640710	3.005060	*Syzygium malaccense*	20.60	20.00	10.50	12.97
	32	101.640720	3.005050	*Campnosperma auriculatum*	20.10	20.70	12.70	12.12
	31	101.640650	3.005010	*Macaranga triloba*	23.50	20.50	12.20	12.36
	30	101.640690	3.005000	*Endospermum diadenum*	21.10	19.80	10.50	12.44
	20	101.640710	3.005050	*Beilschmiedia madang*	26.00	25.10	14.80	12.46
	53	101.640670	3.005130	*Beilschmiedia madang*	22.40	22.50	13.60	13.04
	48	101.640660	3.005090	*Endospermum diadenum*	17.00	18.00	13.00	14.24
	49	101.640660	3.005130	*Endospermum diadenum*	13.40	13.30	14.30	15.09
	45	101.640620	3.005130	*Pouteria malaccensis*	38.30	39.30	14.50	15.27
	42	101.640660	3.005150	*Artocarpus scortechinii*	27.40	26.40	13.30	15.65
	50	101.640620	3.005200	*Artocarpus scortechinii*	31.00	28.80	14.70	16.00
	5	101.640700	3.005170	*Endospermum diadenum*	47.20	45.20	14.90	16.32
	29	101.640720	3.005040	*Syzygium malaccense*	16.00	15.10	12.50	16.45
	39	101.640600	3.005170	*Syzygium malaccense*	17.40	18.20	15.00	16.84
	47	101.640630	3.005250	*Endospermum diadenum*	31.90	31.30	19.90	16.97
	9	101.640750	3.005160	*Beilschmiedia madang*	19.80	18.80	16.50	17.15
	13	101.640770	3.005130	*Artocarpus scortechinii*	13.40	13.00	18.90	18.56
	24	101.640710	3.005060	*Syzygium malaccense*	11.90	11.50	21.30	19.85
	40	101.640600	3.005180	*Syzygium malaccense*	14.20	15.00	22.70	20.68
	44	101.640740	3.005070	*Elaeis guineensis*	11.70	12.40	23.00	22.93
14	73	101.642680	3.004150	*Pertusadina eurhyncha*	23.30	23.90	11.80	12.46
	50	101.642670	3.004170	*Castanopsis acuminatissima*	25.70	27.00	10.60	12.23

	21	101.642740	3.004130	*Nyatoh tembaga*	45.70	43.00	12.40	13.28
	15	101.642750	3.004110	*Syzygium malaccense*	34.90	34.20	12.20	13.42
	57	101.642560	3.004130	*Endospermum diadenum*	31.10	28.50	15.30	13.48
	74	101.642520	3.004120	*Pellacalyx axillaris*	24.20	22.50	14.30	14.00
	58	101.642590	3.004140	*Pellacalyx axillaris*	35.60	36.60	13.50	14.05
	64	101.642650	3.004180	*Endospermum diadenum*	40.40	40.10	15.30	15.87
	71	101.642620	3.004110	*Pellacalyx axillaris*	26.20	25.60	15.60	16.00
	6	101.642660	3.004130	*Syzygium malaccense*	25.20	24.60	15.60	16.01
	54	101.642680	3.004130	*Nyatoh tembaga*	18.20	18.60	11.40	16.16
	75	101.642680	3.004100	*Syzygium malaccense*	47.60	48.00	15.60	16.26
	12	101.642720	3.004080	*Pertusadina eurhyncha*	18.60	17.00	12.50	16.32
	37	101.642650	3.004030	*Nyatoh tembaga*	28.10	28.10	16.00	16.95
	17	101.642620	3.004070	*Memecylon edule*	21.50	21.90	10.92	17.65
	26	101.642580	3.004080	*Porterandia anisophylla*	18.90	17.00	20.00	21.75
	22	101.642600	3.004130	*Aidia densiflora*	15.50	18.00	20.10	21.95
	65	101.642560	3.004180	*Endospermum diadenum*	16.20	15.70	21.30	22.22
	24	101.642670	3.004220	*Endospermum diadenum*	17.70	15.90	22.40	22.88
15	11	101.656820	3.034440	*Scaphium macropodum*	31.00	31.40	10.70	12.62
	39	101.656780	3.034350	*Pometia pinnata*	36.00	33.90	11.90	13.86
	12	101.656850	3.034380	*Gironniera nervosa*	39.30	41.20	13.90	14.04
	2	101.656830	3.034330	*Santiria laevigata*	44.60	45.70	9.90	14.79
	19	101.656840	3.034260	*Santiria laevigata*	42.10	38.40	10.10	15.30
	46	101.656850	3.034250	*Litsea costalis*	33.70	34.40	10.50	16.05
	27	101.656780	3.034330	*Gluta renghas*	36.40	35.10	16.90	16.55
	45	101.656760	3.034260	*Gynotroches axillaris*	36.20	36.20	15.60	16.62
	53	101.656690	3.034380	*Santiria laevigata*	37.60	34.80	9.50	17.28
	44	101.656640	3.034370	*Scaphium macropodum*	52.00	52.50	17.00	17.63
	32	101.656680	3.034350	*Canarium littorale*	35.20	33.60	17.90	18.17
	14	101.656760	3.034420	*Aidia densiflora*	21.80	21.50	17.60	18.22
	4	101.656810	3.034400	*Porterandia anisophylla*	40.00	40.50	17.40	19.15
	40	101.656810	3.034420	*Porterandia anisophylla*	17.50	18.00	20.50	20.92
	48	101.656660	3.034330	*Knema hookeriana*	16.30	15.60	20.20	21.01
	10	101.656750	3.034450	*Endospermum diadenum*	36.00	34.60	21.80	22.01
	36	101.656730	3.034390	*Xerospermum noronhianum*	16.90	15.40	20.80	22.08
	49	101.656720	3.034300	*Elateriospermum tapos*	15.60	15.60	23.40	25.33
	28	101.656830	3.034360	*Lithocarpus edulis*	14.00	11.80	36.30	30.00
16	41	101.657730	3.034420	*Aquilaria malaccensis*	24.00	23.60	12.40	12.93
	38	101.657700	3.034330	*Artocarpus scortechinii*	40.00	39.60	12.20	13.58
	3	101.657680	3.034430	*Mesua grandis*	18.00	19.00	13.80	13.92
	9	101.657680	3.034460	*Shorea macroptera*	34.00	30.00	12.20	14.83
	30	101.657660	3.034460	*Ixonanthes icosandra*	25.00	22.00	10.80	15.30
	55	101.657610	3.034380	*Ochanostachys amentacea*	21.50	19.50	15.90	15.42
	22	101.657680	3.034350	*Gynotroches axillaris*	18.60	18.30	8.10	15.58
	62	101.657720	3.034420	*Pouteria malaccensis*	22.00	20.20	15.60	15.82
	58	101.657690	3.034260	*Ochanostachys amentacea*	16.10	15.30	10.60	16.02
	65	101.657730	3.034380	*Endospermum diadenum*	19.00	17.00	11.60	17.15
	63	101.657750	3.034350	*Pellacalyx axillaris*	16.30	18.00	13.70	17.51

	26	101.657680	3.034330	*Callerya atropurpurea*	16.30	15.70	22.60	23.00
	56	101.657710	3.034370	*Monocarpia marginalis*	12.10	10.30	23.40	30.91
17	40	101.656780	3.033910	*Diospyros malabarica*	21.60	21.50	11.40	12.14
	39	101.656790	3.033880	*Calophyllum biflorum*	32.20	32.20	12.20	13.07
	37	101.656800	3.033920	*Dipterocarpus baudii*	44.00	43.80	15.60	13.89
	47	101.656750	3.033990	*Shorea leprosula*	61.50	61.30	10.80	14.51
	46	101.656800	3.033920	*Ochanostachys amentacea*	39.70	38.20	12.20	15.21
	52	101.656680	3.033940	*Endospermum diadenum*	31.50	31.90	15.90	16.22
	48	101.656750	3.033910	*Iconanthes icosandra*	30.90	30.60	17.10	16.85
	12	101.656680	3.033840	*Pellacalyx axillaris*	29.00	28.00	14.80	17.05
	19	101.656720	3.033750	*Pellacalyx axillaris*	41.00	40.70	17.10	17.29
	8	101.656750	3.033780	*Aidia densiflora*	19.20	18.70	15.30	17.42
	51	101.656760	3.033760	*Gironniera nervosa*	21.80	21.70	19.10	18.95
	20	101.656780	3.033750	*Diospyros malabarica*	17.00	17.20	17.70	20.20
	13	101.656780	3.033770	*Shorea leprosula*	75.60	75.20	22.20	20.67
	4	101.656780	3.033830	*Canarium apertum*	30.50	30.20	20.40	20.79
	70	101.656730	3.033890	*Gironniera nervosa*	19.10	18.90	20.50	21.21
	9	101.656720	3.033840	*Litsea curtisii*	18.50	18.00	20.70	22.13
	21	101.656830	3.033870	*Gardenia tubifera*	23.40	23.90	21.60	22.89
	38	101.656720	3.033930	*Gironniera nervosa*	11.90	11.80	27.70	28.30
18	4	101.657420	3.033870	*Ochanostachys amentacea*	21.70	21.60	29.80	39.34
	21	101.657430	3.033870	*Pometia pinnata*	24.00	23.90	14.10	12.70
	37	101.657360	3.033980	*Pellacalyx axillaris*	33.00	33.00	10.90	12.79
	67	101.657280	3.033980	*Shorea leprosula*	63.10	63.00	12.20	12.00
	13	101.657180	3.033880	*Litsea castanea*	33.00	33.00	14.70	12.81
	48	101.657280	3.033880	*Shorea bracteolata*	35.50	35.40	10.90	13.83
	5	101.657230	3.033860	*Shorea leprosula*	66.80	66.40	15.80	14.03
	52	101.657230	3.033840	*Shorea acuminata*	32.00	31.90	11.70	14.47
	20	101.657260	3.033780	*Shorea acuminata*	35.00	34.90	16.30	14.65
	43	101.657240	3.033850	*Artocarpus scortechinii*	22.90	22.90	16.20	14.97
	8	101.657310	3.033770	*Knema hookeriana*	21.10	21.10	14.90	16.30
	19	101.657300	3.033770	*Diospyros pilosanthera*	17.00	16.90	14.90	16.67
	7	101.657300	3.033750	*Irvingia malayana*	18.00	18.10	20.10	19.85
	11	101.657420	3.033870	*Artocarpus gomezianus*	26.00	26.00	20.60	20.59
	39	101.657420	3.033980	*Heritiera javanica*	16.00	16.10	25.10	20.87
	14	101.657350	3.033940	*Millettia atropurpurea*	18.40	18.40	23.20	25.86
	60	101.657290	3.033940	*Memecylon edule*	26.40	26.20	27.20	28.15
	40	101.657340	3.033980	*Diospyros pilosanthera*	12.60	12.60	29.80	40.34
19	6	101.643400	3.005200	*Macaranga gigantea*	26.60	26.50	10.00	15.04
	38	101.643460	3.005190	*Papaina obscura*	26.70	26.50	14.80	15.09
	55	101.643440	3.005180	*Artocarpus scortechinii*	24.80	24.90	12.90	15.69
	40	101.643500	3.005240	*Elaeocarpus ganitrus*	17.00	17.10	12.90	15.87
	21	101.643490	3.005260	*Gynotroches axillaris*	14.90	14.90	16.70	16.70
	51	101.643490	3.005290	*Litsea costalis*	28.60	28.60	16.20	16.71
	23	101.643520	3.005280	*Litsea costalis*	22.10	22.20	10.60	16.86
	46	101.643510	3.005360	*Guttiferaeand lauraceae*	16.10	16.00	14.50	16.89
	8	101.643500	3.005380	*Rambutan xerospermum*	17.00	17.00	11.80	17.13

	48	101.643440	3.005320	*Pometia pinnata*	34.50	34.40	14.40	17.13
	9	101.643420	3.005240	*Porterandia anisophylla*	30.50	30.30	13.50	17.31
	52	101.643430	3.005310	*Monocarpia marginalis*	24.30	24.20	17.40	17.88
	14	101.643420	3.005350	*Gonystylus affinis*	13.60	13.50	15.90	18.00
	39	101.643390	3.005390	*Knema patentinervia*	21.20	21.00	15.80	18.25
	60	101.643390	3.005370	*Streblus elongatus*	19.60	19.80	22.10	18.78
	25	101.643460	3.005270	*Aglaia acariaeantha*	28.40	28.40	17.20	18.91
	12	101.643420	3.005230	*Porterandia anisophylla*	14.50	14.50	15.50	18.94
	4	101.643420	3.005240	*Guttiferaeand lauraceae*	16.20	16.20	13.20	19.04
	68	101.643440	3.005340	*Elaeocarpus ganitrus*	32.00	31.70	13.30	19.39
	47	101.643450	3.005320	*Syzygium malaccense*	23.60	23.60	17.40	20.61
	69	101.643440	3.005320	*Rambutan xerospermum*	13.30	13.30	25.40	20.84
	70	101.643420	3.005210	*Ochanostachys amentacea*	13.10	13.00	16.40	20.97
20	21	101.643200	3.006530	*Pellacalyx axillaris*	15.70	15.70	14.70	16.64
	53	101.643250	3.006430	*Eugenia grandis*	19.90	19.50	9.40	17.78
	12	101.643250	3.006380	*Litsea elliptica*	29.80	29.40	14.00	18.09
	17	101.643310	3.006460	*Endospermum diadenum*	57.00	57.00	16.50	18.09
	22	101.643230	3.006600	*Ixonanthes icosandra*	15.70	15.70	10.80	18.75
	6	101.643230	3.006590	*Litsea grandis*	26.80	26.60	16.70	19.17
	39	101.643150	3.006520	*Endospermum diadenum*	52.70	52.70	16.40	19.18
	66	101.643300	3.006520	*Sapium baccatum*	32.40	32.30	14.27	19.96
	59	101.643200	3.006440	*Pellacalyx axillaris*	13.00	13.10	13.70	19.99
	4	101.643230	3.006460	*Dyera costulata*	22.10	22.30	11.60	20.71
	51	101.643240	3.006510	*Pellacalyx axillaris*	12.10	12.10	22.60	20.92
	69	101.643310	3.006500	*Litsea elliptica*	15.20	15.10	14.40	21.59
	20	101.643240	3.006520	*Pellacalyx axillaris*	18.30	18.30	14.80	21.64
	9	101.643260	3.006510	*Pellacalyx axillaris*	17.60	17.60	14.50	22.25
	7	101.643250	3.006560	*Gironniera nervosa*	14.70	14.50	13.40	22.27
	5	101.643270	3.006550	*Pellacalyx axillaris*	19.30	19.30	22.46	23.06
	13	101.643230	3.006560	*Gymnacranthera bancana*	14.10	14.10	13.60	23.20
	25	101.643280	3.006530	*Sapium baccatum*	33.60	33.60	30.10	24.57
	44	101.643230	3.006600	*Streblus elongatus*	14.40	14.40	15.90	20.00
	47	101.643230	3.006550	*Baccaurea griffithii*	16.00	16.00	21.20	22.63
21	35	101.644940	3.006240	*Endospermum diadenum*	39.50	39.50	10.90	14.76
	55	101.644970	3.006240	*Endospermum diadenum*	28.50	28.50	19.60	15.73
	42	101.644990	3.006230	*Litsea elliptica*	36.20	36.30	14.30	15.88
	64	101.645010	3.006250	*Endospermum diadenum*	50.70	50.40	19.70	15.93
	24	101.645050	3.006230	*Ixonanthes icosandra*	45.70	45.70	23.50	17.67
	5	101.645070	3.006210	*Pometia pinnata*	23.40	23.40	10.90	17.95
	8	101.645030	3.006200	*Endospermum diadenum*	35.00	31.60	14.20	18.04
	23	101.645070	3.006150	*Endospermum diadenum*	38.60	38.30	12.40	18.55
	50	101.645020	3.006130	*Eugenia grandis*	37.40	37.40	12.70	18.84
	17	101.645000	3.006160	*Ixonanthes icosandra*	20.10	20.20	16.40	18.94
	58	101.644930	3.006130	*Scaphium macropodum*	17.70	17.70	16.40	19.00
	56	101.644940	3.006160	*Phaeanthus ophthalmicus*	22.00	21.90	12.10	19.16
	59	101.644890	3.006120	*Litsea elliptica*	28.00	28.00	14.70	19.20
	45	101.644910	3.006130	*Litsea grandis*	24.20	24.20	16.50	19.95

	9	101.644970	3.006210	*Litsea grandis*	20.70	20.60	15.30	20.00
	3	101.644960	3.006240	*Aporosa symplocoides*	14.90	14.80	17.80	20.01
	65	101.644990	3.006190	*Eugenia grandis*	20.50	20.30	12.50	20.04
	63	101.644940	3.006140	*Ochanostachys amentacea*	18.10	18.10	11.70	20.11
	47	101.644930	3.006160	*Eugenia grandis*	27.00	27.20	15.40	20.94
	75	101.644910	3.006130	*Dipterocarpus verrucosus*	39.90	40.00	10.70	16.99
	1	101.644890	3.006150	*Nephelium juglandifolium*	14.50	14.50	16.20	21.00
	61	101.644880	3.006160	*Artocarpus rigidus*	14.20	14.00	12.30	21.83
	6	101.644950	3.006190	*Kokoona reflexa*	16.30	16.30	26.20	21.90
	54	101.644870	3.006080	*Spondias dulcis*	12.50	12.30	21.30	23.31
	60	101.644950	3.006220	*Heritiera javanica*	12.60	12.50	17.80	19.25
22	35	101.643620	3.007340	*Endospermum diadenum*	27.50	27.20	13.50	12.98
	43	101.643620	3.007290	*Gluta renghas*	23.40	23.20	11.10	12.95
	65	101.643590	3.007340	*Canarium littorale*	19.90	19.20	12.10	14.01
	17	101.643560	3.007310	*Dyera costulata*	84.00	83.60	7.20	14.80
	75	101.643610	3.007370	*Artocarpus scortechinii*	21.50	22.80	12.70	15.38
	1	101.643590	3.007360	*Artocarpus scortechinii*	25.20	24.60	14.40	16.28
	38	101.643550	3.007420	*Endospermum diadenum*	28.50	29.40	11.30	16.36
	42	101.643620	3.007400	*Shorea hypochra*	61.00	60.50	17.20	17.33
	62	101.643640	3.007380	*Sapium baccatum*	27.50	28.20	16.60	17.42
	9	101.643700	3.007400	*Artocarpus scortechinii*	35.60	34.90	15.90	17.48
	46	101.643740	3.007460	*Artocarpus scortechinii*	38.80	35.80	17.50	17.67
	31	101.643720	3.007360	*Adenanthera malayana*	34.50	32.80	11.50	17.70
	2	101.643770	3.007290	*Syzygium spp*	19.80	18.90	16.70	17.99
	25	101.643610	3.007310	*Litsea costalis*	12.40	11.80	17.80	18.04
	33	101.643620	3.007300	*Diospyros malaccensis*	18.50	17.50	20.30	18.97
	65	101.643580	3.007360	*Palaquium gutta*	20.40	19.20	11.70	19.00
	56	101.643550	3.007420	*Pellacalyx axillaris*	14.00	13.30	14.20	19.56
	29	101.643660	3.007380	*Aidia densiflora*	23.00	21.90	14.30	19.73
	71	101.643720	3.007400	*Ochanostachys amentacea*	20.00	18.90	15.30	19.96
	54	101.643530	3.007350	*Canarium littorale*	13.50	13.00	14.50	20.90
	8	101.643580	3.007280	*Endospermum diadenum*	11.70	12.20	14.90	21.99
	26	101.643570	3.007290	*Canarium littorale*	13.70	13.00	22.40	28.62
	50	101.643620	3.007320	*Xerospermum noronhianum*	11.40	11.60	37.80	34.85
23	2	101.643480	3.003020	*Lithocarpus celebicus*	73.20	74.40	17.20	25.19
	49	101.643470	3.002940	*Artocarpus scortechinii*	32.10	33.60	12.10	21.93
	48	101.643490	3.002920	*Lithocarpus celebicus*	32.00	30.40	15.90	12.36
	28	101.643490	3.002990	*Endospermum diadenum*	29.50	30.40	13.20	13.80
	39	101.643440	3.002940	*Endospermum diadenum*	49.40	49.10	8.40	14.88
	60	101.643500	3.003010	*Endospermum diadenum*	31.20	30.40	13.20	16.04
	14	101.643530	3.003040	*Xylotria javanica*	23.60	23.10	13.90	18.71
	21	101.643490	3.003070	*Litsea costalis*	29.50	28.90	16.80	18.86
	19	101.643460	3.003080	*Ficus spp*	19.20	19.40	12.80	19.94
	69	101.643420	3.003010	*Litsea costalis*	25.00	25.50	15.60	20.00
	66	101.643380	3.002980	*Argania spinosa*	17.50	17.90	12.30	20.04
	46	101.643430	3.002990	*Sangal lofong*	14.40	14.20	15.90	21.87
	8	101.643370	3.003160	*Knema hookeriana*	16.50	15.10	13.40	20.92

	43	101.643370	3.003010	*Pouteria malaccensis*	18.50	18.00	30.30	23.99
	74	101.643300	3.002960	*Memecylon pubescens*	14.30	13.60	15.20	22.88
24	37	101.644230	3.005450	*Gynotroches axillaris*	32.00	30.10	7.90	13.92
	57	101.644320	3.005400	*Endospermum diadenum*	22.00	21.10	17.70	15.53
	33	101.644270	3.005380	*Endospermum diadenum*	38.50	38.80	11.50	15.78
	35	101.644350	3.005310	*Endospermum diadenum*	36.50	35.70	17.20	17.03
	50	101.644320	3.005270	*Litsea costalis*	27.50	26.60	14.80	18.54
	58	101.644230	3.005270	*Endospermum diadenum*	35.80	34.20	15.00	19.85
	25	101.644140	3.005380	*Endospermum diadenum*	38.00	36.80	20.60	19.93
	16	101.644160	3.005450	*Endospermum diadenum*	20.40	19.30	13.60	19.94
	40	101.644200	3.005450	*Syzygium griffithii*	49.00	49.40	14.00	21.33
	7	101.644210	3.005510	*Streblus elongatus*	25.00	24.30	22.50	22.76
	17	101.644310	3.005310	*Gironniera nervosa*	17.50	17.20	22.30	23.22
	72	101.644210	3.005420	*Litsea costalis*	18.30	17.30	17.70	23.78
	5	101.64424	3.00542	*Endospermum diadenum*	16.00	15.70	14.10	19.00
25	61	101.644390	3.007070	*Litsea costalis*	31.90	29.60	10.50	13.56
	38	101.644330	3.007060	*Gironniera nervosa*	16.90	16.40	15.20	13.98
	56	101.644360	3.007000	*Pellacalyx axillaris*	45.20	44.50	14.90	15.35
	57	101.644390	3.007030	*Sapium baccatum*	51.90	52.30	14.20	15.58
	44	101.644420	3.007100	*Pellacalyx axillaris*	43.90	43.70	14.40	15.99
	53	101.644360	3.007050	*Litsea costalis*	38.70	38.30	12.80	16.48
	20	101.644420	3.007140	*Pellacalyx axillaris*	16.90	16.00	16.20	17.75
	3	101.644420	3.007040	*Pellacalyx axillaris*	16.30	15.70	13.40	18.98
	47	101.644520	3.007010	*Syzygium myrtifolium*	25.10	22.60	12.60	20.55
	6	101.644470	3.007020	*Syzygium myrtifolium*	22.00	21.90	14.10	22.35
	74	101.644450	3.007020	*Syzygium myrtifolium*	28.00	26.90	15.30	22.90
	66	101.644490	3.007030	*Syzygium myrtifolium*	12.90	12.30	15.20	23.00
	12	101.644370	3.006960	*Litsea curtisii*	22.40	18.20	25.70	23.64
	10	101.644470	3.007050	*Litsea curtisii*	33.20	32.20	25.20	23.97
	69	101.644410	3.007050	*Litsea curtisii*	14.10	13.20	26.20	25.00
26	4	101.645550	3.002210	*Accacia mangium*	44.00	43.40	8.30	8.40
	2	101.645520	3.002100	*Endospermum diadenum*	26.40	25.40	9.60	9.60
	72	101.645480	3.002090	*Accacia mangium*	17.00	17.20	12.30	10.95
	20	101.645600	3.002130	*Accacia mangium*	23.50	23.20	10.40	11.61
	60	101.645660	3.002090	*Accacia mangium*	25.00	24.10	11.50	12.08
	15	101.645680	3.002180	*Accacia mangium*	56.50	56.70	8.60	12.23
	59	101.645660	3.002210	*Accacia mangium*	43.00	42.80	13.70	12.81
	47	101.645560	3.002220	*Syzygium spp*	13.10	12.90	9.40	12.90
	74	101.645560	3.002250	*Syzygium spp*	13.60	13.30	8.70	12.99
	24	101.645520	3.002170	*Azadirachta excelsa*	11.50	11.10	10.80	13.29
	11	101.645490	3.002270	*Cinnamomum iners*	17.50	17.80	11.30	13.83
	43	101.645390	3.002110	*Azadirachta excelsa*	26.00	26.20	11.90	13.99
	5	101.645420	3.002190	*Accacia mangium*	22.10	22.20	9.20	14.31
	43	101.645490	3.002110	*Azadirachta excelsa*	15.40	14.90	9.90	14.78
	57	101.645450	3.002120	*Accacia mangium*	12.40	11.60	12.20	15.21
	52	101.645520	3.002260	*Azadirachta excelsa*	10.60	10.00	12.00	15.78
	54	101.645470	3.002100	*Accacia mangium*	15.20	14.80	14.40	16.79

	65	101.645490	3.002070	*Accacia mangium*	13.50	12.90	12.80	17.93
	39	101.645670	3.002120	*Cinnamomum iners*	15.30	14.90	15.40	17.94
	10	101.645550	3.002250	*Azadirachta excelsa*	11.50	11.20	14.90	20.22
27	33	101.645450	3.002570	*Accacia mangium*	33.00	33.50	11.00	8.88
	54	101.645470	3.002540	*Cinnamomum iners*	18.90	18.60	10.50	11.00
	7	101.645440	3.002500	*Endospermum diadenum*	14.20	14.40	10.00	11.12
	10	101.645430	3.002590	*Azadirachta excelsa*	18.00	18.70	10.00	11.20
	34	101.645460	3.002620	*Vitex pinnata*	12.60	12.50	11.40	12.20
	41	101.645420	3.002630	*Azadirachta excelsa*	23.50	24.00	9.00	12.35
	24	101.645520	3.002660	*Syzygium polyanthum*	16.10	15.50	8.90	12.54
	74	101.645550	3.002690	*Syzygium spp*	15.10	14.90	11.50	12.73
	9	101.645540	3.002660	*Syzygium spp*	17.00	16.80	10.40	12.74
	35	101.645580	3.002640	*Accacia mangium*	18.50	18.90	12.70	12.79
	72	101.645510	3.002550	*Accacia mangium*	29.50	29.80	11.00	13.00
	17	101.645520	3.002560	*Accacia mangium*	17.80	17.20	11.70	13.15
	60	101.645470	3.002530	*Azadirachta excelsa*	12.00	11.80	14.80	13.54
	61	101.645460	3.002590	*Cinnamomum iners*	18.50	18.20	8.20	13.65
	47	101.645450	3.002610	*Azadirachta excelsa*	16.40	16.40	8.40	14.09
	63	101.645440	3.002630	*Cinnamomum iners*	18.70	18.60	12.20	14.64
	25	101.645440	3.002640	*Vitex pinnata*	14.10	13.90	10.80	15.35
	18	101.645460	3.002630	*Azadirachta excelsa*	12.00	12.00	10.90	15.64
	4	101.645480	3.002630	*Azadirachta excelsa*	12.40	12.30	11.60	15.78
	16	101.645520	3.002640	*Azadirachta excelsa*	11.90	11.20	15.50	15.93
	61	101.645480	3.002570	*Cinnamomum iners*	18.90	18.60	12.20	16.04
	52	101.645560	3.002660	*Syzygium spp*	12.50	12.00	9.10	16.60
	37	101.645440	3.002500	*Cinnamomum iners*	11.30	11.00	10.20	16.68
	64	101.645440	3.002550	*Azadirachta excelsa*	10.30	10.40	14.20	16.95
	38	101.645450	3.002580	*Azadirachta excelsa*	11.00	11.20	13.20	17.17
	51	101.645450	3.002600	*Azadirachta excelsa*	10.00	10.30	13.20	17.60
	20	101.645450	3.002610	*Cinnamomum iners*	11.00	10.40	25.40	19.83

Appendix 15. Lower canopy trees GPS location and tree parameter measurements

Plot No.	Tree No.	Long (Deg.)	Lat (Deg.)	Species	Field DBH (cm)	TLS DBH (cm)	TLS Height (m)	Field Height (m)
1	12	101.644840	3.001280	*Syzgium grande*	12	10.0	6.61	6.80
	8	101.644780	3.001230	*Syzgium grande*	8	10.6	6.98	6.48
	6	101.644710	3.001170	*Cinnamomum iners*	6	15.6	5.79	7.03
2	2	101.644133	3.004683	*Elaeocarpus mastersii*	2	18.0	11.82	10.5
	5	101.644050	3.004783	*Knema hookeriana*	5	15.0	7.85	6.80
	8	101.644117	3.004733	*Aquilaria malaccensis*	8	13.0	10.35	8.00
	10	101.644150	3.004733	*Ixonanthes icosandra*	10	12.5	8.01	7.30
	12	101.644167	3.004733	*Millettia atropurpurea*	12	13.0	9.44	8.40
	13	101.644167	3.004733	*Memecylon pubescens*	13	16.2	9.90	140
	15	101.644167	3.004700	*Gironniera nervosa*	15	14.4	10.4	9.40
	16	101.644167	3.004700	*Pellacalyx axillaris*	16	17.5	11.5	12.0
	33	101.644083	3.004750	*Parkia speciosa*	33	11.0	10.73	12.0
	34	101.644083	3.004733	*Gironniera nervosa*	34	12.2	8.00	10.00
	25	101.644000	3.004650	*Syzygium effusum*	25	11.0	7.45	8.00
	35	101.644083	3.004700	*Litsea costalis*	35	12.0	5.10	5.00
	39	101.644117	3.004767	*Monocarpia marginalis*	39	13.0	10.57	10.5
3	72	101.644710	3.004860	*Pellacalyx axillaris*	72	11.0	10.00	9.00
	37	101.644740	3.004960	*Ochanostachys amentacea*	37	17.0	7.33	7.80
	38	101.644630	3.004940	*Arfocarpus scortechinis*	38	10.5	9.81	10.30
	45	101.644630	3.004920	*Ochanostachys amentacea*	45	11.5	8.25	11.0

	48	101.644620	3.004900	*Litsea costalis*	39	15.0	11.90	14.40
	39	101.644700	3.004910	*Pellacalyx axillaris*	35	17.9	10.65	14.00
	35	101.644710	3.004860	*Terminalia subspathulata*	34	11.5	8.73	7.00
	34	101.644660	3.004860	*Pellacalyx axillaris*	63	14.0	12.0	17.00
	63	101.644700	3.004940	*Paropsia verruciformis*	69	11.7	10.09	10.30
	69	101.644730	3.004790	*Ochanostachys amentacea*	55	12.0	6.45	7.00
	55	101.644650	3.004790	*Memecylon edule*	74	12.50	7.70	7.80
	74	101.644710	3.005000	*Strebhus elongatus*	46	12.00	8.70	8.40
	46	101.644620	3.004910	*Xerospermum noronhianum*	36	12.60	9.58	8.42
	36	101.644680	3.004840	*Strebhus elongatus*	5	12.30	11.65	15.00
4	5	101.643940	3.006950	*Litsea costalis*	9	16.4	11.12	15.00
	9	101.643840	3.007040	*Vitex pinnata*	11	14.7	11.71	10.14
	11	101.643910	3.007020	*Pometia pinnata*	31	10.0	7.99	7.60
	31	101.644010	3.006990	*Knema hookeriana*	17	11.0	11.91	14.65
	12	101.643880	3.006970	*Gironniera nervosa*	20	10.6	8.86	11.70
	13	101.643840	3.006980	*Pellacalyx axillaris*	23	10.9	9.69	8.62
	14	101.643880	3.007040	*Lithocarpus edulis*	37	10.3	10.28	9.00
	17	101.643920	3.007040	*Gironniera nervosa*	38	11.0	6.08	7.50
	20	101.643930	3.007080	*Pellacalyx axillaris*	43	10.8	10.59	10.70
	23	101.644040	3.007080	*Cryptocarya griffithiana*	42	11.40	10.15	10.70
5	60	101.643610	3.006700	*Endospermum diadenum*	63	13.7	11.91	15.10
	63	101.643620	3.006680	*Artocarpus rigidus*	58	10.1	12.00	16.00
	58	101.643690	3.006700	*Pellacalyx axillaris*	55	12.5	11.34	14.25
	55	101.643630	3.006800	*Paropsia verruciformis*	52	10.9	10.26	10.40
	52	101.643640	3.006820	*Ochanostachys amentacea*	48	22.3	9.35	11.80
	48	101.643620	3.006750	*Elaeocarpus petiolatus*	46	12.3	9.26	11.80
	46	101.643630	3.006750	*Elaeocarpus petiolatus*	45	14.1	10.85	12.90
	45	101.643620	3.006690	*Litsea glutinosa*	69	11.3	11.30	12.60
	69	101.643630	3.006610	*Garcinia nervosa*	71	13.4	10.63	13.20
	71	101.643550	3.006590	*Pellacalyx axillaris*	50	15.3	11.33	14.60
	50	101.643570	3.006590	*Pellacalyx axillaris*	40	11.4	9.54	11.00
	40	101.643560	3.006700	*Strebhus elongatus*	34	12.5	10.91	11.60
	34	101.643550	3.006700	*Palaquium hispidum*	38	10.4	9.83	10.10
	38	101.643550	3.006710	*Arthrophyllum diversifolium*	62	12.50	11.37	11.80
6	44	101.646870	3.005370	*Syzygium spp*	4	14.7	9.57	10.50
	4	101.646820	3.005240	*Spondias Dulcis*	1	13.5	10.48	11.70
	1	101.646800	3.005340	*Xylopia ferruginea*	12	14.5	9.82	6.97
	12	101.646870	3.005330	*Lepisanthes alata*	36	12.3	9.59	8.26
	36	101.646880	3.005310	*Memecylon edule*	37	11.30	8.11	8.71
	37	101.646850	3.005290	*Pometia pinnata*	7	16.30	11.00	10.60
7	63	101.646450	3.005660	*Syzygium spp*	63	14.0	12.00	16.0
	62	101.646470	3.005690	*Palaquium gutta*	62	12.5	11.71	12.60
	59	101.646420	3.005810	*Atrocarpus odoratissimus*	59	15.1	10.28	11.20
	53	101.646460	3.005870	*Rhodamnia cinerea*	53	10.0	6.96	6.40
	50	101.646530	3.005870	*Syzygium spp*	50	14.6	6.08	7.20
	69	101.646500	3.005750	*Lithocarpus spp*	69	16.5	8.89	10.10
8	18	101.642250	3.005890	*Ochanostachys amentacea*	44	11.2	11.56	11.90
	44	101.642140	3.005900	*Pellacalyx axillaris*	9	16.9	9.76	11.30
	9	101.642120	3.005840	*Pellacalyx axillaris*	12	12.6	11.00	14.20
	12	101.642210	3.005830	*Pellacalyx axillaris*	14	10.5	8.20	7.80
	14	101.642090	3.005770	*Scleropyrum wathchianuni*	15	14.1	8.16	6.20
	15	101.642130	3.005780	*Lithocarpus celebicus*	19	11.6	11.93	13.80
	19	101.642230	3.005790	*Pellacalyx axillaris*	24	16.7	10.64	10.90
	24	101.642270	3.005770	*Polyalthia rumphii*	17	18.15	11.94	12.60
	17	101.642160	3.005820	*Palaquium gutta*	23	20.7	8.09	8.60
	23	101.642220	3.005780	*Baccaurea griffithii*	45	11.7	6.78	7.29
9	45	101.642570	3.006530	*Artocarpus scortechinii*	46	16.4	10.35	12.58
	46	101.642570	3.006560	*Aidia densiflora*	53	13.4	11.72	13.73
	53	101.642520	3.006630	*Baccaurea griffithii*	2	10.0	10.17	9.93
	2	101.642520	3.006620	*Horsfieldia spp*	10	10.0	9.45	8.63
	10	101.642520	3.006530	*Pellacalyx axillaris*	3	10.3	8.87	9.70
	3	101.642520	3.006590	*Pellacalyx axillaris*	13	14.4	9.97	12.21
	13	101.642450	3.006520	*Palaquium gutta*	15	11.5	11.04	12.21
	15	101.642450	3.006510	*Palaquium gutta*	12	10.0	9.57	9.28
	12	101.642520	3.006520	*Horsfieldia spp*	25	10.8	9.24	9.85
	25	101.642480	3.006440	*Monocarpia marginalis*	26	19.5	10.48	11.30

	26	101.642490	3.006500	*Monocarpia marginalis*	35	13.6	11.64	13.69
	35	101.642470	3.006380	*Litsea costalis*	17	20.5	11.19	14.50
	17	101.642430	3.006430	*Litsea costalis*	22	11.5	11.7	14.57
	22	101.642570	3.006420	*Litsea costalis*	43	14.7	9.02	8.76
	43	101.642560	3.006490	*Syzygium spp*	44	11.0	8.17	10.61
10	47	101.641450	3.005100	*Streblus elongatus*	47	14.7	10.95	13.8
	38	101.641460	3.005100	*Syzygium spp*	38	10.0	6.94	7.0
	51	101.641400	3.005120	*Litsea costalis*	51	11.0	10.91	11.7
	42	101.641400	3.005040	*Dialium platysepalum*	42	10.0	8.61	11.2
	50	101.641490	3.005050	*Streblus elongatus*	50	14.7	11.0	10.5
	48	101.641460	3.005070	*Sandaricum koetjape*	48	15.0	12.0	13.9
	53	101.641520	3.005080	*Litsea costalis*	53	10.8	7.37	8.39
	57	101.641570	3.005040	*elateriospermum tapos*	57	11.5	7.81	6.0
	61	101.641580	3.005070	*Pellacalyx axillaris*	61	25.6	8.47	9.4
	62	101.641590	3.005130	*Endospermum diadenum*	62	16.5	10.66	10.5
	67	101.641570	3.005160	*Pellacalyx axillaris*	67	12.0	12.0	14.4
	68	101.641560	3.005160	*Monocarpia marginalis*	68	13.1	11.53	13.2
	66	101.641570	3.005130	*Litsea costalis*	66	10.1	10.66	12.00
11	20	101.664770	3.030950	*Pellacalyx axillaris*	20	16.4	10.7	8.65
	2	101.664800	3.030920	*Telang Kelawar*	2	12.5	10.0	11.45
	11	101.664850	3.030960	*Artocarpus elasticus*	11	12.2	6.3	5.9
	35	101.664840	3.030970	*Mentimum spp*	35	13.2	10.7	8.94
	36	101.664830	3.030980	*Mentimum spp*	36	10.4	8.3	8.4
	12	101.664790	3.031010	*Pternandra echinata*	12	11.8	8.3	7.8
	50	101.664790	3.031100	*Elaeocarpus petiolatus*	50	10	7.5	6.7
	45	101.664740	3.031100	*Burseraceae spp*	45	27.4	10.5	12.7
	73	101.664760	3.031050	*Elaeocarpus petiolatus*	73	12.2	6.0	6.3
	66	101.664720	3.030990	*Litsea costalis*	66	11	7.6	7.2
	5	101.664670	3.030970	*Syzygium spp*	5	13.9	10	9.4
	47	101.664670	3.030940	*Sterculia parvifolia*	47	13.3	10.4	8.8
	69	101.664680	3.030860	*Streblus elongatus*	69	10.4	7.6	6.5
	6	101.664730	3.030870	*Pternandra echinata*	6	10.1	5.2	6.6
	7	101.664660	3.030890	*Maclurodendron porteri*	7	13.5	9.9	11.3
12	61	101.664020	3.032110	*Aidia densiflora*	61	11.5	11.4	14.6
	59	101.664050	3.032050	*Litsea costalis*	59	10	11.3	11.8
	63	101.664000	3.032060	*Garcinia nervosa*	63	10.9	11.4	10.2
	35	101.663990	3.032080	*Maclurodendron porteri*	35	15	11.4	13.83
	56	101.664070	3.032100	*Canarium littorale*	56	13.1	11.4	10.4
	34	101.664140	3.032150	*Pternandra echinata*	34	11.7	8.5	9.6
	64	101.664140	3.032150	*Pometia pinnata*	64	13	8.4	8.4
	1	101.664110	3.032120	*Maclurodendron porteri*	9	10	9.7	9.1
	9	101.664040	3.032050	*Memecylon edule*	41	10.2	7.3	6.4
	41	101.664020	3.032090	*Sterculia parvifolia*	44	14.6	11.9	14.8
	44	101.664080	3.032140	*Dillenia suffruticosa*	22	16.3	9.6	8.3
13	28	101.640720	3.005020	*Tachyphyrnium grif]ithii*	28	15.5	10.7	12.8
	25	101.640720	3.005020	*Syzygium malaccense*	25	10.5	11.3	12.4
	26	101.640720	3.005010	*Antidesma cuspidatum*	26	11.8	10.1	11.6
	17	101.640810	3.005090	*Heritiera javanica*	17	15.1	8.6	11.0
	18	101.640820	3.005100	*Beilschmiedia madang*	18	17.8	9.0	11.0
	22	101.640620	3.005180	*Syzygium malaccense*	22	10	9.0	8.8
14	45	101.642680	3.004150	*Xerospermum noronhianum*	45	13.3	8.6	7.28
	3	101.642680	3.004140	*Litsea costalis*	3	14.4	10.0	10.3
	35	101.642640	3.004080	*Elaeocarpus mastersii*	35	14.6	10.3	12.1
	36	101.642570	3.004100	*Memecylon garcinioides*	36	15	10.8	8.2
	16	101.642590	3.004070	*Guttiferaeand lauraceae*	16	12.2	12.0	8.9
	11	101.642590	3.004050	*Aidia densiflora*	11	16.1	9.5	9.3
	44	101.642590	3.004020	*Knema hookeriana*	44	14.6	8.9	9.7
	42	101.642560	3.004020	*Dactylocladus stenostachys*	42	13.1	8.0	7.2
	4	101.642600	3.004070	*Sandaricum koetjape*	4	14.7	9.8	8.5
	18	101.642580	3.004070	*Sial Menahun*	18	13	7.7	9.6
	38	101.642510	3.004100	*Pternandra echinata*	38	16	10	8.0
	56	101.642570	3.004190	*Pternandra echinata*	56	17.8	7.3	7.2
	35	101.642590	3.004170	*Melicope ptelefolia*	35	12.2	10.0	8.8
	72	101.642700	3.004150	*Dactylocladus stenostachys*	61	15.00	9.40	8.10
15	7	101.656820	3.034430	*Diospyros buxifolia*	7	14	5.8	5.6
	20	101.656890	3.034270	*Actinodaphne sesquipedalis*	20	16.5	9.7	9.4

	21	101.656790	3.034460	*Ochanostachys amentacea*	21	11.00	11.00	12.10
16	10	101.657710	3.034410	*Ochanostachys amentacea*	10	10	10.7	12.4
	24	101.657640	3.034460	*Ochanostachys amentacea*	24	11.1	9.1	8.4
	6	101.657620	3.034500	*Pokok Nyatoh Tembaga*	6	12.8	6.0	5.4
	35	101.657650	3.034480	*Macaranga gigantea*	35	14.9	7.0	5.4
	54	101.657700	3.034510	*Endospermum diadenum*	54	11.4	10.3	10.6
	59	101.657760	3.034490	*Aidia densiflora*	59	11.8	6.9	5.0
	75	101.657780	3.034470	*Aidia densiflora*	75	10.1	9.2	9.3
	1	101.657780	3.034460	*Aidia densiflora*	1	13.9	8.4	9.4
	61	101.657770	3.034510	*Aidia densiflora*	61	18.4	8.5	7.7
	54	101.657780	3.034460	*Artocarpus scortechinii*	54	13.9	10.6	15
	23	101.657680	3.034310	*Ixonanthes icosandra*	23	17.5	7.8	8.7
	2	101.657710	3.034500	*Aidia densiflora*	2	10.60	10.00	9.20
	49	101.657810	3.034460	*Litsea costalis*	49	12.30	9.10	8.30
	60	101.657700	3.034330	*Xerospermum noronhianum*	60	12.00	9.70	8.10
	31	101.657700	3.034380	*Pellacalyx axillaris*	31	13.50	10.30	9.40
17	5	101.656680	3.033920	*Macaranga gigantea*	5	12.1	7.3	6.7
	6	101.656730	3.033880	*Litsea castanea*	6	10	12.0	12.3
	40	101.656660	3.033810	*Aidia densiflora*	40	10.8	11.5	13.3
	25	101.656760	3.033830	*Diospyros malabarica*	25	11.5	10.2	9.6
	11	101.656820	3.033860	*Gardenia tubifera*	11	13.5	10.9	10.5
	14	101.656780	3.033880	*Mezettia leptopoda*	14	17.8	11.3	9.1
	7	101.656780	3.033950	*Artocarpus scortechinii*	7	13.10	11.50	9.30
	43	101.656740	3.033890	*Monocarpia marginalis*	43	11.40	11.76	11.60
18	68	101.657220	3.033960	*Ilex cymosa*	68	23.8	8.0	10.3
	69	101.657230	3.033930	*Aglaia merostela*	69	10.2	11.6	14.4
	6	101.657260	3.033870	*Aidia densiflora*	6	10.5	8.1	8.1
	70	101.657330	3.033900	*Xylopia ferruginea*	70	10	9.6	9.1
	53	101.657250	3.033780	*Heritiera javanica*	53	10	10.0	11
	51	101.657270	3.033750	*Memecylon edule*	51	18.4	11.9	16.6
	9	101.657370	3.033730	*Diospyros malabarica*	9	11	8.4	7.9
	25	101.657390	3.033880	*Diospyros malabarica*	25	13.30	9.00	10.70
	13	101.643420	3.005180	*Gironniera nervosa*	13	12.7	11.7	14.5
	19	101.643490	3.005350	*Kokoona littoralis*	19	14.1	9.2	8.4
	74	101.643450	3.005360	*Litsea costalis*	74	15.5	6.0	6.2
	11	101.643400	3.005260	*Gluta renghas*	11	12.3	11.8	10.9
	53	101.643410	3.005260	*Porterandia anisophylla*	53	25.2	11.1	13.8
	66	101.643490	3.005310	*Pangium edule*	66	12.60	7.10	6.30
20	43	101.643290	3.006470	*Sapium baccatum*	43	16.4	11.3	12.2
	23	101.643300	3.006580	*Shorea leprosula*	23	11.7	9.0	9.1
	14	101.643230	3.006490	*Gonystylus affinis*	14	13.50	6.00	5.70
	40	101.643340	3.006500	*Pellacalyx axillaris*	40	18.70	11.10	10.50
	11	101.643200	3.006530	*Gironniera nervosa*	11	15.90	9.60	7.70
	60	101.643200	3.006470	*Endospermum diadenum*	60	15.90	9.50	10.90
	70	101.643280	3.006430	*Nephelium juglandifolium*	70	11.90	9.70	9.50
	58	101.643330	3.006370	*Pellacalyx axillaris*	58	10.60	9.50	9.90
	46	101.643300	3.006550	*Gironniera nervosa*	46	11.50	10.80	9.80
	38	101.643330	3.006500	*Artocarpus interger*	38	11.60	7.00	6.80
	37	101.643260	3.006580	*Artocarpus interger*	37	10.10	9.10	8.20
21	36	101.644970	3.006210	*Spondias dulcis*	36	10	9.0	9.2
	57	101.645050	3.006230	*Baccaurea griffithii*	57	10.6	7.0	9.1
	26	101.645070	3.006220	*Aidia densiflora*	26	14.3	6.2	6.5
	72	101.645030	3.006140	*Pternandra echinata*	72	12.8	7.1	7.7
	41	101.644940	3.006100	*Pouteria malaccensis*	41	15.4	12	15.9
	38	101.644960	3.006160	*Spondias dulcis*	38	10.2	10.2	9.2
	20	101.644980	3.006240	*Spondias dulcis*	20	10.2	5.8	5.5
	50	101.644960	3.006200	*Eugenia grandis*	50	11.00	9.00	8.80
	43	101.645020	3.006140	*Endospermum diadenum*	43	12.00	10.40	8.20
	29	101.644960	3.006270	*Pellacalyx axillaris*	29	13.00	10.70	10.80
22	3	101.643620	3.007380	*Xanthophyllum vitellinum*	3	10.5	10.9	9.6
	61	101.643580	3.007380	*Diospyros malaccensis*	61	13.4	10.9	9.9
	21	101.643550	3.007440	*Pellacalyx axillaris*	21	22.4	10.0	11.9
	64	101.643610	3.007420	*Madhuca malaccensis*	64	10.8	11.8	14.7
	20	101.643630	3.007400	*Anisophyllea griffithii*	20	10.4	7.1	8.2
	51	101.643530	3.007390	*Gluta renghas*	51	11.90	10.80	9.70
	36	101.643710	3.007440	*Gironniera nervosa*	36	12.50	11.70	11.00

	19	101.643770	3.007420	*Knema hookeriana*	19	10.60	11.10	14.20
	55	101.643590	3.007430	*Litsea grandis*	55	10.20	8.00	7.80
23	6	101.643480	3.003000	*Antidesma cuspidatum*	6	13.4	7.2	6.4
	20	101.643480	3.003020	*Antidesma cuspidatum*	20	10.6	7.2	6.4
	12	101.643510	3.002970	*Canarium littorale*	12	14.3	10.7	11.6
	32	101.643540	3.002930	*Syzygium spp*	32	17	8.2	8.6
	51	101.643420	3.003080	*Lithocarpus celebicus*	51	12.1	9.1	9.0
	68	101.643420	3.003140	*Lithocarpus celebicus*	68	20.9	12.0	14.9
	17	101.643450	3.003000	*Lithocarpus celebicus*	17	17	11.0	9.5
	70	101.643360	3.003090	*Diospyros malaccensis*	70	15.8	8.00	6.6
	9	101.643330	3.003110	*Burseraceae spp*	9	10	7.6	6.5
	44	101.643330	3.003020	*Syzygium spp*	44	16.8	11.4	11.6
	53	101.643520	3.002920	*Gironniera nervosa*	53	13.90	9.00	8.00
	11	101.643350	3.002950	*Memecylon pubescens*	11	12.00	10.00	10.00
24	65	101.644320	3.005290	*Spondias dulcis*	65	18.5	12.0	15.2
	59	101.644330	3.005260	*Gymnacranthera bancana*	59	10	10.7	12.6
	63	101.644240	3.005270	*Strehlus elongatus*	63	10	8.1	8.3
	47	101.644170	3.005250	*Strehlus elongatus*	47	11.5	8.6	7.9
	41	101.644170	3.005290	*Anisophyllea griffithii*	41	15	11.9	10.8
	2	101.644230	3.005370	*Pellacalyx axillaris*	2	11	7.1	6.8
	24	101.644230	3.005370	*Ochanostachys amentacea*	24	10	8.9	9.5
	4	101.644120	3.005440	*Anisophyllea griffithii*	4	14	8.2	8.3
	42	101.644130	3.005400	*Strehlus elongatus*	42	10	11.6	10.4
	11	101.644220	3.005490	*Gironniera nervosa*	11	12.5	9.9	9.6
	61	101.644190	3.005547	*Lithocarpus wallichianus*	61	19	10.1	10.3
	10	101.644240	3.005470	*Endospermum diadenum*	10	15.2	9.5	7.2
	60	101.644290	3.005320	*Lithocarpus wallichianus*	60	11.50	11.20	10.80
	26	101.644220	3.005300	*Litsea costalis*	26	17.50	8.00	8.70
25	64	101.644420	3.007060	*Syzygium myrtifolium*	64	10.5	10	9.8
	1	101.644420	3.006990	*Gardenia tubifera*	1	10.5	8.3	7.2
	2	101.644370	3.006990	*Pellacalyx axillaris*	2	11.6	8.9	9.8
	20	101.644430	3.006980	*Palaquium gutta*	20	11.5	9.1	8.3
	11	101.644470	3.006980	*Memecylon pubescens*	11	19.5	11.4	10.2
	70	101.644480	3.007050	*Memecylon pubescens*	70	13	10.0	10.6
	51	101.644490	3.007110	*Styrax paralleloneurum*	51	10.3	9.1	8.3
	48	101.644420	3.007110	*Pternandra echinata*	48	10.5	6.9	7.9
	17	101.644470	3.007080	*Gynotroches axillaris*	17	12.2	8.7	8.3
	38	101.644510	3.007020	*Memecylon pubescens*	38	11.00	9.20	9.00
26	26	101.645630	3.002190	*Cinnamomum iners*	26	19.5	7.5	7.2
	6	101.645600	3.002200	*Cinnamomum iners*	6	12	6.6	8.0
	9	101.645550	3.002210	*Vitex pinnata*	9	11.6	6.5	6.6
	44	101.645550	3.002250	*Cinnamomum iners*	44	13.5	7.4	5.5
	70	101.645510	3.002210	*Cinnamomum iners*	70	10.6	7.00	6.9
	56	101.645490	3.002200	*Cinnamomum iners*	56	12	5.3	6.6
	35	101.645420	3.002190	*Bridelia tomentosa*	35	14	7.7	7.7
	31	101.645510	3.002100	*Macaranga gigantea*	31	11.3	6.9	6.5
	50	101.645650	3.002150	*Cinnamomum iners*	50	12	5.5	5.3
	67	101.64561	3.00221	*Cinnamomum iners*	67	11.5	7.5	7.3
27	67	101.645480	3.002540	*Cinnamomum iners*	3	14.2	8.0	7.5
	3	101.645440	3.002500	*Bridelia tomentosa*	12	16.7	6.9	8.0
	12	101.645430	3.002560	*Azadirachta excelsa*	39	11.4	7.0	6.7
	39	101.645420	3.002550	*Azadirachta excelsa*	40	11.1	7.7	7.2
	40	101.645420	3.002590	*Cinnamomum iners*	21	12.2	7.4	7.6
	21	101.645410	3.002560	*Cinnamomum iners*	42	10.2	6.0	6.2
	42	101.645490	3.002610	*Cinnamomum iners*	50	13.6	7.0	7.2
	50	101.645510	3.002610	*Azadirachta excelsa*	15	15.4	7.9	7.7
	15	101.645500	3.002570	*Cinnamomum iners*	59	11	7.3	7.8
	59	101.645530	3.002640	*Syzygium spp*	47	12.5	7.1	7.2
	47	101.645480	3.002710	*Azadirachta excelsa*	5	12	7.9	7.9
	5	101.645620	3.002600	*Cinnamomum iners*	31	11.3	7.8	7.7
	31	101.645610	3.002610	*Cinnamomum iners*	70	14.60	7.90	8.80
	70	101.64558	3.00268	*Cinnamomum iners*	44	13.60	8.00	8.70
	44	101.64556	3.00265	*Syzygium spp*	67	10.40	7.80	8.30